Mississippi State University
Scholars Junction

Theses and Dissertations | Theses and Dissertations

12-13-2008

# Analysis Of Exhaust Waste Heat Recovery Techniques From Stationary Power Generation Engines Using Organic Rankine Cycles

Devin Krishna Sham

Follow this and additional works at: https://scholarsjunction.msstate.edu/td

Recommended Citation
Sham, Devin Krishna, "Analysis Of Exhaust Waste Heat Recovery Techniques From Stationary Power Generation Engines Using Organic Rankine Cycles" (2008). *Theses and Dissertations*. 638.
https://scholarsjunction.msstate.edu/td/638

This Graduate Thesis - Open Access is brought to you for free and open access by the Theses and Dissertations at Scholars Junction. It has been accepted for inclusion in Theses and Dissertations by an authorized administrator of Scholars Junction. For more information, please contact scholcomm@msstate.libanswers.com.

www.manaraa.com

# ANALYSIS OF EXHAUST WASTE HEAT RECOVERY TECHNIQUES FROM STATIONARY POWER GENERATION ENGINES USING ORGANIC RANKINE CYCLES

By

Devin Krishna Sham

A Thesis
Submitted to the Faculty of
Mississippi State University
in Partial Fulfillment of the Requirements
for the Degree of Master of Science
in Mechanical Engineering
in the Department of Mechanical Engineering

Mississippi State, MS

December 2008

www.manaraa.com

ANALYSIS OF EXHAUST WASTE HEAT RECOVERY TECHNIQUES

FROM STATIONARY POWER GENERATION ENGINES USING

ORGANIC RANKINE CYCLES

By

Devin Krishna Sham

Approved:

Kalyan K. Srinivasan
Assistant Professor of Mechanical Engineering
(Director of Thesis)

Louay M. Chamra
Professor and Interim Head of Mechanical Engineering
(Committee Member)

Pedro J. Mago
Associate Professor of Mechanical Engineering
(Committee Member)

Steven R. Daniewicz
Professor and Graduate Coordinator of Department of Mechanical Engineering

Sarah A. Rajala
Dean of the Bagley College of Engineering

www.manaraa.com

Name: Devin K. Sham

Date of Degree: December 12, 2008

Institution: Mississippi State University

Major Field: Mechanical Engineering

Major Professor: Dr. Kalyan K. Srinivasan

Title of Study: ANALYSIS OF EXHAUST WASTE HEAT RECOVERY TECHNIQUES FROM STATIONARY POWER GENERATION ENGINES USING ORGANIC RANKINE CYCLES

Pages in Study: 121

Candidate for Degree of Master of Science

Organic rankine cycles (ORC) with turbocompounding harness the waste heat from an internal combustion engine (ICE) to improve efficiency and fuel economy while reducing brake-specific emissions. A mathematical model was developed to explore the potential gains in 1$^{st}$ and 2$^{nd}$ law efficiencies from a practical and theoretical approach. The two approaches were compared with each other and correlated well. This analysis was conducted for R113, a dry fluid, and propane, a wet fluid, in order to analyze the differences in the two types of fluids. R113 showed a 13% – 22% and a 6% – 14.7% increase in 1$^{st}$ and 2$^{nd}$ law efficiencies, respectively. Propane showed a 9% – 17.4% and a 2% – 8.5% increase in 1$^{st}$ and 2$^{nd}$ law efficiencies, respectively. It was also shown that as the pinch point temperature decreases the 2$^{nd}$ law efficiencies increased. The use of ORC with turbocompounding is an effective manner to improve engine efficiency.

www.manaraa.com

TABLE OF CONTENTS





www.manaraa.com

LIST OF TABLES





www.manaraa.com

LIST OF FIGURES





www.manaraa.com

www.manaraa.com

www.manaraa.com

www.manaraa.com

www.manaraa.com

www.manaraa.com

www.manaraa.com

www.manaraa.com

www.manaraa.com

# CHAPTER 1

# INTRODUCTION

In 2006, according to the Annual Energy Review, 24% of world petroleum was consumed by the United States, AER (2007). In recent years the energy security debates and emission regulations have pushed this country, and the rest of the world, to explore alternative forms of energy. Whether it is solar, wind, geothermal energy, fuel cells, or bio-fuels, something must be done to relinquish our dependency on fossil fuels. Although many of these forms of alternative energy will decrease our reliance on fossil fuels, current technology hinders our ability to make this transition. Therefore, it is of the utmost importance to explore innovative measures to improve the fuel economy and efficiency of internal combustion engines (ICE), while simultaneously decreasing their emissions. The measures taken now to improve ICE will decrease the rate of consumption of fossil fuels until technology is able to harness the potential of clean-burning renewable energy resources.

In the automotive and power generation industries, extensive research is underway to improve the efficiency of the ICE. In nearly 150 years, the efficiency of a spark ignited (SI) engine has increased from 5% to nearly 30%, while compression in ignition (CI) engines to more than 40%. The efficiency of an ICE is a function of the engine's compression ratio. Therefore, if the compression ratio is increased, then the engine efficiency will increase, however this is limited to both chemical/combustion and



www.manaraa.com

physical characteristics. In SI engines (compression ratios of 8:1 to 11:1), higher compression ratios induce the phenomena of "knock" or auto-ignition. In SI engines, the fuel is ignited by a spark, however, if the temperature and pressure are high enough, the fuel will auto-ignite creating a shock wave that can be very detrimental to the internals of the engine, Ferguson et al. (2001). CI engines operate at higher compression ratios, 19:1 to 22:1, in order to achieve the higher temperatures and pressures to ignite the fuel. However, higher compression ratios are limited by the friction of the engine and increased emissions. Engines must be optimized to operate at higher compression ratios. This process may begin with the modeling of ICE.

Conventionally, SI engines are modeled using the Otto cycle and CI engines are modeled using the Diesel cycle. To model both ICE as these thermodynamic cycles the assumptions that ICE are open thermodynamic systems and the combustion process is governed by chemical reactions and occur over a finite time must be employed. Although not true, useful information may be ascertained about the specific work, thermal efficiency, and overall performance of the ICE. These simple approximations are helpful when attempting to design optimal ICE for automotive and stationary power generation purposes. Although ICE may be modeled with high thermal efficiencies using thermodynamic cycles, it is important to consider the thermal efficiency losses in an ICE once it is built.

The first law of thermodynamics shows that 60-70% of energy in the combustion process is wasted; therefore the ICE efficiencies range from 30-40%. However, the first law does not indicate how much of the wasted energy is recoverable. Since not all heat can be recovered and converted to useful work, due to the second law of



www.manaraa.com

thermodynamics, it is important to determine the processes where useful work or exergy is destroyed and wasted. The above information is supported by literature on exergy analysis, which is summarized in Table 1 below, Srinivasan (2006). The literature notes the irreversibilities in the combustion process but also indicates that the recovery of waste heat is necessary to increase engine efficiency and performance. Nearly 1/3 of the fuel energy is destroyed in the combustion process, however Caton et al. (2000) report that this may be minimized by high temperature combustion. The authors also note that with higher combustion temperatures, the exhaust temperatures will be higher.

Table 1 Summary of literature review for exergy analysis

| Author(s) & Year | Title & Journal | Salient Conclusions |
|---|---|---|
| Foster & Myers, **1982** | Heavy Duty Diesel Fuel Economy, ASME, Mechanical Engr. | Biggest exergy loss (**about 30%**) is caused by the **large chemical driving forces during combustion** that cause the fuel and air mixture to go to products **Use of exhaust gas energy** and reduction of cooling requirements are two ways **to improve fuel economy** |
| Dunbar et al., **1994** | Sources of Combustion Irreversibilities, Comb. Sci. Tech | Biggest exergy destruction (**about 1/3rd of fuel exergy**) occurs during the **internal thermal energy exchange** between reactants and products during combustion |
| Caton, J., **2000** | On the destruction of availability (exergy) due to combustion processes — with specific application to internal-combustion engines, Comb. Sci. Tech | To minimize destruction of the fuel's available energy due to combustion processes, combustion processes should be conducted at higher temperatures.<br>Higher combustion temperatures may result in higher exhaust temperatures and higher levels of availability in the exhaust. **Exhaust recovery devices such as turbo-compounding** may be needed to capture this high availability. |

In ICE, the combustion process is always accompanied by heat transfer to the cylinder walls, engine coolant, and heat rejection to the atmosphere through the exhaust gases; therefore, waste heat recovery (WHR) techniques are of significant interest. Recovering some of the waste heat will increase the potential work and efficiency of an



www.manaraa.com

ICE. Second law exergy analysis indicates that more than one-third of the potential energy of the fuel escapes through the exhaust gases, therefore indicating the immense potential for WHR techniques, Srinivasan et al. (2008). Figure 1 below, from Srinivasan (2008), shows that 65% of the exergy is destroyed and/or unused in an air standard diesel cycle. The figure gives a process by process evaluation of exergy losses for a diesel engine with a maximum temperature at 2300 K and a compression ratio of 22:1. The combustion process has 26% exergy destruction while the exhaust process has unused exergy of 34%, indicating ample potential for WHR to increase engine efficiency. This potential for exhaust WHR is the primary motivation for the research presented in this thesis.

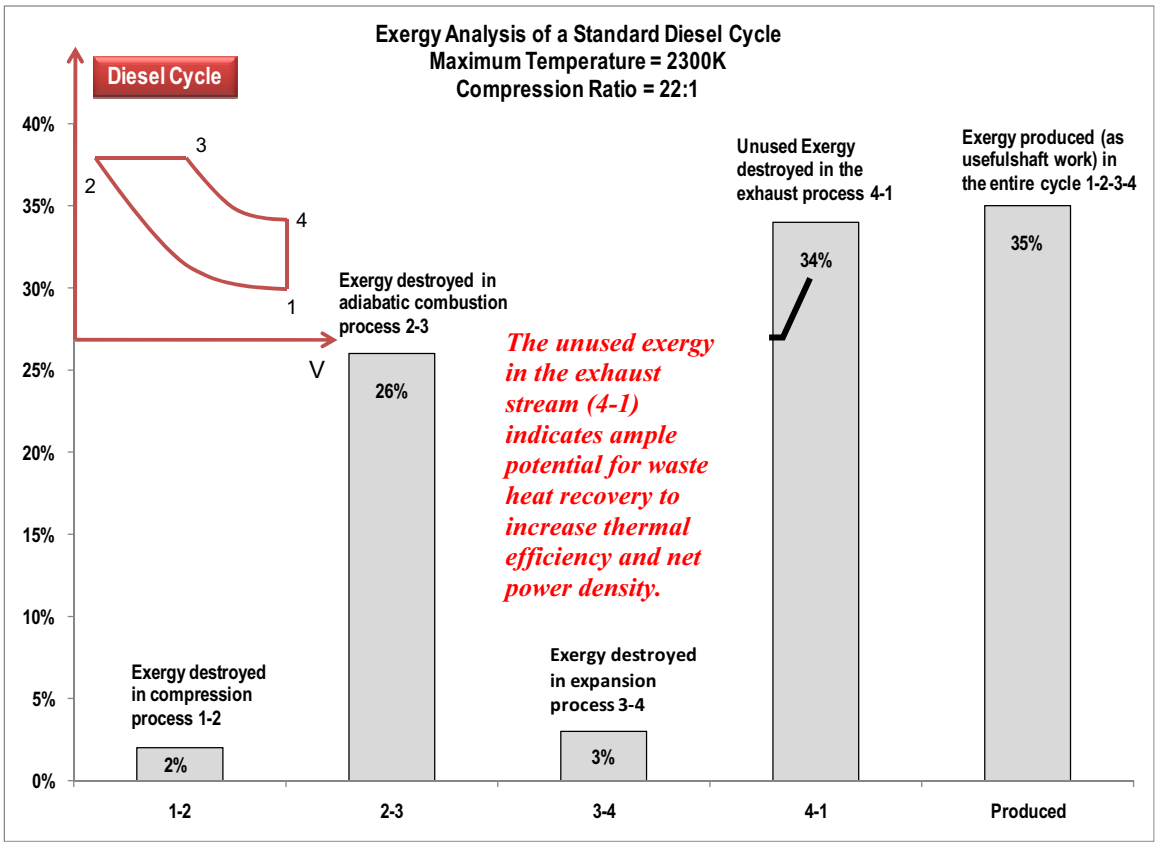


Figure 1 Exergy analysis of a standard diesel cycle



www.manaraa.com

Turbocharging and turbocompounding are two methods of WHR techniques that are of considerable interest. Turbocharging uses expanding gas in the exhaust to spin a turbine. The turbine is connected to a compressor through a shared shaft. The compressor is used to compress the inlet air to the engine. By being able to force more air into the engine, the power output is increased. Since only the energy from the exhaust is used, the extra power doesn't consume extra fuel. Turbocompounding, on the hand, uses the expanding hot gas to spin a turbine that is directly connected to the drive shaft through a series of gears. Turbocompounding can also be used with bottoming cycles, such as Rankine cycles. In this method the hot exhaust is used to heat a fluid, favorably to a saturated vapor, and then the vapor is used to spin the turbine. Results vary depending on the fluid chosen. Organic Rankine Cycles (ORC) use primarily refrigerants as their working fluid due to their low critical points and toxicity characteristics. Organic rankine fluids can be classified as isentropic, wet, and dry depending on the slope of the saturation curve on the temperature versus entropy curve. Typically dry fluids are chosen because they do not need to be superheated and because they do not condense when going through a turbine, Srinivasan et al. (2008). For the analysis presented in this thesis, R113 was chosen as the dry fluid and propane was chosen as the wet fluid for comparison purposes. More details on the specific setup of the ORC and selection process for organic fluids will be discussed later. WHR techniques, such as ORC, have been explored in the automotive and power generation industry since the late 1970s. Research indicates that improvements of 10% to 15% in fuel economy are possible, as well as reductions in brake specific emissions due to improvements in power output.



www.manaraa.com

## Literature Review

A selective literature review, on WHR in ICE, points toward several attempts in WHR in the late 1970s accompanying the first oil crisis of the country. However, 30 years later the country is faced with a similar crisis and renewed efforts are being pursued to bring such technologies back to life. Liesing et al. (1978) investigated turbocompounding in the hope to improve thermal efficiencies by 10% to 15%. Shortly after, Brands et al. (1981) used turbocompounding on a Cummins (Cummins Engine Company) heavy duty diesel engine to improve the 400 hp power rating by 12.5% and increase fuel economy by 14.8%; followed by Foster et al. (1982), who reiterated the possibility of turbocompounding to increase thermal efficiencies by 15%. The authors also noted that the implementation of vapor compression cycles could yield an efficiency increase of 10%. To further improve the thermal efficiency of ICE, in both automotive and stationary power generation applications, they recommended the use of ORC. Chen et al. (1983) reviewed many strategies to improve the thermal efficiency in ICE, such as advanced thermal cycles including turbocompounding and Rankine cycles. Additionally, DiBella et al. (1983) utilized a long-haul diesel truck engine in conjunction with an (ORC) operating with trifluoroethanol to demonstrate fuel economy improvements of about 12.5%. Further, Cerri et al (1983) used regenerative supercharging to increase power of medium speed diesel engines by over 8%. More than 10 years later, Hung et al. (1997), explored various refrigerants for ORC and found that R113 and R12 provided high thermal efficiencies due to their latent heats at low pressures. Arias et al. (2006) explored various configurations for Rankine cycles with engines and found that if the fluid is used as the engine coolant and then superheated by exhaust gas, then



www.manaraa.com

approximately 8.1% of useful energy was recovered. Chakravarthy et al. (2006) used exhaust heat to preheat inlet fuel and air in hopes to improve overall engine efficiency in a homogeneous charge compression ignition (HCCI) engine. However, due to the limited work produced, the authors suggest the use of cycle compounding to increase efficiency. Teng et al. (2006) reported the use of ORC operating on dry fluids increased the power output of the engine by 20%. Finally, Srinivasan et al. (2008) exhibited improvements of 10% to 15% in overall thermal efficiency using an advanced low pilot injection natural gas engine (ALPING) with an ORC. The authors also mentioned that this combination would be ideal for stationary power generation applications due to the high thermal efficiencies and low emissions. Table 2, below, is a summary of the above discussion of literature on turbocompounding and ORC, reiterating important conclusions.



www.manaraa.com

Table 2 Summary of literature review for turbocompounding and ORC

| Author(s) & Year | Title and Journal | Salient Conclusions |
|---|---|---|
| Leising et al., **1978** | Using waste heat boosts diesel efficiency, SAE 0098-2571/78 | **Turbocompounding** with Rankine Cycles improves efficiency by 10-15% |
| Brands et al., **1981** | **Turbocompounding** increases diesel power, improves economy, SAE 0098-2571/81 | Test conducted by Cummins Inc. found that turbocompounding improves power rating by 12.5%, and fuel economy improved by almost 15% |
| Foster and Myers, **1982** | Heavy Duty Diesel Fuel Economy, ASME, Mechanical Engr. | **Turbocompounding** to increase efficiency by 10-15%<br>Mention a study that used a combustion air refrigeration system (vapor compression cycle) to improve almost 10% increase in efficiency<br>Mention a study that uses **Organic Rankine Cycle**, but the problem was the **prohibitive cost**. Maybe **suitable for stationary power gen**. applications |
| Chen et al., **1983** | A review of engine advanced cycle and **Rankine bottoming cycle** and their loss evaluations, SAE 830124 | A comprehensive review discussing the theory and practice behind adopting advanced thermal cycles including **turbocompounding and Rankine cycles** |
| Teng et al., **2006** | Achieving High Engine Efficiency for Heavy-Duty Diesel Engines by Waste Heat Recovery Using **Supercritical Organic-Fluid Rankine Cycle** | A **"dry" organic fluid** was selected in this study. For the case-study discussed, the power of the engine increased by 20% without any additional fuel consumption |

Soaring electricity costs and low emission regulations in recent years have generated sizeable public interest for concepts such as combined heating and power (CHP) and combined cooling, heating, power (CCHP) systems. CHP and CCHP systems supply on-site electricity while using the wasted thermal energy from the prime mover to satisfy additional cooling and heating requirements. Micro-scale CHP systems can cater to office spaces and residential applications to provide a cheaper alternative to producing electricity (and heating and cooling) rather than obtaining it from a central grid. Aceves et al. (2006) reported that the cogeneration of a CHP with WHR had an efficiency of 70%. Cogeneration in these units can be achieved by an assortment of prime movers,



www.manaraa.com

such as SI and CI engines, micro-turbines, and fuel cells, however, ICE are good candidates due to their low setup and operational costs and ease of operation and maintenance. Therefore, investigation of ICE for CHP and CCHP applications from an efficient energy utilization stand point is of enormous interest. In the following section, the setup of the analysis will explained.

## Objectives

The purpose of this thesis is to present a mathematical analysis of turbocompounding with the use of ORC using a wet and dry fluid. The goal is to use ORC to increase the fuel economy and efficiency of ICE while reducing its emissions. Although specific dimensions and characteristics of each component (pump, turbine, condenser, and evaporator) are not discussed, the purpose of this thesis is to present the analysis of ORC and the performance requirements for certain components. The following chapters of this thesis will include a description of the model setup, then the methodology explaining the mathematical approach to this analysis. The results and discussion will follow the methodology and the conclusion and future recommendations will be at the end.



www.manaraa.com

# CHAPTER 2

## MODEL SETUP

Turbocompounding in an ICE is used to increase the potential power output of the system by harnessing the energy in exhaust gas. As the hot gas expands, the turbine, which is connected to a shared drive, will rotate, thereby generating useful shaft work or power. The increase in potential power will increase efficiency and fuel economy, while reducing brake-specific emissions. A bottoming cycle can be used in conjunction with turbocompounding as an alternative method of increasing system efficiency. Although there are many forms of bottoming cycles, in this case the bottoming cycle uses the waste heat from the ICE exhaust to produce useful work. This bottoming cycle follows the configuration and characteristics of Rankine Cycle, a power generation cycle.



www.manaraa.com

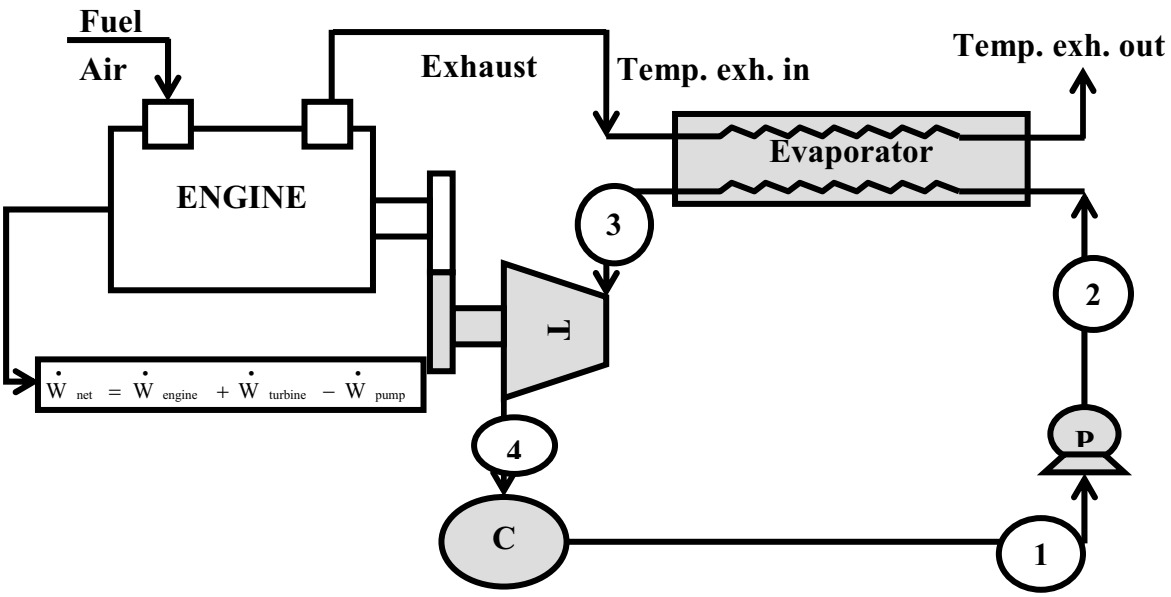


Figure 2 Engine and ORC schematic

The above figure, from Srinivasan et al. (2008), shows the configuration of engine and ORC. The exhaust gas, from the ICE, heats the organic fluid to a saturated vapor from States 2 to 3 through the evaporator and then is rejected to the ambient. The evaporator is a counter-flow heat exchanger which is used due to its packaging and superior heat transfer characteristics. In this configuration the temperature difference between the heating fluid (exhaust gas) and the working fluid (the organic fluid) is minimized, therefore reducing exergy destruction. At State 3 the organic fluid is sent through a turbine, T, where the expanding fluid will cause the turbine to rotate. This turbine is connected to a common drive shaft, shared by the ICE, through a series of gears. The rotating work increases the power output of the system. The fluid at State 4 is condensed through the condenser, C, and then at State 1 enters the pump, P, and it is sent through the cycle again.



www.manaraa.com

As mentioned earlier, the analysis in this thesis uses an ORC, which are Rankine cycles that use organic fluids as the working fluids. Organic fluids are best used in low temperature waste heat recovery applications. Due to the low temperatures and pressures of the waste heat, organic fluids are good choices due to their low critical temperatures and safety characteristics. Table 3 presents a literature review of organic fluid selection. The table highlights important thermodynamic and safety characteristics as well as the fluids chosen in each analysis.



www.manaraa.com

Table 3 Summary of literature review of organic fluid selection

| Author(s) & Year | Fluids analyzed | Salient Conclusions |
|---|---|---|
| Ulli Drescher and Dieter Bru¨ggemann, **2006** | Octanemethyltrisil-oxane (OMTS)<br>Toluene<br>Ethylbenzene<br>Propylbenzene<br>Butylbenzene | Organic fluids are best for low temperatures and/or the power plant is small. At low temperatures, organic fluids lead to higher cycle efficiency than water.<br><br>To use water, high pressures are needed, therefore it is a safety and economical risk<br><br>Properties good for ORCs: stability of the fluid and compatibility with materials in contact, safety, health, and environmental aspects, availability and costs<br><br>Efficiency correlates with a low minimum temperature and high vaporization temperature. The alkybenzenes showed the highest efficiencies |
| V. Maizza and A Maizza, **2001** | HCF-22<br>HC-40 Methyl chloride<br>HCFC-123<br>HCFC-124a<br>HFC-125<br>HFC-134a<br>HCFC-142b<br>HFC-152a<br>HC-170 Ethane<br>HC-290 Propane<br>HC-600a Iso-butane<br>R-401A (a)<br>R-401B (a)<br>R-401C (a)<br>R-402A (b)<br>R-402B (b)<br>HFC-404A (b)<br>HFC-407C (c)<br>HFC-410A (d)<br>R-508B | Organic fluids should have low critical temperature and pressure, small specific volume, low viscosity and surface tension, high thermal conductivity, suitable thermal stability, non corrosive, non-toxic and compatible with engine material and lubricating oil.<br><br>Some favorable thermodynamic properties include high latent heat and low liquid specific heat, a near vertical saturated liquid line to prevent the need for superheating and condensation during expansion in the turbine<br><br>Of the fluids analyzed in this study R-123 and R-124 couple good system performance with high operative elasticity |
| G Angelino, C Invernizzi, and G Molteni, **1999** | Ammonia<br>R123<br>HFC-245 ca | Organic fluid Rankine cycle (ORC) use organic fluids with optimized thermodynamic properties capable of taking full advantage of the lowest possible heat sink temperatures.<br><br>Organic fluids must be safe and technically suitable. Toxic fluids or substances harmful to the ambient in general are not taken into consideration, appropriate safety measures required.<br><br>Refrigerants have long been considered as typical working media for moderate-temperature applications.<br><br>Fluid characteristics such as molecular weight and critical pressure are of significant interest |



www.manaraa.com

Table 3 Literature review of organic fluid selection (continued)

| | | |
|---|---|---|
| Sanjay Vijayaraghavan, **2003** | Hydrocarbons<br>Halocarbons<br>Refrigerants<br>Aromatics<br>Water<br>Ammonia | Organic fluids have lower heats of vaporization than water, which requires larger flow rates, smaller turbine sizes are obtained due to the higher density at the turbine exit conditions<br><br>stable, non fouling, non corrosive, non toxic, and non flammable fluids simplify the design and cost of a power plant significantly<br><br>Molecular weight, melting, boiling, and critical temperatures as well as critical pressures are of significant interest in fluid selection |
| P J Mago, L M Chamra, and C Somayaji, **2007** | R134a, R113, R245ca, R245fa, R123, isobutane, and propane<br>water | Organic fluid is selected on the basis of safety and technical feasibility<br><br>Important fluid properties were: molecular weight, boiling point, density, and critical temperature and pressure<br><br>The higher the boiling point of the fluid, the better the cycle thermal efficiency. Dry fluids show better thermal efficiencies than wet fluids because they do not condense after the fluid goes through the turbine.<br><br>Organic fluids need not be superheated as the cycle thermal efficiency remains approximately constant when the inlet temperature of the turbine is increased<br>However, using the second-law analysis, it can be seen that superheating organic fluids increase the irreversibility. Therefore, organic fluids must be operated at saturated conditions to reduce the total irreversibility of the system<br><br>Thermal efficiency of ORC increases when the condenser temperature is decreased<br><br>Some organic fluids show better performance within a range of temperatures |

Important fluid properties are the molecular weight, density, boiling point, and critical temperature and pressures. In analysis presented in Mago et al. (2007), the boiling point (saturation temperature) had a direct influence on the efficiency of the ORC. The higher the boiling point (saturation temperature) the better the efficiency. Another important characteristic, when selecting an organic fluid, is its slope on the saturation curve in a temperature versus entropy diagram. The slope of the curve affects the fluid



www.manaraa.com

adaptability, cycle efficiency, and the arrangement of equipment in power generation systems. Referring to Figure 3 below from Mago et al. (2007), the fluid can be classified into 3 three categories depending on the slope of the curve.

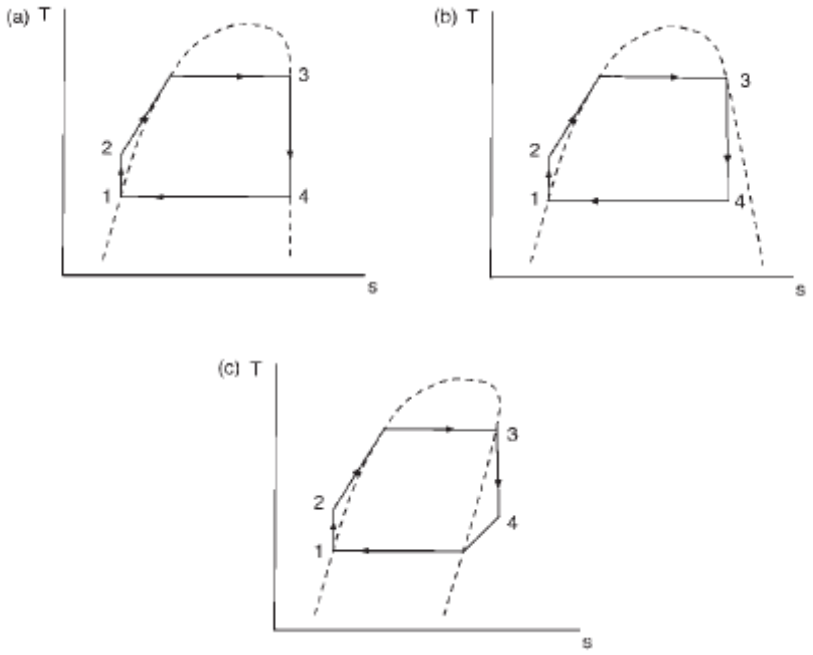


Figure 3 Organic fluid slope comparison, (a) isentropic fluid, (b) wet fluid, and (c) dry fluid

An isentropic fluid as an infinitely large slope, a wet fluid has a negative slope, and dry fluid has a positive slope. Mago et al. (2007) reported that, generally, isentropic and dry fluids are better working fluids because they do not condense while going through the turbine and they do not need superheating. The lower temperatures and pressures needed to reach saturation for organic fluids make them good candidates for waste heat recovery. Other fluids, such as water, could be used for these applications, but the need for superheating would be required in order to reach its saturation point.



www.manaraa.com

Superheating would require higher temperatures and pressures which increase cost and safety concerns. Organic fluids must also exhibit good safety characteristics.

Maizza et al. (2001) state that a good working fluid exhibits the following characteristics: low toxicity, good material compatibility, low flammability, low corrosion, and low fouling characteristics. Lee et al. (1993) reported that refrigerants are good working fluids due to their low toxicity characteristics. The combination of the good thermodynamic and safety properties make organic fluids suitable for WHR applications.

The analysis presented in this thesis used propane, a wet fluid, and R113, a dry fluid, for its working fluids. Previously reported engine data from Srinivasan et al. (2008) is used for the ICE in this analysis. The Advanced injection Low Pilot Ignition Natural Gas (ALPING) engine utilizes very small diesel pilot sprays injected during early compression stroke (approximately 60 ° BTDC) to ignite a lean premixed mixture of natural gas and air. It has been shown that these engines produce very low nitrogen oxide (NOx) emissions (less than 0.2 g/kWh) with high thermal efficiencies (about 41%), Krishnan et al., 2004. In an effort to further improve the efficiency of the ALPING engine, ORC turbo compounding is analyzed in this thesis. Engine data taken at various pilot diesel injection timings at half and quarter loads that correspond to engine brake power of 21 kW and 10.5 kW, respectively were used for the present analysis. In particular, the analysis was performed at pilot diesel injection timings of 20, 30, 40, 50, and 60 degrees before top dead center (BTDC) at half load, and 20, 30, 40, 50, and 55 degrees BTDC. For the ORC, the evaporator pressures were varied in 0.5 MPa increments as well as the exit temperatures for the exhaust gas, through the heat



www.manaraa.com

exchanger. This method was analyzed from two perspectives, a practical and theoretical method. A description of the calculations for this analysis is presented in the methodology, followed by a discussion of the results. Calculations are shown in Appendix A, *MathCAD* analysis of evaluations 1 & 2 for R113 at half load.



www.manaraa.com

CHAPTER 3

METHODOLOGY

Modeling of the ORC system is broken into two sections: ORC analysis and evaporator analysis. The ORC analysis is modeled using a standard rankine cycle, while the evaporator analysis is modeled by using heat exchanger design principles. Figure 4 below is a temperature versus entropy diagram. Refer to figure 2, in Chapter 2, for the engine and ORC setup.

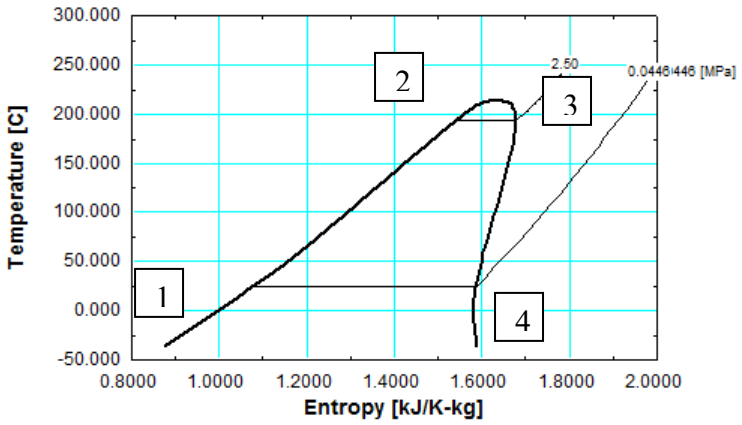


Figure 4 R113 T-s diagram for states 1-4 at an evaporator pressure of 2.5 MPa.

The modeling begins with ORC at State 1. State 1 is located after the condenser and before the pump. We define State 1 to be at a saturated liquid and to have an ambient temperature of 25 degrees Celsius. Then using *CATT2* (2002) and/or *ALLPROPS* (1999),



www.manaraa.com

a computer aided software, the pressure, specific volume, specific, enthalpy, and specific entropy were found.

State 2 is located after the pump and before the evaporator. Evaporator pressures were selected to start at 1 MPa and increase in increments of 0.5 MPa to 3.15 MPa. The 3.15 MPa was the highest value allowable pressure before the critical pressure of 3.4 MPa for R113. From States 1 to 2 there is a reversible adiabatic process through the pump. Therefore from the first law the work of the pump is:

$$w_{pump} = h_2 - h_1 \tag{1}$$

Since the process is reversible:

$$s_2 = s_1 \tag{2}$$

By assuming the liquid to be incompressible the work of the pump can be defined as:

$$w_{pump} = \int v \cdot dP = v \cdot (P_2 - P_1) \tag{3}$$

This is the ideal specific work for the pump, assuming a pump efficiency of 80%, the actual specific work needed for the pump can be found by:

$$\eta_{pump} = \frac{w_{ideal_{pump}}}{w_{actual_{pump}}} \tag{4}$$

Once the actual work is found the actual specific enthalpy at State 2 can be found using Equation 1. Using the pressure and actual specific enthalpy the rest of the thermodynamic states can be found using *CATT2*.

States 2 to 3 have constant pressure heat addition through the evaporator. At State 3 we forced the condition that the fluid would be a saturated vapor. Since the pressure from State 2 to State 3 will be the same and the quality of the fluid is known, the



www.manaraa.com

rest of the thermodynamic States can be found. From the first law, the heat addition can be found:

$$q_H = h_3 - h_2 \tag{5}$$

From States 3 to 4 the fluid goes through adiabatic reversible expansion in the turbine. The first law gives:

$$w_{turbine} = h_3 - h_4 \tag{6}$$

The reversible process gives:

$$s_3 = s_4 \tag{7}$$

From States 4 to 1, the fluid goes through constant pressure heat transfer in the condition. Therefore pressure at State 4 will equal the pressure at State 1. Knowing the pressure and ideal specific entropy the rest of the thermodynamic properties can be found. The ideal turbine work can be found using Equation 6. The actual turbine work can be found if the efficiency of the turbine is known. We will assume the turbine efficiency to be 85%. Therefore the actual specific turbine work can be found by:

$$\eta_{turbine} = \frac{w_{actual_{turbine}}}{w_{ideal_{turbine}}} \tag{8}$$

Now using the actual turbine work, the actual specific enthalpy at State 4 can be found by using Equation 6. Using the actual specific enthalpy and the pressure the rest of the thermodynamic properties at State 4 can be found.

The thermal efficiency of the rankine cycle is defined as the ratio of net work to the heat added:

$$\eta_{ORC_{1stlaw}} = \frac{W_{net}}{Q_{addition}} \tag{9-a}$$



www.manaraa.com

This can simplify to the differences in specific enthalpies:

$$\eta_{ORC_{1stlaw}} = \frac{(h_3 - h_{4_{actual}}) - (h_{2_{actual}} - h_1)}{(h_3 - h_{2_{actual}})} \quad \text{(9-b)}$$

This is a complete analysis of the ORC; however the following will analyze the specifics of the evaporator. This is done by two different methods, in the first method a design constraint is employed to prevent condensation in the evaporator. In the second method a range of effectiveness values is used to analyze the pinch point of the evaporator. Both methods were compared to each other.

For both methods of analysis, previously recorded engine data was provided to use in the analysis of the evaporator. The data for the engine was given by Srinivasan et al. (2008). The data is summarized in the table below. The engine data was given half and quarter load and for a range of injection timings, however only five were used. All calculations were for both half and quarter engine loads. The mass flow rates and the properties of the exhaust gases were given for all injection timings and load conditions.

Table 4 ALPING engine data

| Inj.timing | Diesel_flow | NG_flow | Exhaust | Texh in | Ex.Pr | Power | Eff |
|---|---|---|---|---|---|---|---|
| degBTDC | g/min | g/min | g/min | evap C | psig | bhp | % |
| | | | | | | | |
| Half Load | | | | | | | |
| 20 | 3.37 | 89.52 | 3643.19 | 319.589 | 11.11 | 28.23 | 28.16 |
| 30 | 3.36 | 78.84 | 3650.67 | 281.8488 | 10.61 | 28.15 | 31.89 |
| 40 | 3.36 | 71.05 | 3661.31 | 270.1401 | 10.81 | 28.20 | 35.14 |
| 50 | 3.35 | 68.92 | 3693.04 | 264.8569 | 10.36 | 28.12 | 36.12 |
| 60 | 3.35 | 70.88 | 3640.52 | 266.1079 | 10.37 | 28.23 | 35.19 |
| Qtr. Load | | | | | | | |
| 20 | 3.36 | 64.29 | 2824.91 | 253.4269 | 3.88 | 13.74 | 18.73 |
| 30 | 3.37 | 55.74 | 2835.06 | 238.568 | 3.84 | 14.14 | 22.07 |
| 40 | 3.36 | 50.76 | 2831.75 | 236.5363 | 3.70 | 14.26 | 24.33 |
| 50 | 3.38 | 53.46 | 2837.16 | 244.5775 | 3.79 | 14.57 | 23.67 |
| 55 | 3.36 | 57.59 | 2836.96 | 250.7884 | 3.80 | 14.00 | 21.20 |



www.manaraa.com

In this analysis we set the design constraint that the exhaust gas temperature, exiting the evaporator, will not be below the dew point temperature. Employing this constraint will prevent condensation in the evaporator, which interferes with heat exchanger performance characteristics. At different injection timings the exhaust pressure was slightly different, the pressure that gave the lowest dew point temperature was chosen for simplicity. This approach also gives a "cushion" to the higher pressures.

The saturation temperature was found using the pressure of the exhaust gas and a quality of one for water. Once the saturation temperature was found, a range of the temperature values were added. This range started with zero and went to twenty degrees Celsius, in increments of five. These temperatures were set to be outlet temperatures of the evaporator.

With inlet and outlet exhaust temperatures known the mean temperature was found. The mean temperature is needed to find the specific heat of air at this temperature. The specific heat was found using the following equation from Sonntag et al. (2002):

$$c_{p\,air} = \frac{kJ}{kg \cdot K} \cdot [1.05 - 0.365 \cdot \frac{T}{1000 \cdot K} + 0.85 \cdot (\frac{T}{1000 \cdot K})^2 - 0.39 \cdot (\frac{T}{1000 \cdot K})^3] \quad (10)$$

The heat transfer through a heat exchanger is defined as:

$$Q_{actual} = (\dot{m} \cdot c_p)_{hot} \cdot (T_{in} - T_{out})_{hot} \quad (11)$$

The maximum heat transfer can be found using the inlet temperature difference (ITD) method:

$$Q_{\max} = C_{\min imum} \cdot (T_{in_{hot}} - T_{in_{cold}}) \quad (12)$$



www.manaraa.com

The $C_{minimum}$ is the minimum heat capacity of the two fluids. For our case the minimum fluid will be the exhaust due to the imposed design criterion of a forced phase change in the ORC fluid. $C_{min}$ is defined as:

$$C_{\min imum} = (\dot{m} \cdot c_p)_{\min imum} \tag{13}$$

The effectiveness of the evaporator can be found using the maximum heat transfer and the actual heat transfer by:

$$\varepsilon = \frac{Q_{actual}}{Q_{\max}} \tag{14}$$

The actual heat transfer can also be written as (since the heat transfer between two fluids has to be equal):

$$Q_{actual} = (\dot{m} \cdot c_p) \cdot (T_{in} - T_{out}) = \dot{m}_{ORC} \cdot (h_3 - h_{2_{actual}}) \tag{15}$$

Using Equation (15) the mass flow rate of the ORC can be determined since actual heat transfer and the specific enthalpies are known. With mass flow rate known, the net power of ORC can be found by:

$$\dot{W}_{ORC} = \dot{m}_{ORC} \cdot [(h_3 - h_{4_{actual}}) - (h_{2_{actual}} - h_1)] \tag{16}$$

The power output of the engine and the mass flow rates of the fuel, which were provided above in Table 1, are used to calculate the engine efficiency. The 1st law engine efficiency can be calculated by dividing the net work by the mass flow rate of the fuel and lower heating value of the fuel:

$$\eta_{engine_{1stlaw}} = \frac{\dot{W}_{engine}}{(\dot{m} \cdot LHV)_{fuel}} \tag{17}$$



www.manaraa.com

To find the 1st law efficiency of the engine combined with the ORC, we simply add the net power of the ORC to the engine power as shown in Equation (18) below.

$$\eta_{Combined_{1stlaw}} = \frac{\dot{W}_{engine} + \dot{W}_{ORC}}{(\dot{m} \cdot LHV)_{fuel}} \tag{18}$$

The percentage increase in first law efficiency with combined engine and ORC with respect to the engine can be found by:

$$Percent_{increase\,1stlaw} = \frac{\eta_{Combined_{1stlaw}} - \eta_{engine_{1stlaw}}}{\eta_{engine_{1stlaw}}} \tag{19}$$

In a similar manner the 2nd law efficiency and percentage increase can be found replacing the lower heating value of the fuel with the chemical exergy of the fuel:

$$\eta_{Combined_{2ndlaw}} = \frac{\dot{W}_{engine} + \dot{W}_{ORC}}{(\dot{m} \cdot x_{exergy})_{fuel}} \tag{20}$$

$$Percent_{increase\,2ndlaw} = \frac{\eta_{Combined_{2ndlaw}} - \eta_{engine_{2ndlaw}}}{\eta_{engine_{2ndlaw}}} \tag{21}$$

In the second analysis a range of effectiveness was used for the evaporator. Then by assuming linear temperature profiles the pinch point of the evaporator is determined and analyzed.

First, the maximum heat transfer is found using Equations (12) and (13) from above. Then by using choosing a range of effectiveness (60, 65, 70, 75, 80) the actual heat transfer can be found by Equation (14).

By rearranging Equation (11) for the exhaust side heat transfer, the outlet exhaust temperature can be found.



www.manaraa.com

$$T_{hot_{out}} = T_{hot_{in}} - \frac{Q_{actual}}{(\dot{m} \cdot c_p)_{hot}} \tag{22}$$

In a manner similar to the first analysis, the mass flow rate and work of the ORC can be found using Equations (15) and (16). The 1st and 2nd law thermal efficiencies as well as percentage increases can also be found using Equations (18), (19), (20), and (21).

Assuming linear temperature profiles the pinch point temperature difference can be found. The pinch point temperature difference is the minimum temperature difference between the hot and cold fluid and tells how effective an evaporator or process operates. In this case the pinch point will occur at point where ORC reaches its saturation temperature. To begin this analysis plot Temperature vs. Change in Enthalpy for the evaporator. By subtracting the enthalpy of State 2 from the points on the graph the graph was shifted to the left, making Point 2, the enthalpy of State 2 of the ORC, zero. Point 2' is the difference between the saturated liquid enthalpy and $h_2$ and Point 3 is the difference between the $h_2$ and $h_3$ for the ORC. Change in enthalpy at State 3 is equal to the total heat transfer in the evaporator. Point 4 has the same change in enthalpy but is at the inlet temperature for the exhaust gas. Point 5 is the exit temperature for the exhaust gas with a change in enthalpy of zero.



www.manaraa.com

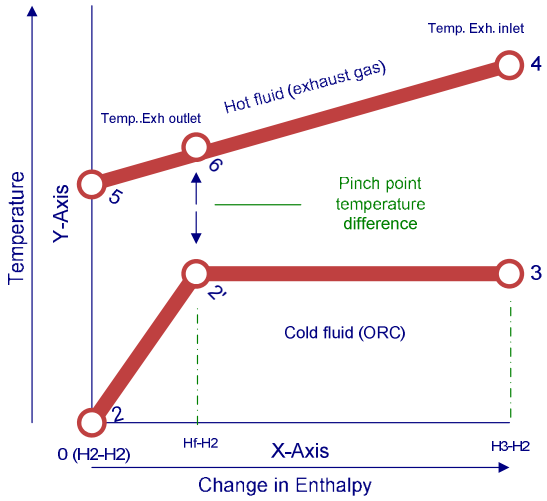


Figure 5 Pinch point plot

Using the x and y coordinates of Points 4 and 5 the slope could be found for the temperature profile of the exhaust gas:

$$m_{slope} = \frac{T_{exh_{in}} - T_{exh_{out}}}{\dot{m}_{ORC} \cdot (h_3 - h_2) - \dot{m}_{ORC} \cdot (h_2 - h_2)} \tag{23}$$

With the slope known, the y-intercept could be found using Point 4 or 5 with the slope-intercept equation:

$$T_{exh_{in}} = m_{slope} \cdot [\dot{m}_{ORC} \cdot (h_3 - h_2)] + b_{y-\text{int}} \tag{24}$$

Now that all the variables of the slope-intercept equation are known, the temperature at Point 6 can be found for exhaust gas by using the change in enthalpy at Point 2'.

$$T_{pinch} = m_{slope} \cdot [\dot{m}_{ORC} \cdot (h_f - h_2)] + b_{y-\text{int}} = T_6 \tag{25}$$

Subtracting the temperatures T pinch (Point 6) the ORC saturation temperature (Point 2) will give the pinch point temperature difference.

$$\Delta T_{pinch} = T_6 - T_{2'} \tag{26}$$



www.manaraa.com

# CHAPTER 4

# RESULTS AND DISCUSSION

Current energy security and emissions debates have supplied sufficient motivation to investigate methods of increasing internal combustion engine (ICE) performance and efficiency. The increase in efficiency, fuel consumption, and emissions may be investigated from various avenues. In this research, methods of waste heat recovery (WHR) techniques were explored in order to investigate the potential increases and viability of turbocompounding with organic rankine cycle (ORC). In particular, experimental data from a pilot ignited natural gas engine (Srinivasan et al., 2008) were used in conjunction with an analytical thermodynamic model in which R113, a dry fluid, and propane, a wet fluid were investigated as possible candidates for exhaust waste heat recovery using an organic rankine cycle. As mentioned in the Methodology (Chapter 3), two methods of evaluation were conducted in this research. Evaluation 1 uses a practical design constraint to limit the outlet temperature of the evaporator for the exhaust gas to slightly above saturation temperature. This method will prevent condensation in the evaporator, which generally has negative effects on its performance. Evaluation 2 uses a theoretical approach to vary the effectiveness of the evaporator in order to vary the pinch point temperature difference. Other characteristics of the ORC and engine were varied in order to give a wide range of results for this research. ORC evaporator pressures were



www.manaraa.com

varied, depending on fluid, while the injection timing and load were varied for the engine.

The goal of this research, in evaluation 1, was to find the increase in 1st and 2nd law efficiencies with the implementation of an ORC. Figures 6 and 7 below show the cycle thermal efficiency of an ORC versus evaporator pressure for R113 and propane, respectively.

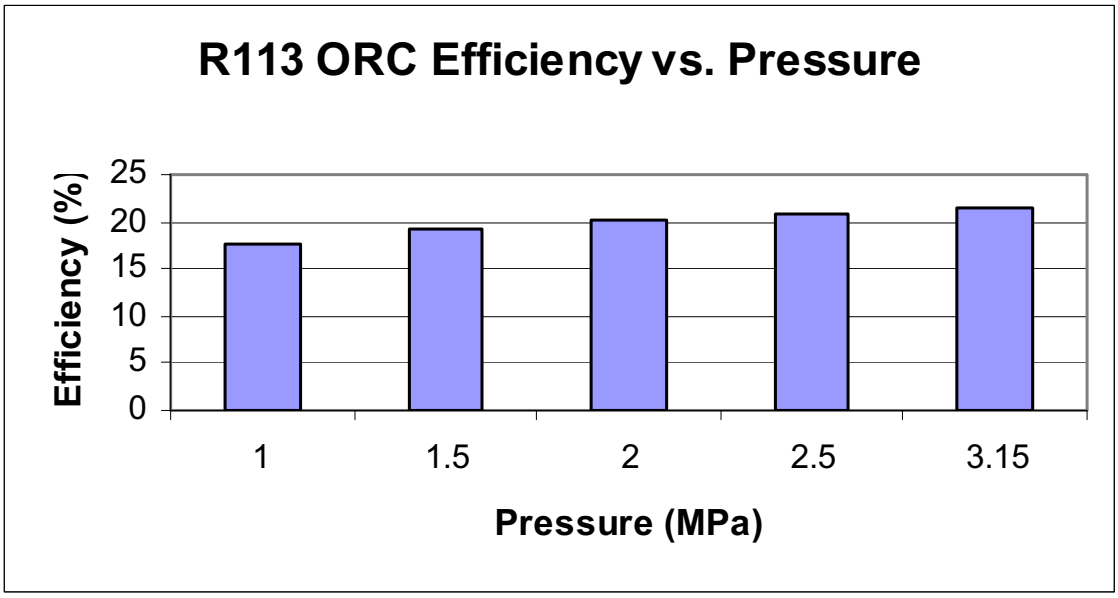


Figure 6 R113 ORC plot of efficiency versus evaporator pressure.



www.manaraa.com

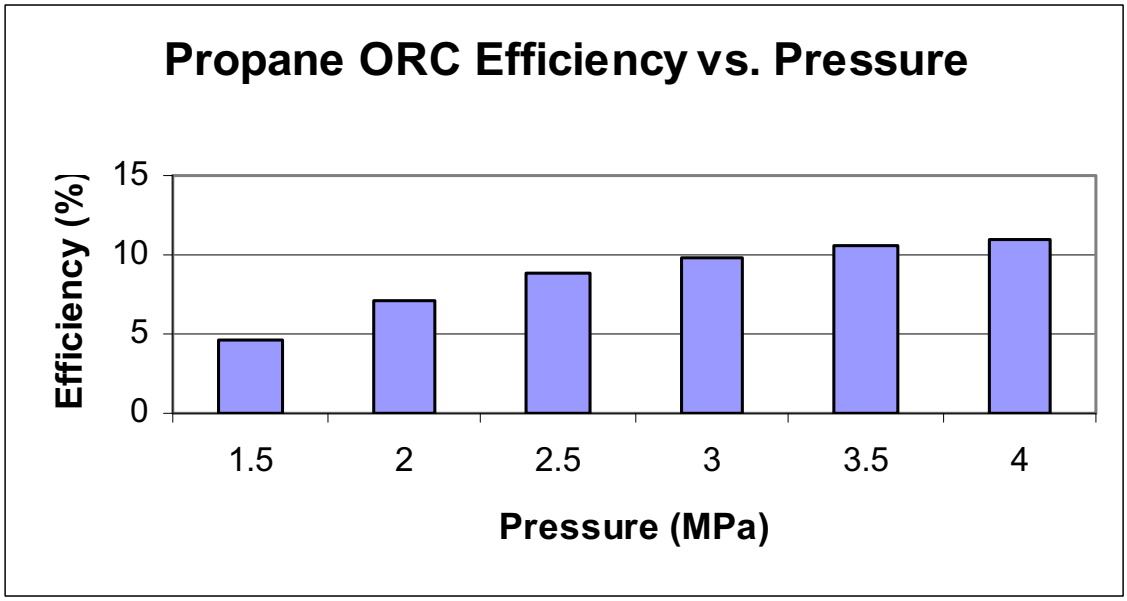


Figure 7 Propane ORC plot of efficiency versus evaporator pressure

Regardless of evaporator pressure, the R113 ORC shows a much higher thermal efficiency even though propane can utilize an evaporator pressure of 4 MPa. The difference in available pressures for each fluid is due to the respective critical points of the fluids. R113's critical temperature is 214.06 degrees Celsius and critical pressure is 3.392 MPa. Propane's critical temperature is 96.70 degrees Celsius and critical pressure is 4.248 MPa, Mago et al. (2006). Contrasting similar evaporator pressures of 1.5, 2.0, 2.5 MPa propane has ORC efficiencies of 4.6 %, 7.1%, and 8.8%, while R113 has ORC efficiencies of 19.3%, 20.2%, and 20.9%, respectively. The larger efficiencies of R113 are due to its higher boiling point (saturation temperature). It is also important to note that with the increase in evaporator pressure, regardless of fluid, the cycle efficiency increases. The higher evaporator pressure causes the boiling point for the fluid to rise thereby increasing the efficiency.



www.manaraa.com

The engine data, supplied by Srinivasan et al. (2008), showed that the 1st law efficiencies of 28 – 35% at half load and 18% - 21% at quarter load, depending on injection timings. Injection timings investigated in this research for half load were 20, 30, 40, 50, and 60 degrees before top dead center (BTDC), while quarter load injection timings were 20, 30, 40, 50, and 55 degrees BTDC. Figures 8 and 9 show the total 1st law efficiencies at half load with respect to injection timing and ORC evaporator pressure for R113 and propane, respectively. Each bar on the graph represents a specific injection timing at a particular evaporator pressure. The injection timings increase from left to right, starting at 20 degrees BTDC. An important observation from these figures is that the range of operating pressures for R113 was 1-3.15 MPa, whereas, with propane the operating pressure range was extended to 1.5 – 4.0 MPa. It is instructive to compare the performance of these two working fluids at the same evaporator pressures, i.e., 1.5, 2.0, 2.5 MPa, respectively, at all injection timings investigated.

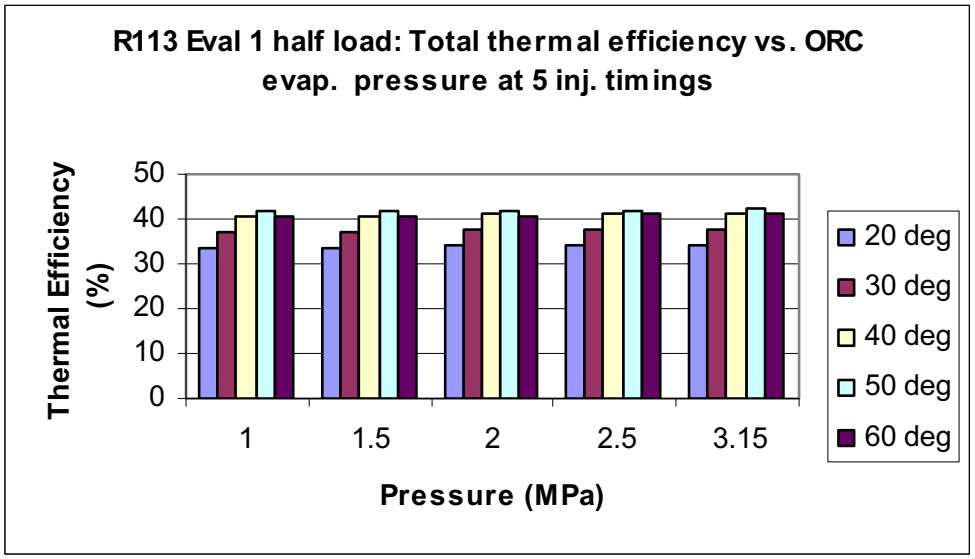


Figure 8 Total 1st law efficiency for R113 at half load versus ORC evaporator pressure and injection timing.



www.manaraa.com

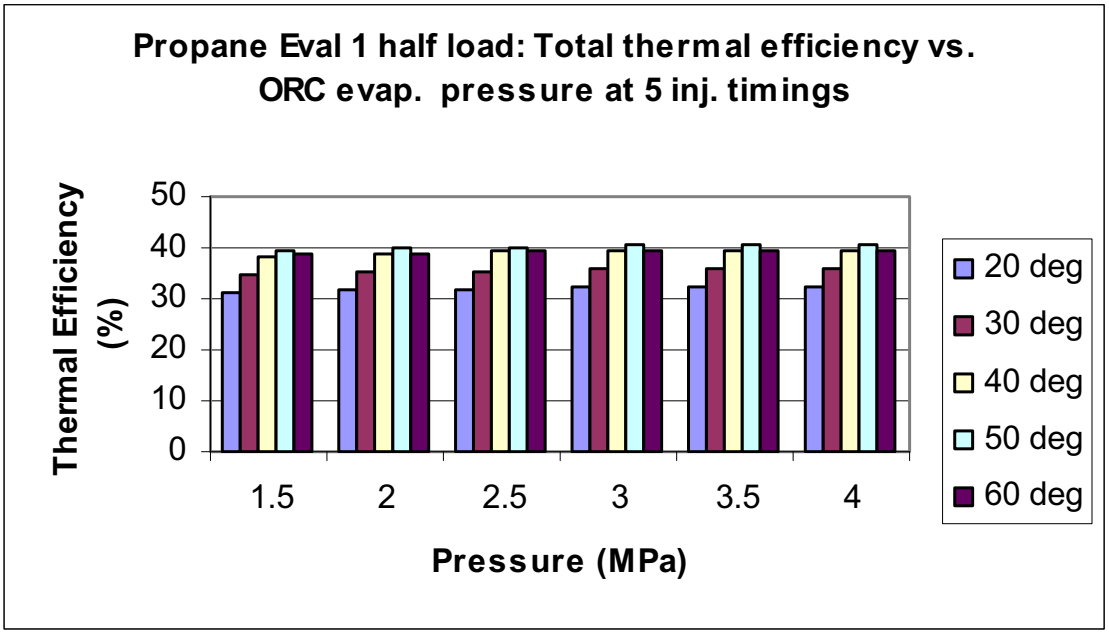


Figure 9 Total 1st law efficiency for propane at half load versus ORC evaporator pressure and injection timing.

At 50 degrees BTDC the thermal efficiency was the highest at all evaporator pressures. At half load with a evaporator pressure of 2.5 MPa and injection timing of 50 degrees BTDC the 1st law efficiencies of R113 and propane are 42% and 40%, respectively. With this particular ORC and engine configuration R113 and propane produced a 14% and 10% increase in 1st law efficiency, respectively. Figures 10 and 11 below show the percent increase in 1st law efficiency versus ORC evaporator pressure and injection timing. Depending on the evaporator pressure and injection timing, R113 is able to produce up 19.5% increase in 1st law efficiency while propane produced a 16.1% increase in 1st law efficiency; however this is at two different operating conditions. As evaporator pressure increases the percent increase in efficiency increases. At 40 degrees BTDC the highest increases in efficiency were seen.



www.manaraa.com

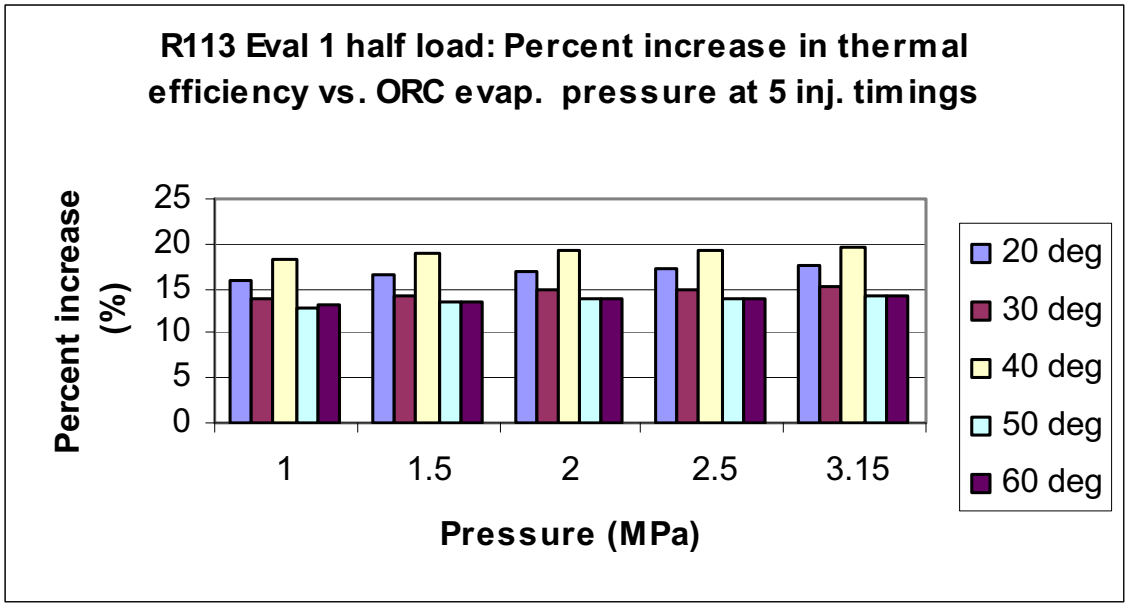


Figure 10 R113 percent increase in 1st law efficiency versus ORC evaporator pressure and injection timing at half load.

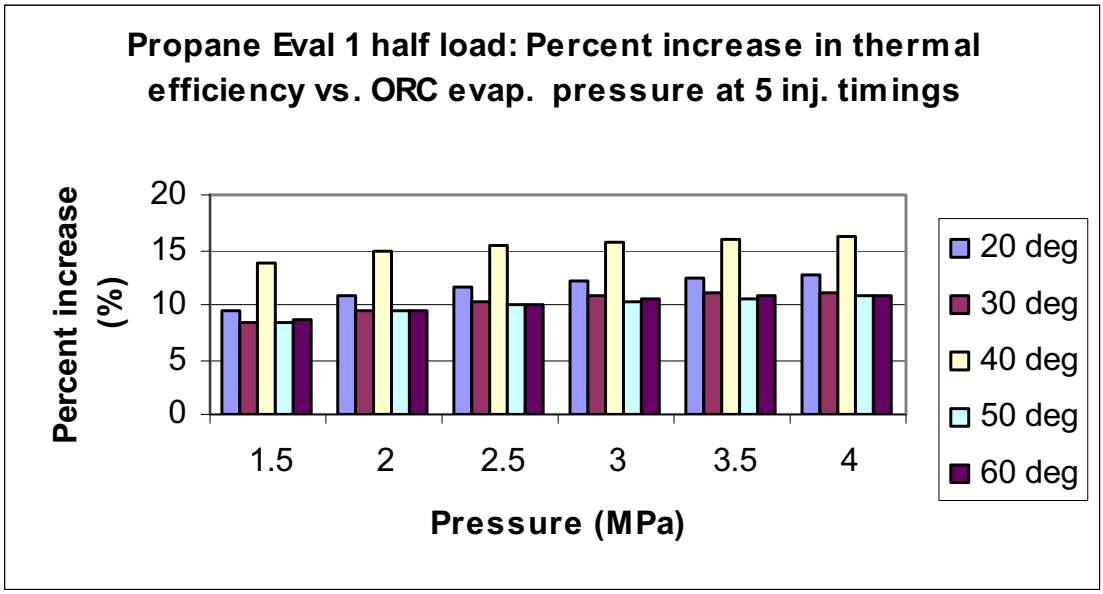


Figure 11 Propane percent increase in 1st law efficiency versus ORC evaporator pressure and injection timing at half load.



www.manaraa.com

At quarter load operation the 1st law efficiencies are slightly lower than half load due to the lower power output of the engine and the lower exhaust temperatures. The small inlet temperature difference between working fluid and the exhaust gas results in poor operation and performance of the evaporator and ORC.

Due to the lower exhaust temperatures of the engine at quarter load the ORC operated at lower evaporator pressures for R113. By reducing the evaporator pressure for the ORC the higher saturation temperatures for R113 were reduced. The evaporator pressures used at quarter load operation for R113 were 1.0, 1.5, and 2.0 MPa. Propane was able to operate normally because its saturation temperatures were much lower. At quarter load operation the engine efficiency ranged from 18% - 21%. Figures 12 and 13 below show the total 1st law efficiency for engine plus the ORC at quarter load operation.

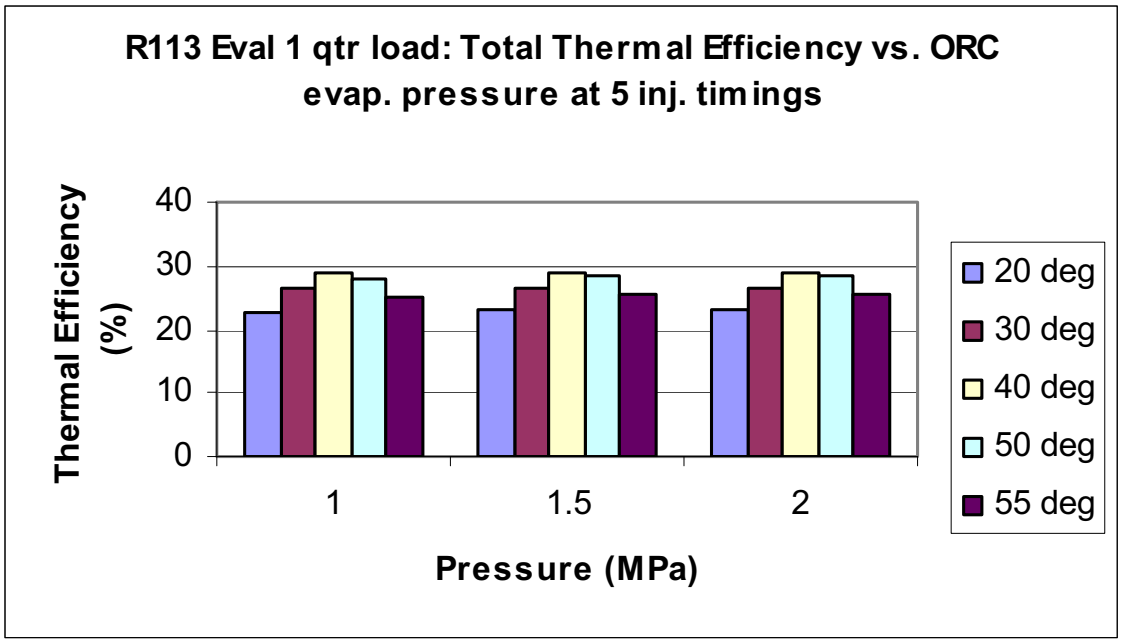


Figure 12 Total 1st law efficiency for R113 at quarter load versus ORC evaporator pressure and injection timing.



www.manaraa.com

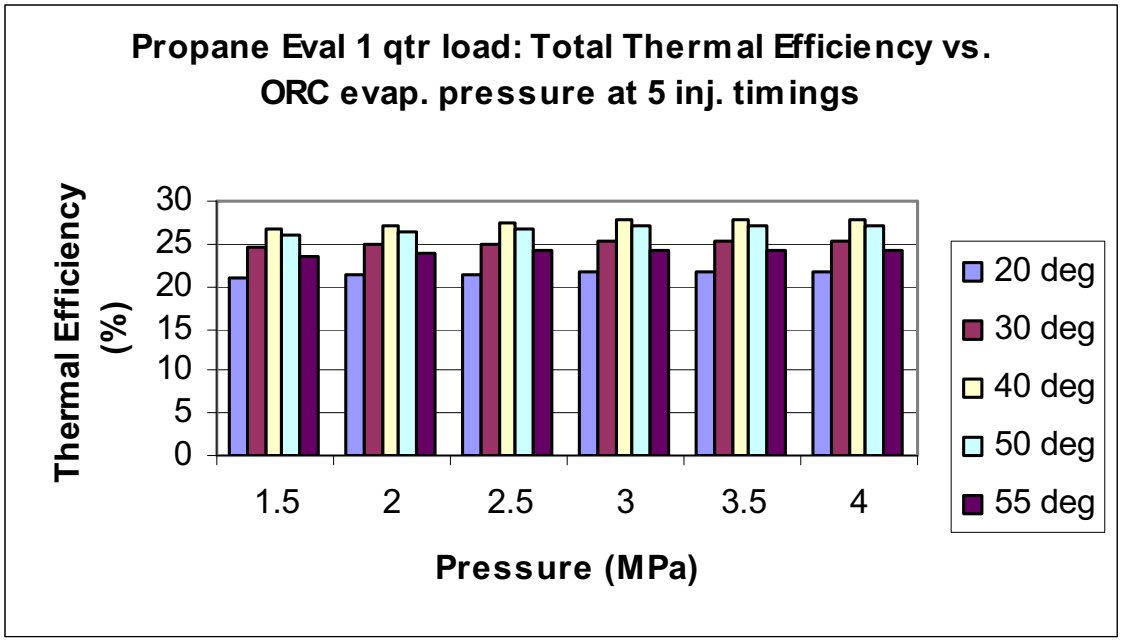


Figure 13 Total 1st law efficiency for propane at quarter load versus ORC evaporator pressure and injection timing.

Once again, it is instructive to note that the common range of ORC evaporator operating pressures for the fluids, R113 and propane, is 1.5 and 2 MPa, respectively. At these pressures, the R113 dry fluid performed much better than propane (average overall efficiencies for all injection timings ranged between 20-25% for propane, whereas the efficiencies ranged between 20 and 30% for R113)

At quarter load operation, an injection timing of 40 degrees BTDC had the highest efficiency for all evaporator pressures compared 50 degrees at half load. At evaporator pressure of 2.0 MPa and an injection timing 40 degrees BTDC the 1st law efficiencies of R113 and propane were 29.2% and 27.2%, respectively. This equates to a 16.5% and 10.5% increase in 1st law efficiency for R113 and propane, respectively. However by varying the conditions of operation R113 yielded an 18.77% increase in efficiency, while



www.manaraa.com

propane produced a 13.9% increase in efficiency. A graphical representation of the percent increase in 1st law efficiency versus evaporator pressure and injection timing is shown below in figures 14 and 15. Once again the increase in evaporator pressure increases the percent increase in efficiency, however for quarter load operation 20 degrees BTDC had the higher increases, compared to 40 degrees at half load.

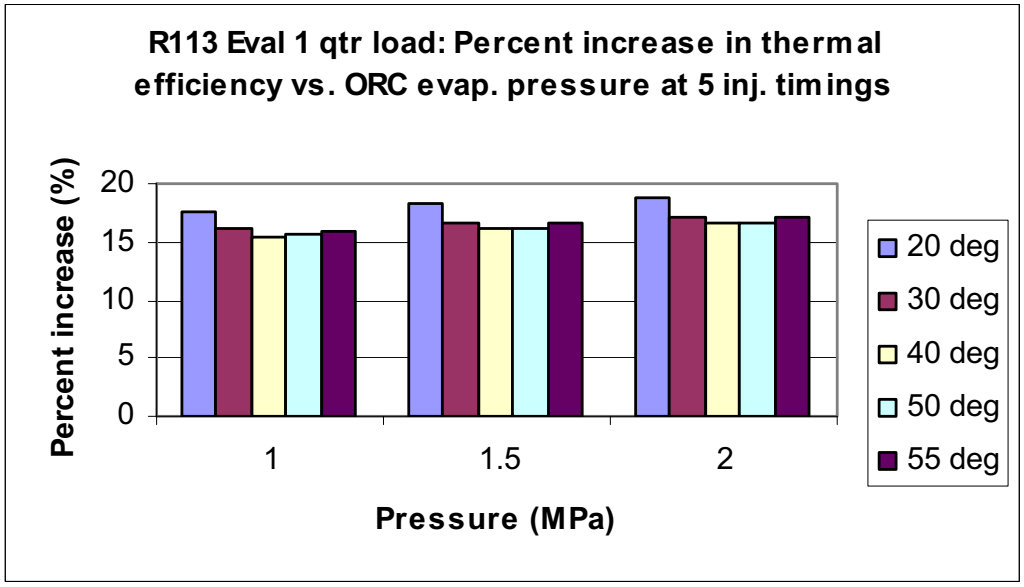


Figure 14 R113 percent increase in 1st law efficiency versus ORC evaporator pressure and injection timing at quarter load.



www.manaraa.com

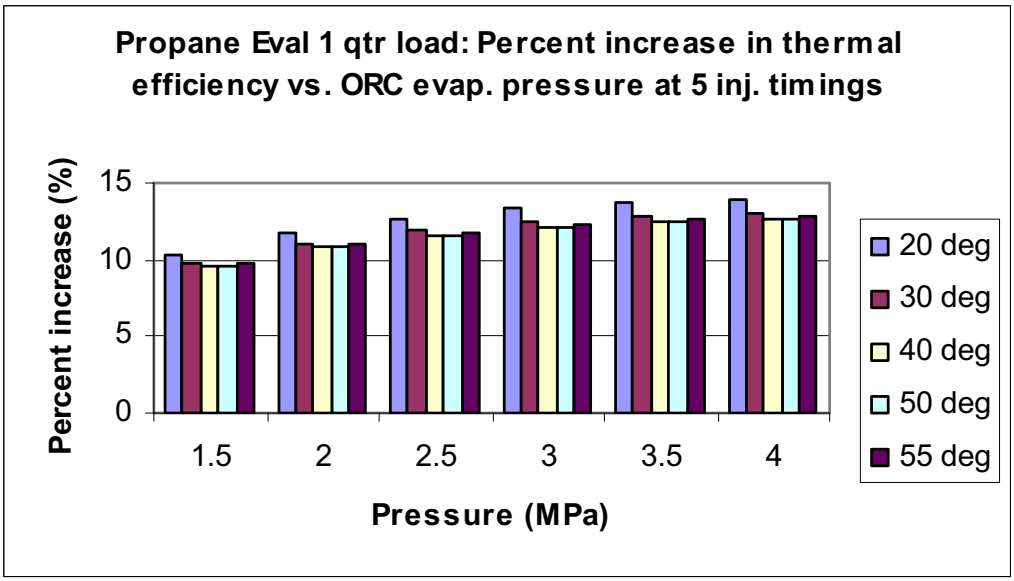


Figure 15 Propane percent increase in 1st law efficiency versus ORC evaporator pressure and injection timing at quarter load.

The 2nd law efficiency, which is defined as the ratio of the actual available work output from the crankshaft to the rate at which chemical exergy is supplied to the engine, can be determined by knowing the chemical exergy of the fuel (in this case diesel and natural gas). The values of chemical exergies were obtained from Table A.23, pp. A 53, Russell & Adebiyi (1993). An interesting observation is that the second and first law efficiencies for the engine are of similar magnitude. For instance, for the engine operating alone at half load the 2nd law efficiency is 26.3% - 33%, and the first law efficiency is 28% - 35%. This is because, the chemical exergy of hydrocarbon fuels are very similar in magnitude to their respective heating values (Russell and Adebiyi, 1993). However, with exhaust WHR using the ORC, the second law efficiencies are expected to be higher. With the aid of the ORC at evaporator pressure of 2.5 MPa and an injection timing of 50 degrees BTDC the 2nd law efficiency was 36.6% for R113, a 7.7% increase,



www.manaraa.com

and 34.9% for propane, a 3.4% increase. It is important to note that the second law efficiencies are low due to the employed design constraint in evaluation 1. By limiting the outlet temperatures for the exhaust gas, the ability to recover waste heat is hindered, however if the outlet temperatures were not limited, condensation would develop in exhaust gas side of the evaporator, which could lead to corrosion and fouling in the long run. Figures 16 and 17 are graphical representations of the 2nd law efficiencies for R113 and propane at half load with respect to engine injection timing and ORC evaporator pressure.

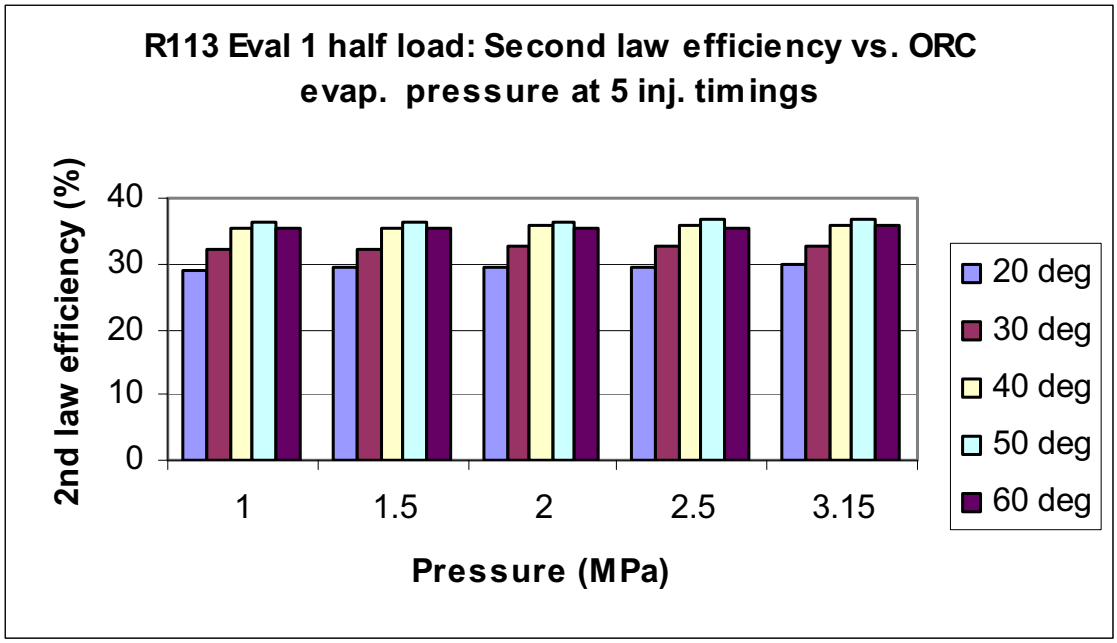


Figure 16 Second law efficiency for R113 at half load versus ORC evaporator pressure and injection timing.



www.manaraa.com

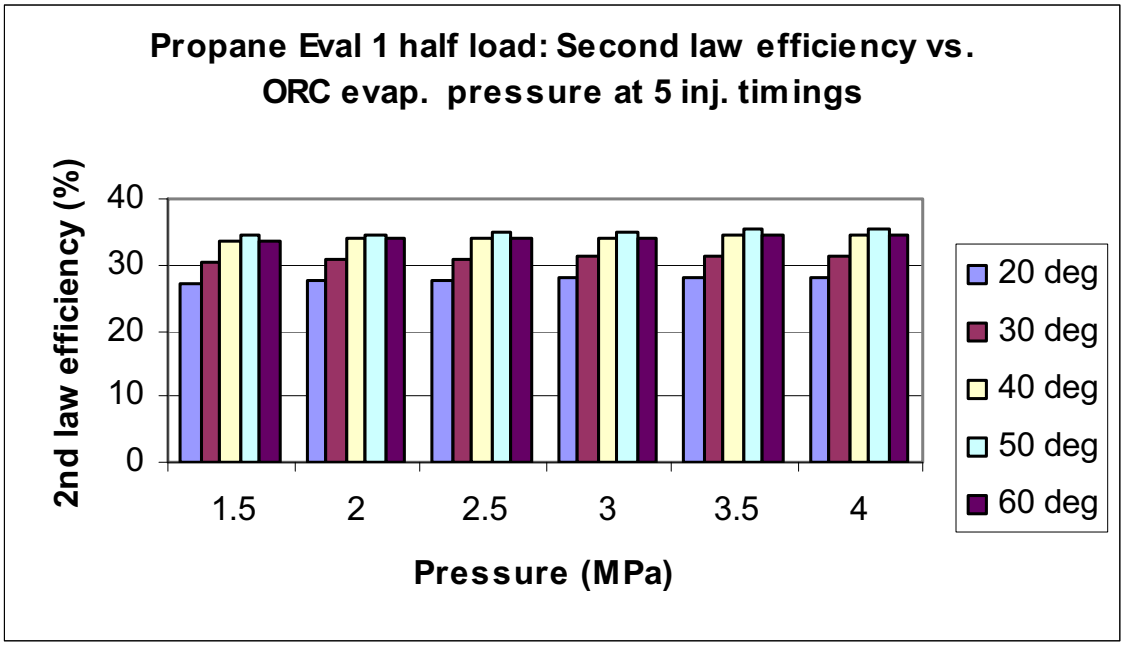


Figure 17 Second law efficiency for propane at half load versus ORC evaporator pressure and injection timing.

Similar to the first law efficiencies, the injection timing of 50 degrees BTDC show the highest 2nd law efficiencies as evaporator pressures increased. By varying operating conditions larger percentage increases in 2nd law efficiencies were obtained. R113 was able to achieve an 11.4% increase in 2nd law efficiency while propane achieved a 6.2% increase. Graphs of the percent increase in 2nd law efficiency with respect to evaporator pressure and injection timing are shown in figures 18 and 19 below. Once again the 20 degrees BTDC show the highest percentage increase in efficiency and increased with respect to evaporator pressure.



www.manaraa.com

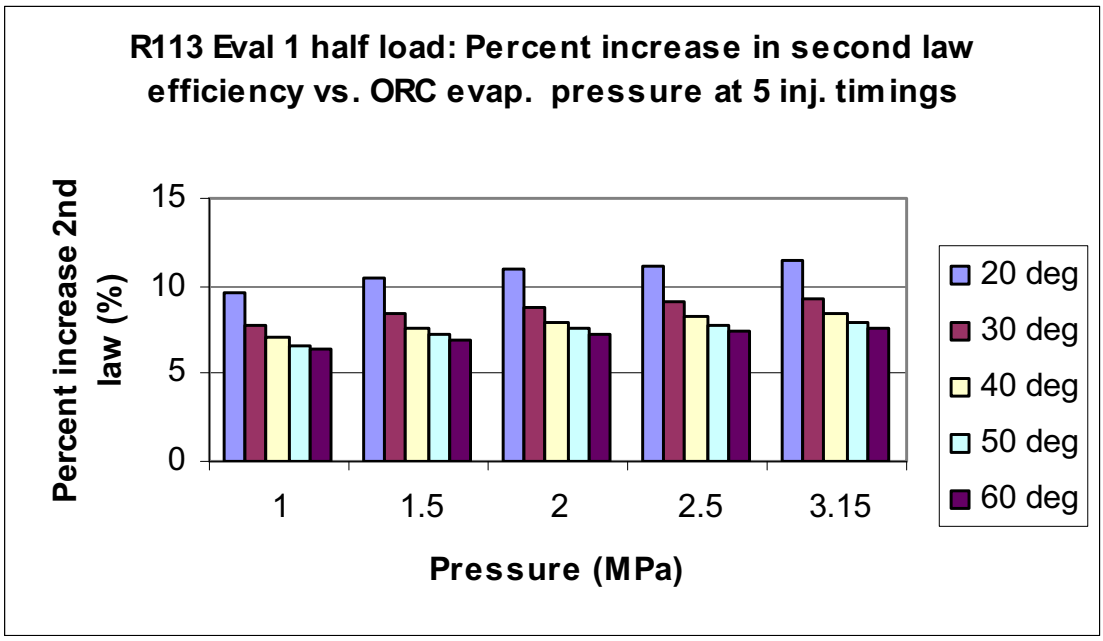


Figure 18 R113 percent increase in 2nd law efficiency versus ORC evaporator pressure and injection timing at half load.

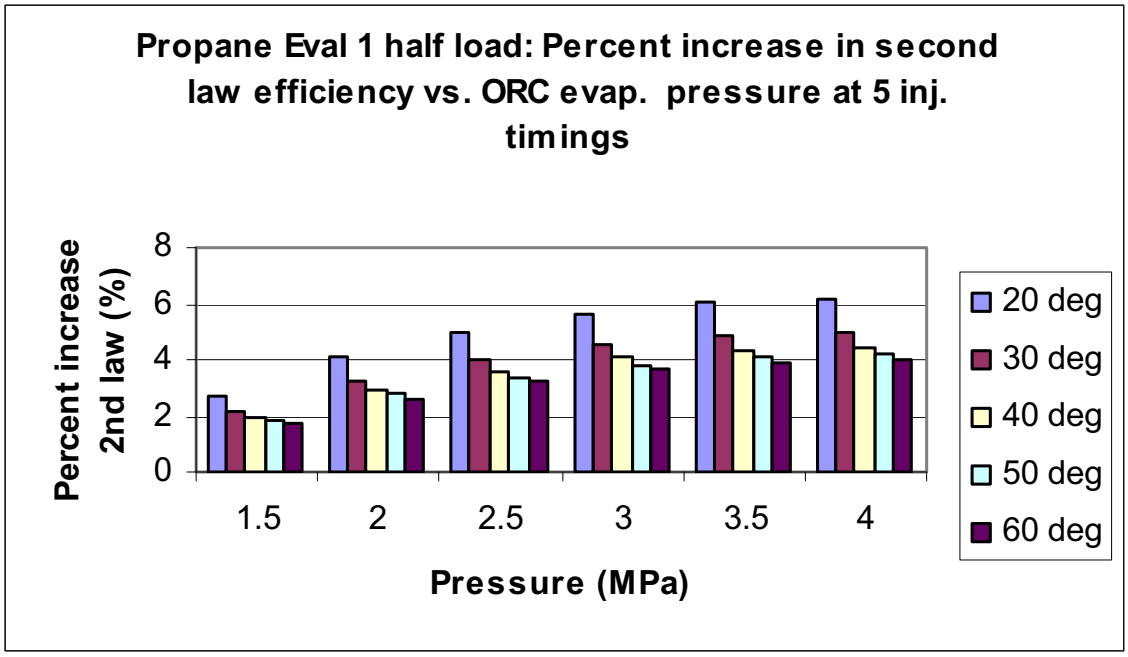


Figure 19 Propane percent increase in 2nd law efficiency versus ORC evaporator pressure and injection timing at half load.



www.manaraa.com

At quarter load operation 2nd law efficiencies followed similar trends to that of 1st law efficiencies. The 2nd law efficiency of the engine was found to be between 17.6% and 19.9%. Once again efficiencies are slightly lower at quarter load for the engine plus ORC than at half load, due to the lower power output and lower exhaust gas temperatures. As mentioned earlier the ORC evaporator pressures for R113 are limited to less than 2.0 MPa for quarter load, due to small inlet temperature difference, i.e. difference between exhaust gas temperature entering the evaporator and saturation temperature of R113 at a given pressure. Figures 20 and 21 below show the 2nd law efficiency for R113 and propane at various evaporator pressures and injection timings.

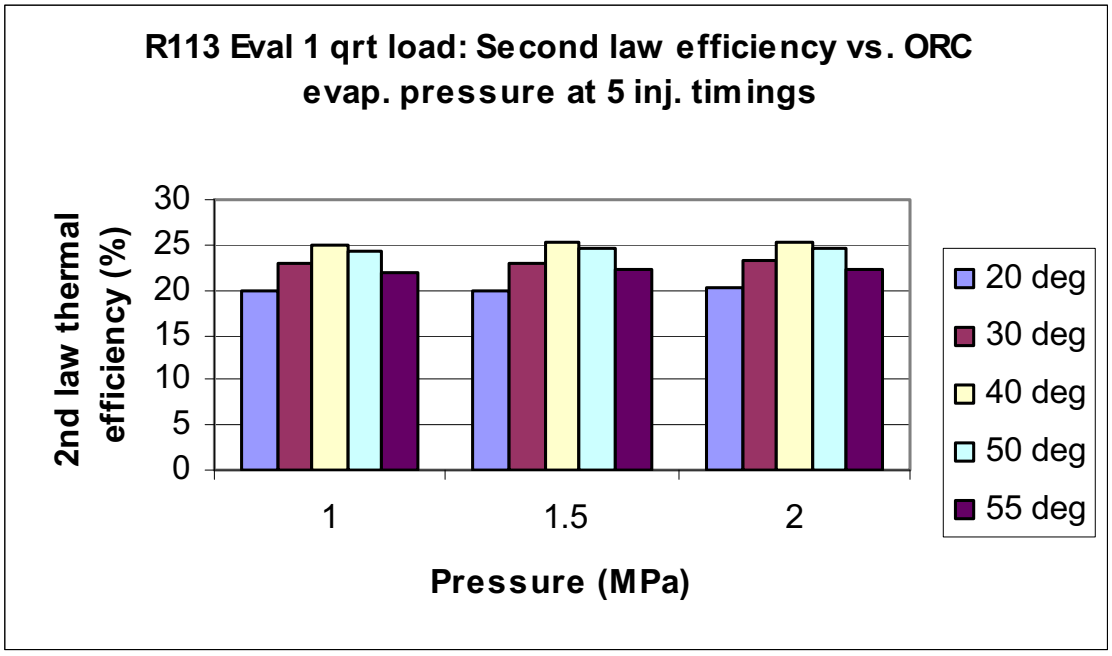


Figure 20 Second law efficiency at quarter load for R113 versus ORC evaporator pressure and injection timing.



www.manaraa.com

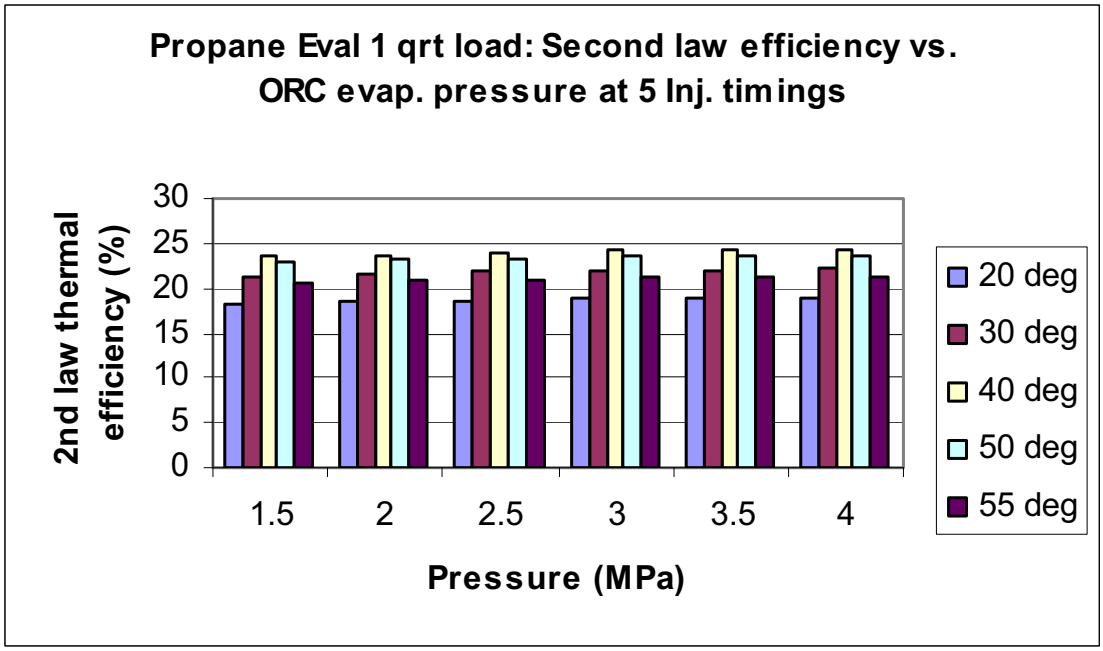


Figure 21 Second law efficiency at quarter load for propane versus ORC evaporator pressure and injection timing.

At 40 degrees BTDC and an evaporator pressure of 2.0 MPa the 2nd law efficiency for R113 is 25.4%, a 9.9% increase, where propane is 23.8%, a 3.7 increase in 2nd law efficiency. A 12.2% increase in 2nd law efficiency was achievable at 20 degrees BTDC and an evaporator pressure of 2.0 MPa for R113. Propane was able to achieve a 7.01% increase in 2nd law efficiency at 20 degrees BTDC and an evaporator pressure of 4.0 MPa. The percent increase in 2nd law efficiency is shown in graphical from in figures 22 and 23. As mentioned earlier, the 2nd law efficiencies are lower than at half load due to the exhaust gas outlet temperatures being limited in the evaporator.



www.manaraa.com

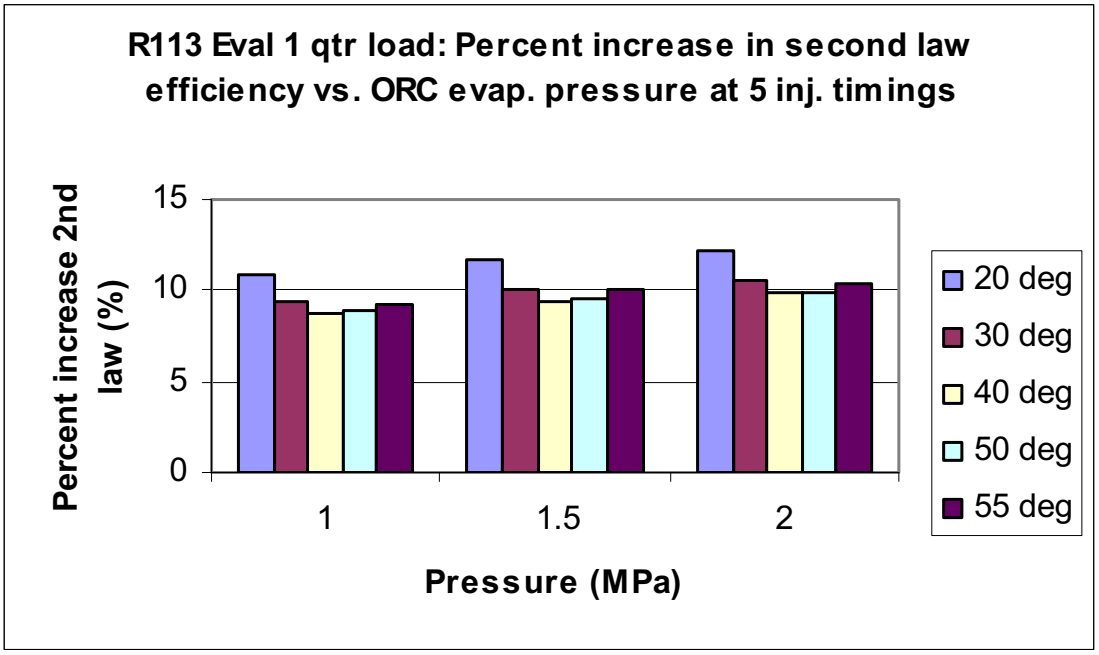


Figure 22 R113 percent increase in 2nd law efficiency at quarter load versus ORC evaporator pressure and injection timing.

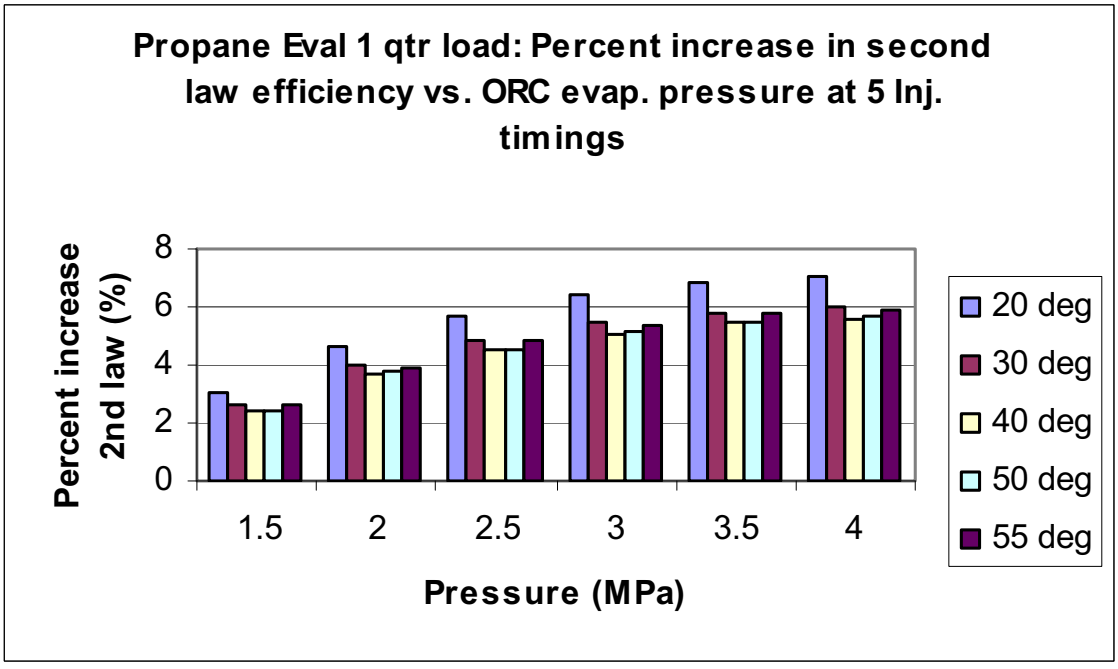


Figure 23 Propane percent increase in 2nd law efficiency at quarter load versus ORC evaporator pressure and injection timing.



www.manaraa.com

In evaluation 2, however, the evaporator operated at higher effectiveness range, 60-80%, compared to evaluation 1 where the evaporator effectiveness ranged from 53-70%. The higher effectiveness allows more waste heat to be recovered due to enhanced heat transfer rates; this also allows greater 2nd law efficiencies. The higher effectiveness also produce lower outlet exhaust gas temperatures and smaller pinch point temperatures, which will be discussed in more detail later. The lower exhaust gas temperatures may produce condensation in the exhaust gas, as discussed earlier, due to being below the saturation temperature of water in the exhaust. The 2nd law efficiencies were calculated in the evaluation 2 and reached as high as 37.8%, a 10.7% increase, for R113 and 35.4%, a 4.8% increase, for propane at 2.5 MPa of evaporator pressure and an engine injection timing of 50 degrees BTDC at half load. At different evaporator pressures and injection timings slightly higher efficiencies were seen, this is shown in figures 24 and 25 below. The figures are the graphs for the 2nd law efficiencies for R113 and propane at half load with respect to ORC evaporator pressure and engine injection timing at 80% effectiveness.



www.manaraa.com

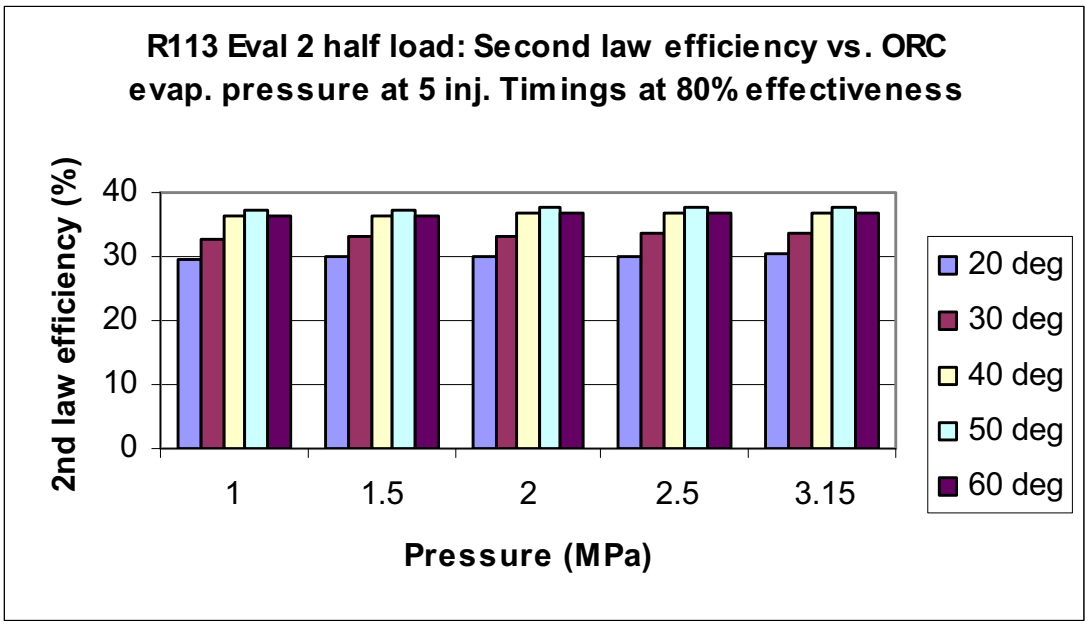


Figure 24 Second law efficiency at half load for R113 versus ORC evaporator pressure and injection timing at 80% effectiveness.

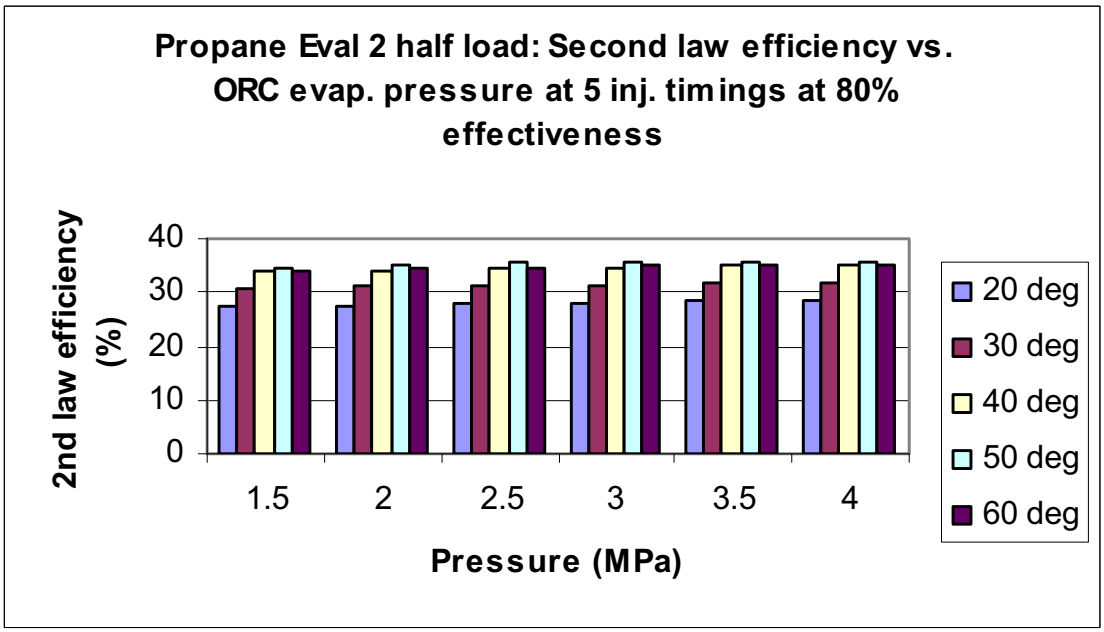


Figure 25 Second law efficiency at half load for propane versus ORC evaporator pressure and injection timing at 80% effectiveness.



www.manaraa.com

It is important to note that in evaluation 1 the effectiveness for the evaporated ranged from 53% to 70%. By comparing the results from evaluation 1 to evaluation 2 at load with an effectiveness of 60%, it can be seen that the results are very similar, thus validating both methods. The second law efficiencies for evaluations 1 and 2 (at 60% effectiveness for R113 at half load) are shown in figure 26 below.

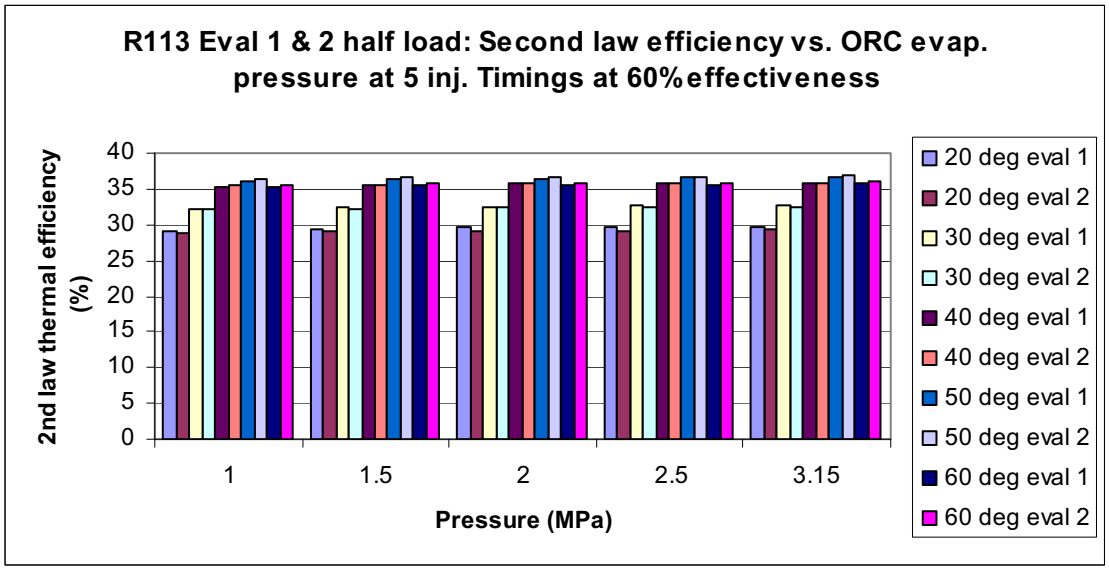


Figure 26 R113 evaluations 1 & 2 second law efficiency comparison at half load

As mentioned earlier percent increase in 2nd law efficiency also increased marginally for 80% effectiveness at half load for R113 and propane. R113 was able to achieve a 12.9% increase in 2nd law efficiency at a evaporator pressure of 3.15 MPa and an engine injection timing of 20 degrees BTDC, while propane achieved a 7.1% increase at a evaporator pressure of 4.0 MPa and an engine injection timing of 20 degrees BTDC. Graphs of the percent increase in 2nd law efficiency for 80% effectiveness at half load with respect to evaporator pressure and engine injection timing are shown in figures 27 and 28.



www.manaraa.com

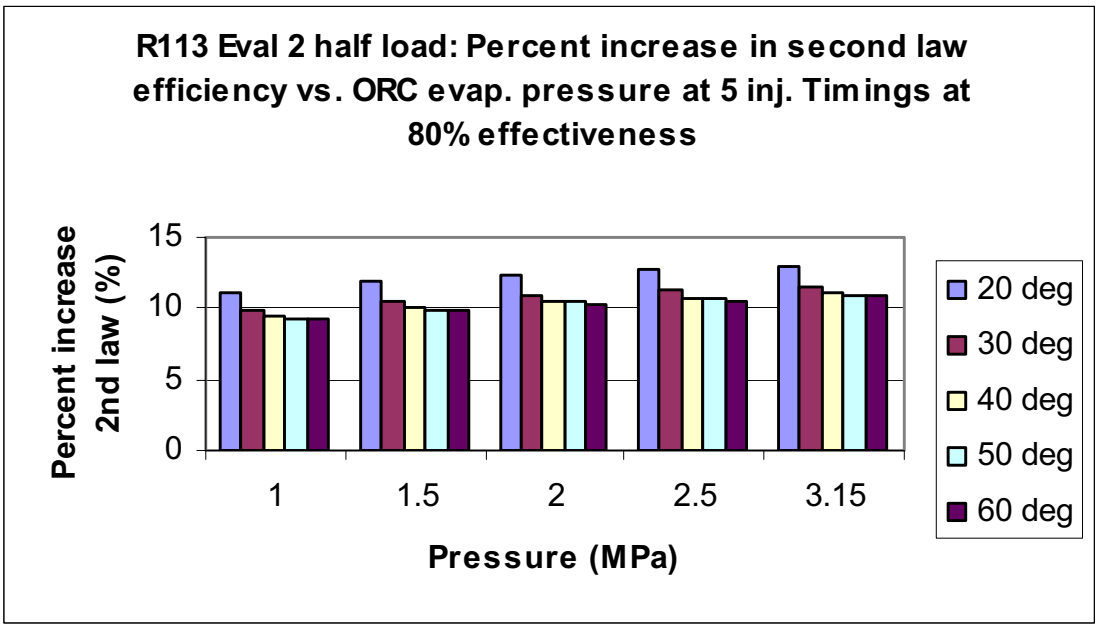


Figure 27 R113 percent increase in 2nd law efficiency at half load versus ORC evaporator pressure and injection timing at 80% effectiveness.

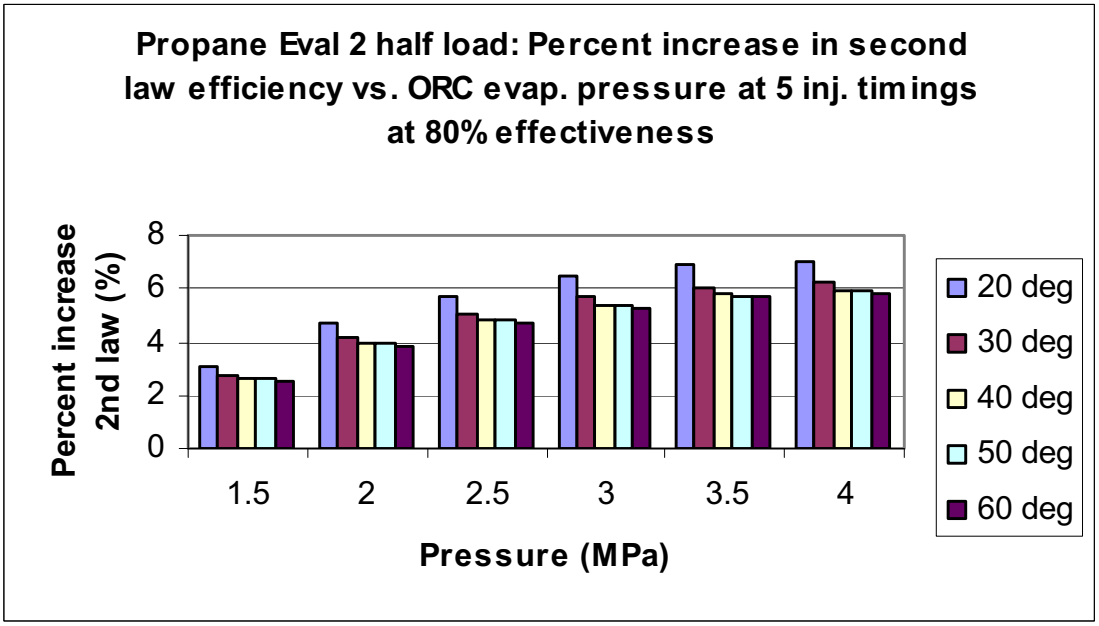


Figure 28 Propane percent increase in 2nd law efficiency at half load versus ORC evaporator pressure and injection timing at 80% effectiveness.



www.manaraa.com

For quarter load operation similar results were found for the 2nd law efficiencies at 80% effectiveness. At evaporator pressure of 2.0 MPa and an engine injection timing of 40 degrees BTDC the 2nd law efficiencies were 26.4% for R113, a 13.4% increase, and 24.1% for propane, a 5.1% increase. Figures 29 and 30 show graphs of the 2nd efficiencies at quarter load with 80% effectiveness with respect to engine injection timing and ORC evaporator pressure, while figures 31 and 32 show the percent increases in 2nd law efficiencies. Once again the evaporator pressures for R113 were reduced to small inlet temperature difference at quarter load operation.

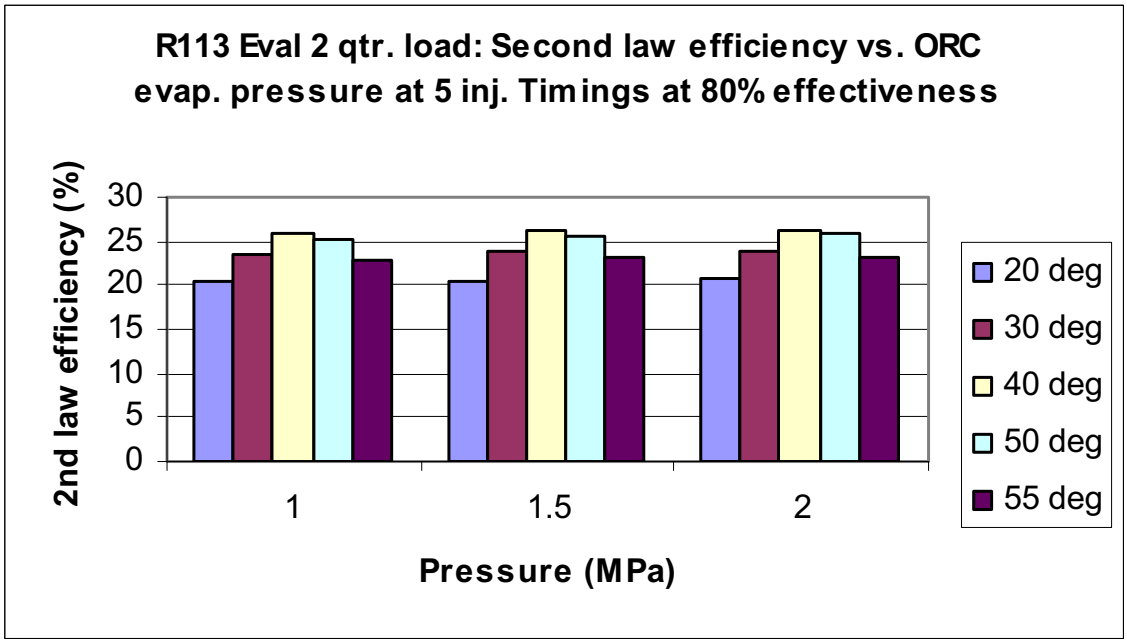


Figure 29 Second law efficiency at quarter load for R113 versus ORC evaporator pressure and injection timing at 80% effectiveness.



www.manaraa.com

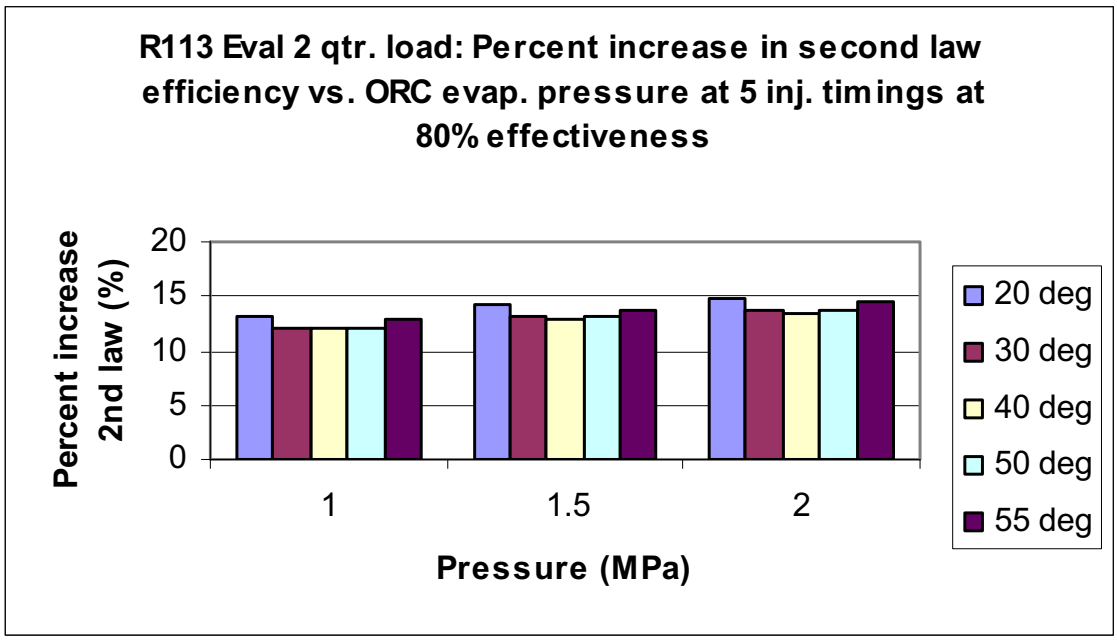


Figure 30 R113 percent increase in 2nd law efficiency at quarter load versus ORC evaporator pressure and injection timing at 80% effectiveness.

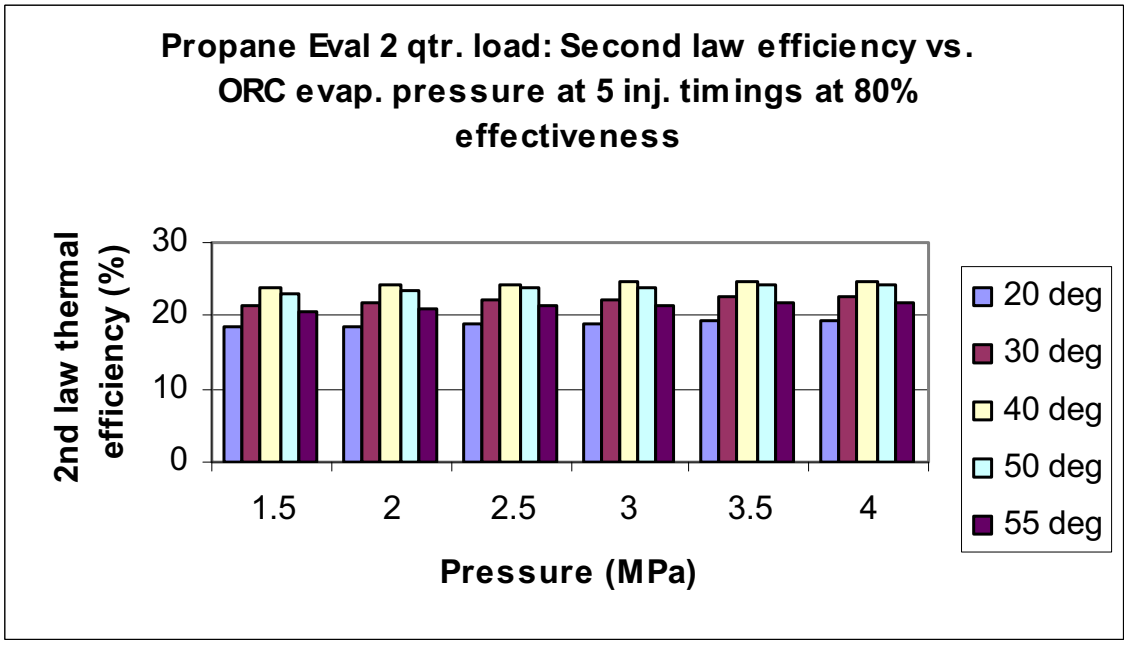


Figure 31 Second law efficiency at quarter load for propane versus ORC evaporator pressure and injection timing at 80% effectiveness.



www.manaraa.com

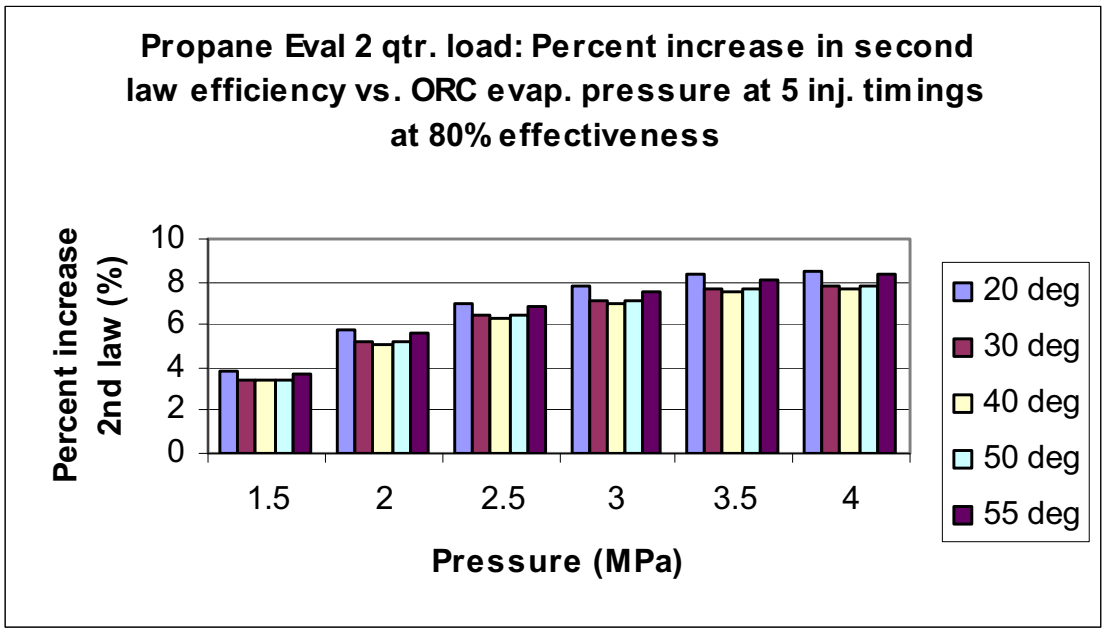


Figure 32 Propane percent increase in 2nd law efficiency at quarter load versus ORC evaporator pressure and injection timing at 80% effectiveness.

The increases in 1st and 2nd law efficiencies are due to the additional work done by the turbine in the ORC. The calculation for efficiency, as shown earlier in the Methodology (Chapter 3), is dependent on the work done by the system and the amount of fuel used. By increasing the amount of work done by the system without additional fuel the efficiency can be increased. Since no additional fuel is required to operate the ORC, the additional work of the ORC is considered "free". At half load the engine operated at 21 kW (28 hp) and at quarter load 10.5 kW (14 hp), depending on the working fluid and operating conditions, of the engine and the ORC, the ORC was able to add between 0.281kW (0.377 hp) to 3.12 kW (4.2 hp).

Evaluation 2 was a fundamental heat transfer approach to the analysis. The effectiveness was varied in order to examine the effect of the pinch point on the evaporator and the entire cycle as well. This calculation was completed only for R113, in



www.manaraa.com

order to analyze the effects of a dry fluid. The pinch point is minimum temperature difference between the two fluids in a heat exchanger; refer to figure 5 in the Methodology (Chapter 3). The smaller pinch point temperature difference results in a higher effectiveness, higher cycle efficiencies and lower heat transfer irreversibilities, however this also increases the cost of operation due to larger and hence more expensive heat exchangers and turbines. Larger pinch point temperature differences have the opposite effect, therefore there will be larger temperature differences, a lower effectiveness, lower cycle efficiencies, and larger irreversibilities, however equipment and operation will be less costly because the size of the heat exchanger is smaller, El-Wakil (2002). Therefore pinch point optimization takes in to account performance, sizing, and cost characteristics.

At half load and 80% effectiveness with an injection timing of 50 degrees BTDC and an evaporator pressure of 2.5 MPa, R113 had a pinch point temperature difference of 18.2 degrees. However at 60% effectiveness with same conditions the pinch point temperature difference was 30.9 degrees for R113. The following are graphs of the pinch point temperature difference with respect to evaporator pressure and injection timing at 80% and 60% effectiveness for R113 at half load, shown in figures 33 and 34.



www.manaraa.com

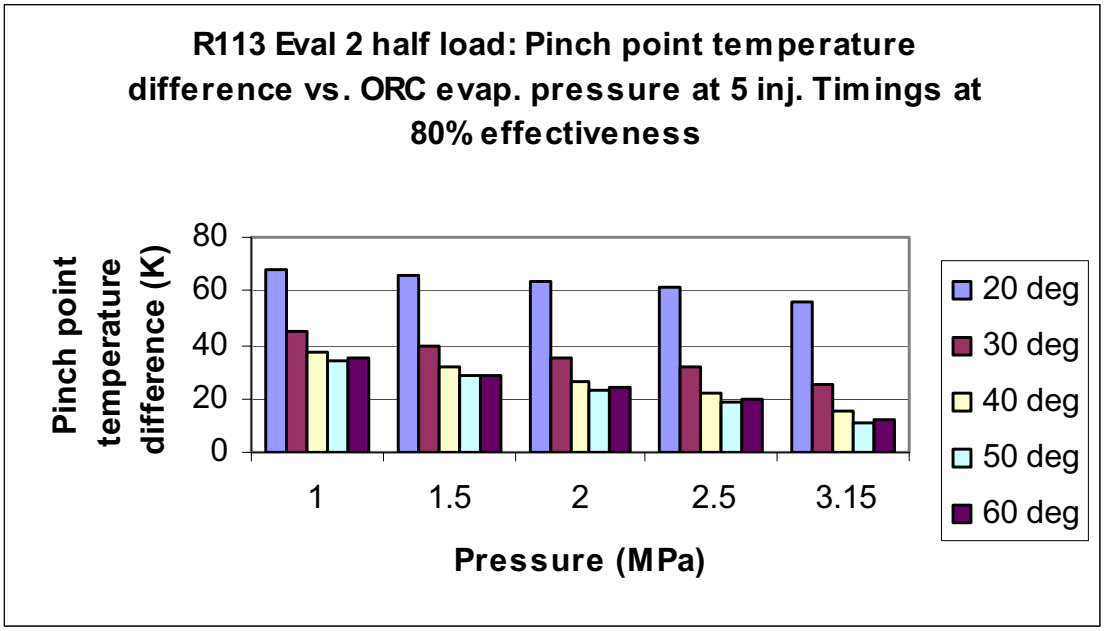


Figure 33 R113 pinch point temperature difference at 80% effectiveness versus ORC evaporator pressure and injection timing at half load.

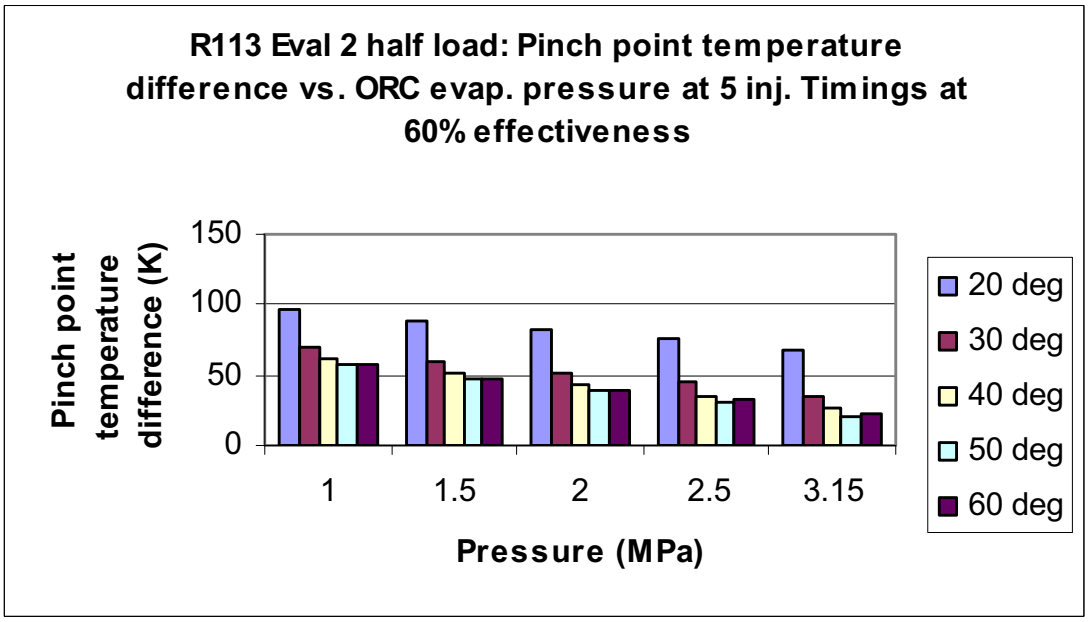


Figure 34 R113 pinch point temperature difference at 60% effectiveness versus ORC evaporator pressure and injection timing at half load.



www.manaraa.com

At quarter load operation the pinch point temperature differences follow similar trends compared to half load. In some instances the pinch point temperature differences were very small. For example, at an injection timing of 40 degrees BTDC and a evaporator pressure of 2.0 MPa, the pinch point difference for R113 was 1.9 degrees. At 60% effectiveness the pinch point temperature differences were still small with 15.4 degrees for similar conditions. The smaller pinch point temperature differences are due the lower exhaust temperatures of the engine while operating at quarter load. Graphs for the pinch point temperature difference at quarter load operation for R113 at 60 and 80% effectiveness are shown in figures 35 and 36 below.

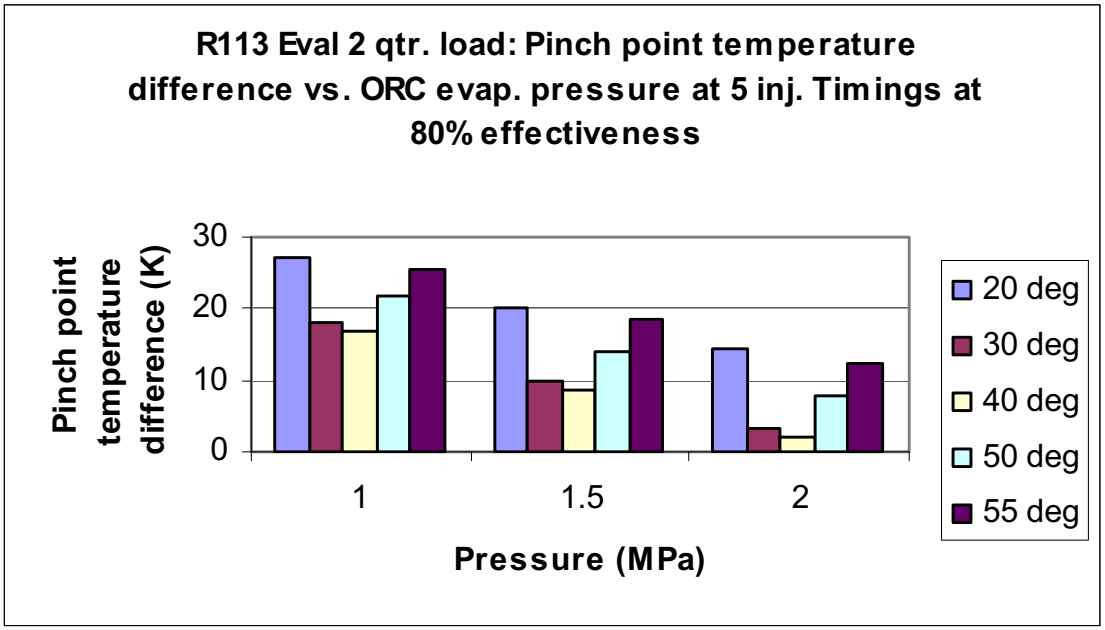


Figure 35 R113 pinch point temperature difference at 80% effectiveness versus ORC evaporator pressure and injection timing at quarter load.



www.manaraa.com

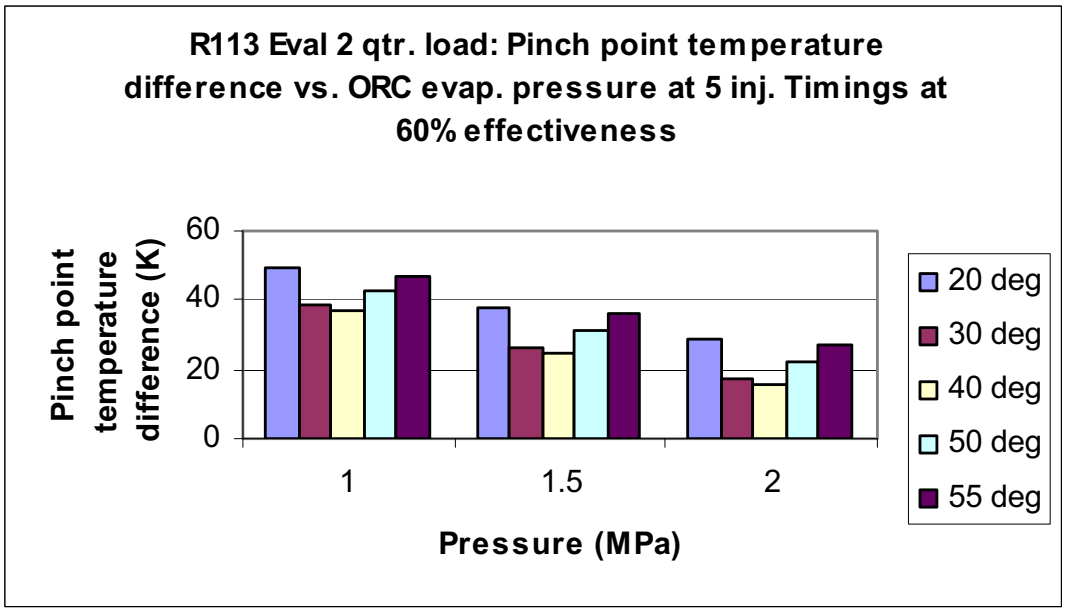


Figure 36 R113 pinch point temperature difference at 60% effectiveness versus ORC evaporator pressure and injection timing at quarter load.

The pinch point temperature difference decreases as the evaporator pressure increases. This is also true for 1st and 2nd law efficiencies. Therefore it can be determined that as the evaporator pressure increases, the pinch point temperatures decrease, therefore increasing 2nd law efficiencies. This is shown graphically half and quarter load at 80% effectiveness in figures 37and 38 below. In figures 37 and 38 the second law efficiencies decrease as the pinch point temperatures decrease. This is evidence that with a smaller pinch point temperature difference the irreversibilities decrease.



www.manaraa.com

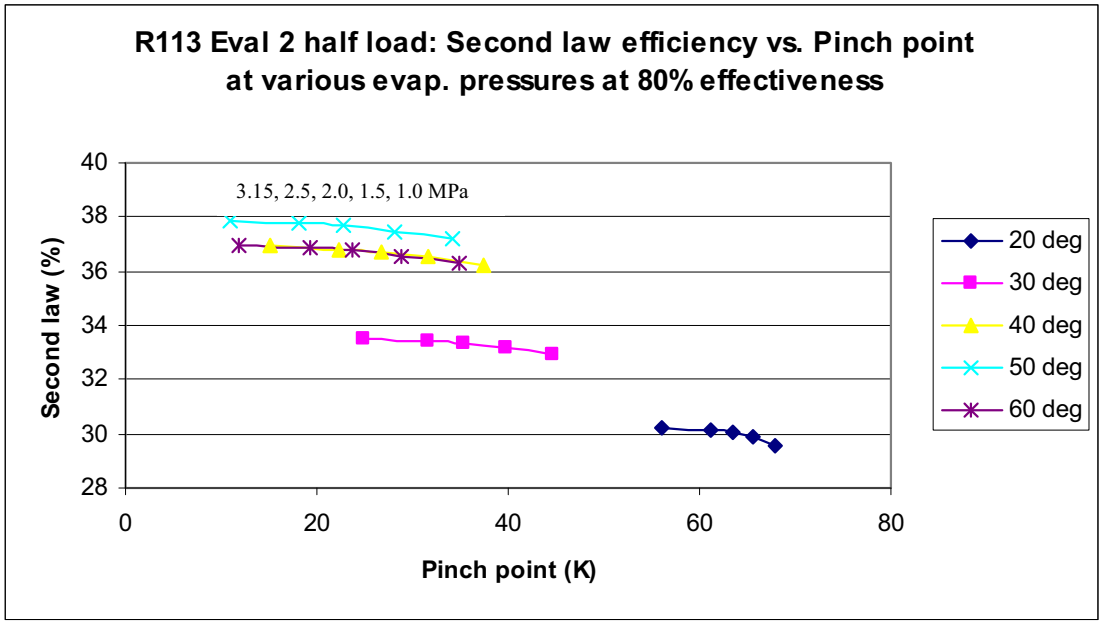


Figure 37 Second law efficiency versus pinch point temperature difference at various evaporator pressures at 80 % effectiveness for R113 at half load.

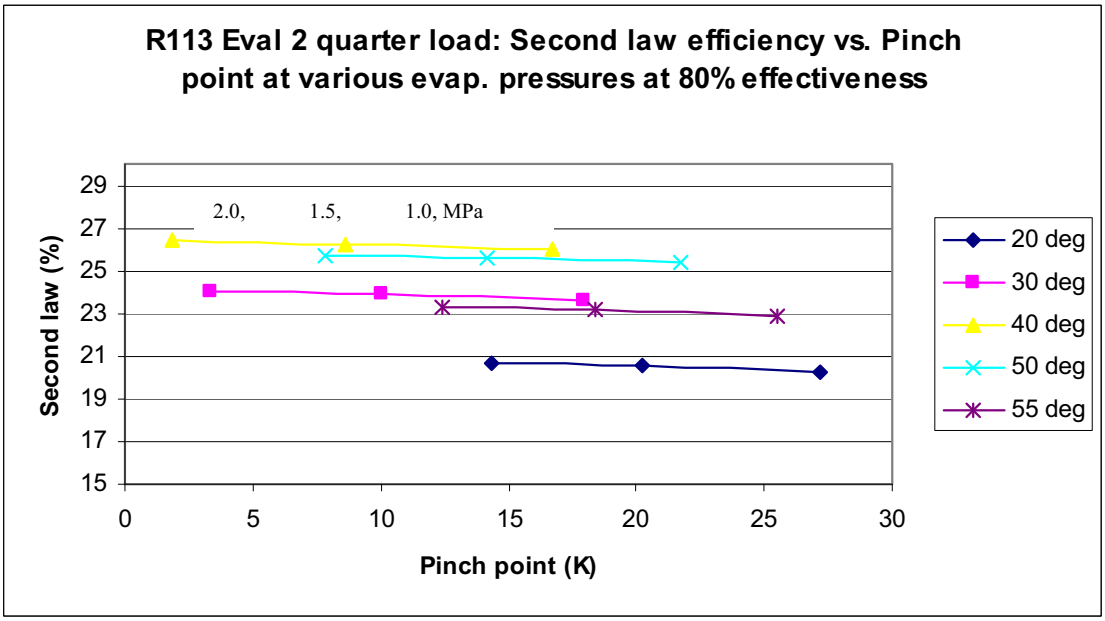


Figure 38 Second law efficiency versus pinch point temperature difference at various evaporator pressures at 80 % effectiveness for R113 at quarter load.



www.manaraa.com

# CHAPTER 5

# CONCLUSIONS

Recent emissions and security debates have spurred extensive research in alternative fuels and renewable energies. This situation has also created ample demand for waste heat recovery techniques for internal combustion engines in order to increase their efficiency and fuel economy while reducing brake specific emissions. Due to the fact that 1/3$^{rd}$ of the chemical exergy of the fuel is wasted through the exhaust, WHR techniques are of the utmost importance. Organic rankine cycles with turbocompounding are an effective method of harnessing the rejected energy in the exhaust gas to produce useful work and increase efficiency.

For this analysis a mathematical model was developed to analyze and compare the efficiency benefits of using Organic Rankine Cycles (ORCs) powered by R113, a dry fluid, and propane, a wet fluid, to recover waste heat from the exhaust of a pilot ignited natural gas engine. The pilot ignited natural gas engine employed very small diesel pilot sprays to compression-ignite a premixed mixture of natural gas and air (Srinivasan et al., 2008). The injection timing of the pilot diesel sprays were varied from 20 degrees to 60 degrees BTDC, while the engine was operated at two different power ranges, 21 kW of half load and 10.5 kW of quarter load. Organic fluids, such as R113 and propane, are used due to their low critical points, crucial for low temperature applications, technical feasibility, and safety characteristics. The model was developed from both a practical



www.manaraa.com

and a design approach. In evaluation 1, the outlet temperatures of the exhaust gas for the evaporator were limited to slightly above the saturation temperature of water in the exhaust in order to prevent condensation which promotes fouling and corrosion. In evaluation 2, the effect of pinch point was analyzed on the evaporator and the entire cycle. The pinch point was varied through the effectiveness of the evaporator.

First and second law efficiencies were increased using the ORC with both R113 and propane. The increases in 1$^{st}$ law efficiencies ranged from 13% – 22% for R113 and 9% – 17.4% for propane depending on operating conditions of the ORC evaporator and the engine injection timings (that were varied from 20 degrees BTDC to 60 degrees BTDC). The increases in 2$^{nd}$ law efficiencies ranged from 6 % – 14.7% for R113 and 2% – 8.5% for propane depending on operating conditions. Efficiencies were higher with R113 due to the higher boiling point. Trends in the data showed that the efficiencies increased with ORC evaporator pressure due the higher saturation temperature at higher pressures. This point was found to be true in literature as well. Mago et al. (2007) found that for fluids with higher boiling points (saturation temperatures) there were higher cycle efficiencies. Drescher et al. (2007) reported that higher maximum process temperatures generally lead higher efficiencies between fluids, correlating to higher vaporization temperatures. Finally, Hung et al. (1997) stated that system efficiency increased as system pressure increased. Mago et al. (2007) mentioned, however, superheating fluids typically increased irreversibilities and therefore should be operated at their saturated conditions.

Trends were also seen with regards to engine injection timing. Engine injection timings of 50 degrees and 40 degrees BTDC showed the highest efficiencies for half load



www.manaraa.com

and quarter load, respectively, while injection timings of 20 degrees BTDC showed the highest percentage increases in efficiencies. Varying the effectiveness of the evaporator varied the pinch point temperature difference in the analysis. The pinch point showed an inverse relationship with both 1st and 2nd law efficiencies for R113. As the pinch point temperature difference decreased both the 1st and 2nd law efficiencies increased. Therefore it is verified that by decreasing the pinch point temperature difference the irreversibilities are also decreased. However, it is important to note that smaller pinch point temperature differences result in costly capital and operational expenditures primarily due to the requirement of larger heat exchangers. Therefore, the pinch point temperature difference must be optimized on a cost and performance basis.

Propane showed lower increases in efficiencies due to propane's critical points being lower than that of R113. However, propane is a wet fluid and typically needs to be superheated in order to achieve similar results to that of a dry fluid. Propane was chosen in this analysis regardless of its results, since it may be used as the working fluid for the ORC and the fuel for the ICE. By using one fluid for both it would simplify packaging and the need or additional components.

Future work will involve creating additional models exploring a variety of working fluids, examining fluids in their superheated range and closer to their critical points, especially, wet fluids, as well as exploring other Waste Heat Recovery (WHR) techniques for comparison purpose. In conjunction with mathematical models, the implementation of ORC for use in experimental settings could be used to verify and validate results seen in modeling and simulation.



www.manaraa.com

ORC with turbocompounding is a viable alternative to increasing efficiency for ICE. By harnessing the waste heat of the engine, the additional work of the ORC consumes no extra fuel, thereby directly increasing efficiency. This application could be applied to stationary power generation applications such as Combined Heating and Power (CHP). If packaging was designed properly the application could be used in the automotive industry to increase fuel economy and reduce emissions. Many automakers are exploring techniques such as engine downsizing as ways to fuel economy and reduce emissions. By using a smaller engine, say in-line 4 instead of a V6, and then using a turbocharger, the vehicles fuel consumption would be reduced while still maintaining sufficient power through the turbocharger. ORC with turbocompounding could be used in a similar manner, since more room will be created in the engine compartment with a smaller motor. Research is being conducted for the use of organic fluids to be used as the engine coolant for ICE. This process will capture waste heat from the cylinder walls and preheat the working fluid before it is sent to the evaporator where it is superheated. By using one fluid for the engine cooling purposes and waste heat recovery, packing designs are simplified. Recovering heat from the cylinder walls and the exhaust gas will increase 2$^{nd}$ law efficiencies and decrease irreversibilities, Arias et al. (2006).



www.manaraa.com

BIBLIOGRAPHY

Aceves, S. M., Martinez-Frias, J., & Reistad, G. M. (2006). Analysis of Homogeneous Charge Compression Ignition (HCCI) Engines for Cogeneration Applications. *ASME Journal of Energy Resource Technology*, *128*, 16-36.

Angelino, G., Invernizzi, C., & Molteni, G. (1999). The potential role of organic bottoming Rankine cycles in steam power stations. *Proceedings of the Institution of Mechanical Engineers*, *214*(Part A), 75-81.

Annual Energy Review (AER) 2007. (2008, June 23).*Energy Information Administration*. Retrieved from http://www.eia.doe.gov/aer/.

Arias, D., Shedd, T., & Jester, R. (2006). Theoretical Analysis of Waste Heat Recovery from an Internal Combustion Engine in a Hybrid Vehicle. *SAE Technical Paper Series*, SAE Technical Paper Series.

Brands, M. C., Werner, J. R., Hoehne, J. L., & Kramers, S. (1981). Vehicle Testing of Cummins Turbocompounded Diesel Engine. *SAE Technical Paper Series*.

Caton, J. A. (2000). On the Destruction of Availability (exergy) Due to Combustion Processes - With Specific Application to Internal Combustion Engines. *Energy*, *25*, 1097-1117.

Cerri, G. (1983). Regenerative Supercharging for Four Stroke Internal Combustion Engines. *SAE Technical Paper Series*, SAE Technical Paper Series.

Chakravarthy, V., Draw, C., Graves, R., Druecke, B., Foster, D., & Klein, S. (2006). Second Law Comparisons of Volumetric and Flame Combustion in an Ideal Engine with Exhaust Heat Recovery.

Chen, S., & Lin, R. (1983). A Review of Engine Advance Cycle and Rankine Bottoming Cycle and Their Loss Evaluation. , SAE Technical Paper Series., 51-82.

DiBella, F. A., DiNanno, L. R., & Koplow, M. D. (1983). Laboratory and On-Highway Testing of Diesel Organic Rankine Compound Long-Haul Vehicle Engine. *SAE Technical Paper Series*.



www.manaraa.com

Drescher, U., & Bruggemann, D. (2007). Fluid selection for the Organic Rankine Cycle (ORC) in biomass power and heat plants. *Applied Thermal Engineering*, *27*, 223-228.

Dunbar, W. R., & Lior, N. Sources of Combustion Irreversibility. *Combustion Science and Technology*, *41*, 41-61.

El-Wakil, M. (2002). *Powerplant Technology* (pp. 30-46). New York: McGraw-Hill Science, Engineering & Mathematics.

Ferguson, C., & Kirkpatrick, A. (2001). *Internal Combustion Engines: Applied Thermosciences* (Second., pp. 259-264). New York: John Wiley & Sons, Inc.

Foster, D. E., & Myers, P. S. (1982). Heavy-Duty Diesel Fuel Economy. *Mechanical Engineering* , *104*(12), 50-55.

Hung, T. C., Shai, T. Y., & Wang, S. K. (1997). A Review of Organic Rankine Cycles (ORCs) for the Recovery of Low-Grade Waste Heat. *Energy*, *22*(7), 661-667.

Krishnan, S. R., Srinivasan, K. K., Singh, S., Midkiff, K. C., Bell, S. R., Gong, W., et al. (2004). Strategies for Reduced $NO_x$ Emissions in Pilot-Ignited Natural Gas Engines. *ASME Journal Eng. Gas Turbines Power*, *126*(3), 665-671.

Lee, M. J., Tien, D. L., & Shao, C. T. (1993). Thermophysical Capability of Ozone Safe Working Fluids for an Organic Rankine-Cycle System. *Heat Recovery System CHP*, *13*, 409-418.

Leising. Using Waste Heat Boots Diesel Efficiency. *SAE Technical Paper Series*.

Mago, P. J., Chamra, L. M., & Somayaji, C. (2007). Performance analysis of different working fluids for use in organic Rankine cycles. *Proceedings of the Institution of Mechanical Engineers*, *221*(Part A), 255-264.

Maizza, V., & Maizza, A. (2001). Unconventional Working Fluids in Organic Rankine-Cycles for Waste Heat Recovery Systems. *Applied Thermal Engineering*, *21*(3), 225-263.

Russell, L. D., & Adebiyi, G. A. (1993). *Classical Thermodynamics* (p. A53). Fort Worth, TX: Saunders College.

Sonntag, R. E., Borgnakke, C., & Wylen, G. J. (2002). *Fundamentals of Thermodynamics* (6th ed.). New York: Wiley.



www.manaraa.com

Srinivasan, K., Mago, P., Zdaniuk, G., & Chamra, L. (2008). Improving the Efficiency of the Advanced Injection Low Pilot Ignited Natural Gas Engine Using Organic Rankine Cycle. *Journal of Energy Resources Technology*, *130*.

Srinivasan, K. (2006, February 26). Overview of Organic Rankine Cycles. . University of Alabama, Tuscaloosa.

Srinivasan, K. K. (2008, September 1). Private communications with Dr. Srinivasan.

Teng, H., Regner, G., & Cowland, C. (2006). Achieving High Engine Efficiency for Heavy-Duty Diesel Engines by Waste Heat Recovery Using Supercritical Organic-Fluid Rankine Cycle. *SAE Technical Paper Series*.

Vijayarahgavan, S. (2003). *Thermodynamic Studies on Alternative Binary Working Fluid Combinations and Configurations for a Combined Power and Cooling Cycle*. University of Florida.



www.manaraa.com

APPENDIX A

*MATHCAD* ANALYSIS OF EVALUATIONS 1 & 2 FOR R113 AT HALF LOAD



www.manaraa.com

***Organic rankine cycle:***

$kJ := 1000 \cdot J \qquad MJ := 1000 \cdot kJ \qquad i := 1, 2 .. 5 \qquad j := 1, 2 .. 5$

*Organic rankine cycle will be used to recover heat from the exhaust of internal combustion engine in order to use it for useful work.*

*At State 1: We will have ambient temperature with a quality of 0 (saturated liquid) before the pump for this cycle. Using a computerized aid for thermodynamic tables (CATT2) the other values at this state can be found for R113.*

*State 1:* $T_1 := 298.15 \cdot K \qquad x_1 := 0$ *using CATT2* $\qquad P_1 := 0.04455 \cdot MPa$

$$\nu_1 := 6.39 \cdot 10^{-4} \cdot \frac{m^3}{kg} \qquad \boxed{h_1 := 55.75 \cdot \frac{kJ}{kg}} \qquad s_1 := 0.2105 \frac{kJ}{kg \cdot K}$$

*At state 2: After the pump a range of pressures will be used to determine the work done by the pump which will then be used to determine the other values at the this state. Pressures will be limited by the critical pressure of the working fluid. Assuming an ideal pump, the work will be equal to the specific volume times the pressure difference. The efficiency of the pump will yield the actual work required, which will give the enthalpy. From the pressure and enthalpy all other values can be determined.*

*State 2:* $s_2 = s_1 \qquad P_2 := \begin{pmatrix} 1 \\ 1.5 \\ 2 \\ 2.5 \\ 3.15 \end{pmatrix} \cdot MPa \qquad \nu_2 = \nu_1$

*Ideal pump work:* $w_{p.s_i} := \nu_1 \cdot \left( P_{2_i} - P_1 \right) \qquad w_{p.s} = \begin{pmatrix} 0.611 \\ 0.93 \\ 1.25 \\ 1.569 \\ 1.984 \end{pmatrix} \cdot \frac{kJ}{kg}$

*Pump efficiency:* $\eta_p := 80\% \qquad \eta_p = \frac{w_{p.s}}{w_{p.a}}$



www.manaraa.com

*Actual pump work:* $w_{p.a_i} := \frac{w_{p.s_i}}{\eta_p}$ $w_{p.a} = \begin{pmatrix} 0.763 \\ 1.163 \\ 1.562 \\ 1.961 \\ 2.48 \end{pmatrix} \cdot \frac{kJ}{kg}$

$w_{p.a} = h_2 - h_1$ $h_{2_i} := h_1 + w_{p.a_i}$ $\boxed{h_2 = \begin{pmatrix} 56.513 \\ 56.913 \\ 57.312 \\ 57.711 \\ 58.23 \end{pmatrix} \cdot \frac{kJ}{kg}}$

*With:* $P_2 = \begin{pmatrix} 1 \\ 1.5 \\ 2 \\ 2.5 \\ 3.15 \end{pmatrix} \cdot 1MPa$ $h_2 = \begin{pmatrix} 56.513 \\ 56.913 \\ 57.312 \\ 57.711 \\ 58.23 \end{pmatrix} \cdot \frac{kJ}{kg}$ *Using CATT2:*

$T_2 := \left[ 273.15 + \begin{pmatrix} 25.85 \\ 26.29 \\ 26.73 \\ 27.17 \\ 27.74 \end{pmatrix} \right] \cdot K$ $\nu_2 := \begin{pmatrix} 6.398 \\ 6.403 \\ 6.407 \\ 6.411 \\ 6.417 \end{pmatrix} \cdot 10^{-4} \cdot \frac{m^3}{kg}$ $s_2 := \begin{pmatrix} 0.213 \\ 0.2144 \\ 0.2157 \\ 0.217 \\ 0.2188 \end{pmatrix} \cdot \frac{kJ}{kg \cdot K}$

$x_2 := 0$

*At state 3: The fluid went through a constant pressure heat exchanger where the fluid was heated to the point of being saturated vapor (quality of 1). With pressure from state 2 and quality, the rest of the values are found before the fluid enters the turbine.*

*State 3:* $P_3 := P_2$ $x_3 := 1$ *using CATT2* $T_3 := \left[ 273.15 + \begin{pmatrix} 139 \\ 162.1 \\ 180.4 \\ 195.8 \\ 213 \end{pmatrix} \right] \cdot K$



www.manaraa.com

$$\nu_3 := \begin{pmatrix} 0.01455 \\ 0.009275 \\ 0.006548 \\ 0.004903 \\ 0.003693 \end{pmatrix} \cdot \frac{m^3}{kg} \qquad h_3 := \begin{pmatrix} 277.2 \\ 288.4 \\ 295.7 \\ 300.4 \\ 304.8 \end{pmatrix} \cdot \frac{kJ}{kg} \qquad s_3 := \begin{pmatrix} 0.7918 \\ 0.8048 \\ 0.8124 \\ 0.8163 \\ 0.82 \end{pmatrix} \cdot \frac{kJ}{kg \cdot K}$$

*At state 4:* *The fluid leaves the turbine and is about to enter a condenser. The turbine is considered to be an ideal turbine so the entropy from state 3 to state 4 will be equal. The condenser is considered to be a constant pressure heat exchanger so the pressure from state 4 to state 1 will be equal. With the pressure and entropy, the enthalpy can be determined using the tables. Having the values of enthalpy from state 3 to state 4, work of the ideal turbine can evaluated. With turbine efficiency the actual work of the turbine can be be found, yielding the actual enthalpy at state 4. The pressure and the actual enthalpy will then be used to find the other values at this state.*

*State 4:* $P_4 := P_1$ $s_4 = s_3$ *therefore using CATT2:* $h_{4.s} := \begin{pmatrix} 230.2 \\ 234.6 \\ 237.1 \\ 238.5 \\ 239.7 \end{pmatrix} \cdot \frac{kJ}{kg}$

*Ideal turbine work:* $w_{t.s_i} := h3_i - h_{4.s_i}$ $w_{t.s} = \begin{pmatrix} 47 \\ 53.8 \\ 58.6 \\ 61.9 \\ 65.1 \end{pmatrix} \cdot \frac{kJ}{kg}$

*Turbine efficiency:* $\eta_t := 85 \cdot \%$ $\eta_t = \frac{w_{t.a}}{w_{t.s}}$

*Actual turbine work:* $w_{t.a_i} := \eta_t \cdot w_{t.s_i}$ $w_{t.a} = \begin{pmatrix} 39.95 \\ 45.73 \\ 49.81 \\ 52.615 \\ 55.335 \end{pmatrix} \cdot \frac{kJ}{kg}$



www.manaraa.com

$w_{t.a} = h_3 - h_{4.a}$ $\quad h_{4.a_i} := h_{3_i} - w_{t.a_i}$ $\quad h_{4.a} = \begin{pmatrix} 237.25 \\ 242.67 \\ 245.89 \\ 247.785 \\ 249.465 \end{pmatrix} \cdot \frac{kJ}{kg}$

*With:* $h_{4.a} = \begin{pmatrix} 237.25 \\ 242.67 \\ 245.89 \\ 247.785 \\ 249.465 \end{pmatrix} \cdot \frac{kJ}{kg}$ $\quad P_4 = 44.55 \cdot kPa$ $\quad$ *Using CATT2*

$T_4 := \left[ 273.15 + \begin{pmatrix} 67.23 \\ 75.2 \\ 79.89 \\ 82.63 \\ 85.08 \end{pmatrix} \right] \cdot K$ $\quad \nu_4 := \begin{pmatrix} 0.3347 \\ 0.3428 \\ 0.3475 \\ 0.3503 \\ 0.3528 \end{pmatrix} \cdot \frac{m^3}{kg}$ $\quad s_4 := \begin{pmatrix} 0.8132 \\ 0.829 \\ 0.8381 \\ 0.8435 \\ 0.8482 \end{pmatrix} \cdot \frac{kJ}{kg \cdot K}$

*The organic rankine cycle thermal efficiency is the net work divided by that heat addition:*

*Thermal efficiency:*

$$\eta_{th.ORC_i} := \frac{\left(h_{3_i} - h_{4.a_i}\right) - \left(h_{2_i} - h_1\right)}{h_{3_i} - h_{2_i}}$$

$$\eta_{th.ORC} = \begin{pmatrix} 17.757 \\ 19.253 \\ 20.239 \\ 20.872 \\ 21.436 \end{pmatrix} \cdot \%$$



www.manaraa.com

***Evaporator evaluation 1:***

*To vary the pinch point difference is difficult since the actual temperature profiles along the evaporator are unknown. But varying the outlet temperature of the exhaust will in turn vary the pinch point. As a design constraint we set the outlet exhaust temperature to be no less than the dew point temperature of water at the given exhaust pressure. This will prevent the condensing of water which could promote fouling inside the heat exchanger. Once the dew point temperature is found, 5 degree increments are added to the dew point temperature to vary the pinch point and to see effects on the evaporator.*

*All exhaust data came from previous engine experiments. Half load for injection timings of 20, 30, 40, 50, and 60 degrees BTDC:*

*Exhaust mass flow rate:*

$$m'_{exh.half} := \begin{pmatrix} 3643.19 \\ 3650.07 \\ 3661.31 \\ 3693.04 \\ 3640.52 \end{pmatrix} \cdot \frac{gm}{min} \qquad m'_{exh.half} = \begin{pmatrix} 0.061 \\ 0.061 \\ 0.061 \\ 0.062 \\ 0.061 \end{pmatrix} \frac{kg}{s}$$

*Exhaust inlet temperature:*

$$T_{exh.in.half} := \left[ 273.15 + \begin{pmatrix} 319.589 \\ 281.8488 \\ 270.1401 \\ 264.8569 \\ 266.1079 \end{pmatrix} \right] \cdot K \qquad T_{exh.in.half} = \begin{pmatrix} 592.739 \\ 554.999 \\ 543.29 \\ 538.007 \\ 539.258 \end{pmatrix} K$$

*Exhaust pressure:*

$P_{exh.half} := (11.11 + 14.7) \cdot psi$ $\quad P_{exh.half} = 0.178 \cdot MPa$ $\quad x := 1$

*using CATT2 the dew point at these conditions for water are:*

$T_{dew.half} := (273.15 + 116.6) \cdot K$ $\quad T_{dew.half} = 389.75\,K$



www.manaraa.com

*Exhaust outlet temperature:*

$$T_{exh.out.half} := T_{dew.half} + \begin{pmatrix} 0 \\ 5 \\ 10 \\ 15 \\ 20 \end{pmatrix} \cdot K \qquad T_{exh.out.half} = \begin{pmatrix} 389.75 \\ 394.75 \\ 399.75 \\ 404.75 \\ 409.75 \end{pmatrix} K$$

*The mean exhaust temperature:*

$$T_{m.exh.half_j} := \frac{T_{exh.in.half_j} + T_{exh.out.half_j}}{2} \qquad T_{m.exh.half} = \begin{pmatrix} 491.245 \\ 474.874 \\ 471.52 \\ 471.378 \\ 474.504 \end{pmatrix} K$$

*Specific heat of air as a function of temperature:*

$$Cp_{air}(T) := \frac{kJ}{kg \cdot K} \cdot \left[ 1.05 + -0.365 \cdot \frac{T}{1000K} + 0.85 \cdot \left( \frac{T}{1000 \cdot K} \right)^2 + -0.39 \cdot \left( \frac{T}{1000 \cdot K} \right)^3 \right]$$

*Reference: Sonntag et al. (2002)*

$$cp_{exh.half_j} := Cp_{air}\left(T_{m.exh.half_j}\right) \qquad cp_{exh.half} = \begin{pmatrix} 1.03 \\ 1.027 \\ 1.026 \\ 1.026 \\ 1.027 \end{pmatrix} \cdot \frac{kJ}{kg \cdot K}$$

*Heat transfer:*

$$Q_{half_j} := m'_{exh.half_j} \cdot cp_{exh.half_j} \cdot \left(T_{exh.in.half_j} - T_{exh.out.half_j}\right) \qquad Q_{half} = \begin{pmatrix} 12.69 \\ 10.008 \\ 8.987 \\ 8.415 \\ 8.066 \end{pmatrix} \cdot kW$$



www.manaraa.com

*The effectiveness of the evaporator can be found by using the maximum heat transfer and the actual heat transfer:*

*It is stated that the maximum heat transfer between two fluid occurs when:*

$Q_{max} = C_{min} \cdot (T_{hot.in} - T_{cold.in})$ where $C_{min} = m' \cdot cp$ *the minimum heat capacity of the two fluids*

*For our case will we assume the exhaust gas (hot fluid) to be the fluid with the minimum heat capacity due to a forced phase change in the ORC, an imposed design condition.*

$Q_{max} = m'_{exh} \cdot cp_{exh} \cdot (T_{exh.in} - T_2)$ $\quad Q_{max.half_{i,j}} := m'_{exh.half_j} \cdot cp_{exh.half_j} \cdot (T_{exh.in.half_j} - T2_i)$

Injection timing: 20 30 40 50 60 — pressure

$$Q_{max.half} = \begin{pmatrix} 18.363 & 15.988 & 15.294 & 15.093 & 14.964 \\ 18.336 & 15.96 & 15.267 & 15.065 & 14.937 \\ 18.308 & 15.933 & 15.239 & 15.037 & 14.91 \\ 18.281 & 15.905 & 15.212 & 15.01 & 14.882 \\ 18.245 & 15.87 & 15.176 & 14.974 & 14.847 \end{pmatrix} \cdot k$$

1.5 / 2 / 2.5 / 3.15

*The above matrix varies with engine injection timing and pump pressures. From left to right the numbers vary with injection timing (20, 30 40, 50, 60 degrees BTDC). From top to bottom the numbers vary with pump pressure (1.0, 1.5, 2.0, 2.5, 3.15 MPa). The following matrices have similar setup.*

*Effectiveness:* $\varepsilon = \frac{Q_{actual}}{Q_{max}}$ $\quad \varepsilon_{1.half_{i,j}} := \frac{Q_{half_j}}{Q_{max.half_{i,j}}}$

$$\varepsilon_{1.half} = \begin{pmatrix} 69.105 & 62.597 & 58.758 & 55.754 & 53.904 \\ 69.209 & 62.705 & 58.864 & 55.857 & 54.003 \\ 69.313 & 62.813 & 58.97 & 55.96 & 54.102 \\ 69.417 & 62.922 & 59.077 & 56.064 & 54.201 \\ 69.553 & 63.063 & 59.216 & 56.199 & 54.331 \end{pmatrix} \cdot \%$$



www.manaraa.com

*From actual heat transfer the mass flow rate of the ORC can be found:* $Q = m'_{orc} \cdot (h_3 - h_2)$

$$m'_{orc.half_{i,j}} := \frac{Q_{half_j}}{h_{3_i} - h_{2_i}}$$

$$m'_{orc.half} = \begin{pmatrix} 0.058 & 0.045 & 0.041 & 0.038 & 0.037 \\ 0.055 & 0.043 & 0.039 & 0.036 & 0.035 \\ 0.053 & 0.042 & 0.038 & 0.035 & 0.034 \\ 0.052 & 0.041 & 0.037 & 0.035 & 0.033 \\ 0.051 & 0.041 & 0.036 & 0.034 & 0.033 \end{pmatrix} \frac{kg}{s}$$

*Now the power output of the ORC can be found:*

$$W_{orc.half_{i,j}} := m'_{orc.half_{i,j}} \cdot \left[ \left( h_{3_i} - h_{4.a_i} \right) - \left( h_{2_i} - h_1 \right) \right]$$

$$W_{orc.half} = \begin{pmatrix} 2.253 & 1.777 & 1.596 & 1.494 & 1.432 \\ 2.443 & 1.927 & 1.73 & 1.62 & 1.553 \\ 2.568 & 2.026 & 1.819 & 1.703 & 1.633 \\ 2.649 & 2.089 & 1.876 & 1.756 & 1.684 \\ 2.72 & 2.145 & 1.926 & 1.804 & 1.729 \end{pmatrix} \cdot kW$$

*Power output of the engine and thermal efficiency without ORC:*

$$W_{half.engine} := \begin{pmatrix} 28.23 \\ 28.15 \\ 28.20 \\ 28.12 \\ 28.23 \end{pmatrix} \cdot hp \qquad W_{half.engine} = \begin{pmatrix} 21.051 \\ 20.991 \\ 21.029 \\ 20.969 \\ 21.051 \end{pmatrix} \cdot kW \qquad \eta_{th.half.engine} := \begin{pmatrix} 28.16 \\ 31.89 \\ 33.14 \\ 36.12 \\ 35.19 \end{pmatrix} \cdot \%$$

*Mass flow rates and lower heating values of diesel and natural gas:*

$$Q_{LHV.d} := 43.2 \cdot \frac{MJ}{kg} \qquad Q_{LHV.ng} := 45 \cdot \frac{MJ}{kg}$$

*Reference: Russell et al. (1993)*

$$m'_{d.half} := \begin{pmatrix} 3.37 \\ 3.36 \\ 3.36 \\ 3.35 \\ 3.35 \end{pmatrix} \cdot \frac{gm}{min} \qquad m'_{ng.half} := \begin{pmatrix} 89.52 \\ 78.84 \\ 71.05 \\ 68.92 \\ 70.88 \end{pmatrix} \cdot \frac{gm}{min}$$



www.manaraa.com

*Total thermal efficiency of engine plus ORC:*

$$\eta_{th.total.half_{i,j}} := \frac{W_{half.engine_j} + W_{orc.half_{i,j}}}{\left(m'_{d.half_j} \cdot Q_{LHV.d}\right) + \left(m'_{ng.half_j} \cdot Q_{LHV.ng}\right)}$$

$$\eta_{th.total.half} = \begin{pmatrix} 33.5 & 36.992 & 40.614 & 41.52 & 40.458 \\ 33.772 & 37.236 & 40.855 & 41.753 & 40.675 \\ 33.952 & 37.396 & 41.014 & 41.906 & 40.819 \\ 34.068 & 37.499 & 41.116 & 42.005 & 40.91 \\ 34.171 & 37.591 & 41.207 & 42.093 & 40.992 \end{pmatrix} \cdot \%$$

*Percentage increase in thermal efficiency:*

$$Pct_{inc.half_{i,j}} := 1 - \frac{\eta_{th.half.engine_j}}{\eta_{th.total.half_{i,j}}}$$

$$Pct_{inc.half} = \begin{pmatrix} 15.939 & 13.793 & 18.402 & 13.006 & 13.021 \\ 16.618 & 14.356 & 18.884 & 13.491 & 13.486 \\ 17.06 & 14.724 & 19.198 & 13.808 & 13.789 \\ 17.341 & 14.958 & 19.399 & 14.01 & 13.983 \\ 17.59 & 15.165 & 19.577 & 14.189 & 14.154 \end{pmatrix} \cdot \%$$

*Chemical exergy* $\Psi_d := 47.4 \cdot \frac{MJ}{kg}$ $\Psi_{ng} := 51.8 \cdot \frac{MJ}{kg}$

*Reference: Russell et al. (1993)*

*Second law thermal efficiency for the engine:*

$$\eta_{th.2nd.engine.half_j} := \frac{W_{half.engine_j}}{\left(m'_{d.half_j} \cdot \Psi_d\right) + \left(m'_{ng.half_j} \cdot \Psi_{ng}\right)}$$

$$\eta_{th.2nd.engine.half} = \begin{pmatrix} 26.331 \\ 29.683 \\ 32.86 \\ 33.741 \\ 32.975 \end{pmatrix} \cdot \%$$



www.manaraa.com

*Second law thermal efficiency for the engine plus the ORC:*

$$\eta_{th.2nd.total.half_{i,j}} := \frac{W_{half.engine_j} + W_{orc.half_{i,j}}}{\left(m'_{d.half_j} \cdot \Psi_d\right) + \left(m'_{ng.half_j} \cdot \Psi_{ng}\right)}$$

$$\eta_{th.2nd.total.half} = \begin{pmatrix} 29.15 & 32.195 & 35.354 & 36.145 & 35.219 \\ 29.387 & 32.407 & 35.564 & 36.348 & 35.408 \\ 29.544 & 32.547 & 35.703 & 36.481 & 35.532 \\ 29.644 & 32.636 & 35.791 & 36.567 & 35.612 \\ 29.734 & 32.716 & 35.871 & 36.643 & 35.684 \end{pmatrix} \cdot \%$$

*Percentage increase in 2nd law thermal efficiency:*

$$Pct_{inc.2nd.half_{i,j}} := 1 - \frac{\eta_{th.2nd.engine.half_j}}{\eta_{th.2nd.total.half_{i,j}}}$$

$$Pct_{inc.2nd.half} = \begin{pmatrix} 9.669 & 7.805 & 7.053 & 6.652 & 6.371 \\ 10.399 & 8.407 & 7.602 & 7.172 & 6.87 \\ 10.874 & 8.8 & 7.961 & 7.512 & 7.197 \\ 11.176 & 9.05 & 8.189 & 7.729 & 7.405 \\ 11.443 & 9.272 & 8.392 & 7.921 & 7.59 \end{pmatrix} \cdot \%$$



www.manaraa.com

***Evaporator evaluation 2:***

*The following is the information from the organic rankine cycle analysis:*

*State 1:* *Ambient conditions before going into the pump.*

$$T_1 = 298.15\,K \qquad P_1 = 0.045\cdot MPa \qquad h_1 = 55.75\cdot\frac{kJ}{kg}$$

*State 2:* *Conditions after the pump before going into the evaporator.*

$$T_2 = \begin{pmatrix} 299 \\ 299.44 \\ 299.88 \\ 300.32 \\ 300.89 \end{pmatrix} K \qquad P_2 = \begin{pmatrix} 1 \\ 1.5 \\ 2 \\ 2.5 \\ 3.15 \end{pmatrix}\cdot MPa \qquad h_2 = \begin{pmatrix} 56.513 \\ 56.913 \\ 57.312 \\ 57.711 \\ 58.23 \end{pmatrix}\cdot\frac{kJ}{kg}$$

*State 3:* *Conditions after the evaporator before going into the turbine.*

$$T_3 = \begin{pmatrix} 412.15 \\ 435.25 \\ 453.55 \\ 468.95 \\ 486.15 \end{pmatrix} K \qquad P_3 = \begin{pmatrix} 1 \\ 1.5 \\ 2 \\ 2.5 \\ 3.15 \end{pmatrix}\cdot MPa \qquad h_3 = \begin{pmatrix} 277.2 \\ 288.4 \\ 295.7 \\ 300.4 \\ 304.8 \end{pmatrix}\cdot\frac{kJ}{kg}$$

*State 4:* *Conditions after the turbine before going through a condenser.*

$$T_4 = \begin{pmatrix} 340.38 \\ 348.35 \\ 353.04 \\ 355.78 \\ 358.23 \end{pmatrix} K \qquad P_4 = 0.045\cdot MPa \qquad h_{4.a} = \begin{pmatrix} 237.25 \\ 242.67 \\ 245.89 \\ 247.785 \\ 249.465 \end{pmatrix}\cdot\frac{kJ}{kg}$$

*Thermal efficiency:*

$$\eta_{th.ORC} = \frac{(h_3 - h_{4.a}) - (h_2 - h_1)}{h_3 - h_2}$$

$$\eta_{th.ORC} = \begin{pmatrix} 17.757 \\ 19.253 \\ 20.239 \\ 20.872 \\ 21.436 \end{pmatrix}\cdot\%$$



www.manaraa.com

*The following is the engine experiment data, please note that only 20, 30, 40, 50, 60 degrees BTDC and 20, 30, 40, 50, 55 degrees BTDC were used for half and quarter load, respectively, Srinivasan et al.(2008):*

| Inj.timing | Diesel_flow | NG_flow | Exhaust | Texh in | Ex.Pr | Power | Eff |
|---|---|---|---|---|---|---|---|
| degBTDC | g/min | g/min | g/min | evap C | psig | bhp | % |
| | | | | | | | |
| Half Load | | | | | | | |
| 20 | 3.37 | 89.52 | 3643.19 | 319.589 | 11.11 | 28.23 | 28.16 |
| 30 | 3.36 | 78.84 | 3650.67 | 281.8488 | 10.61 | 28.15 | 31.89 |
| 40 | 3.36 | 71.05 | 3661.31 | 270.1401 | 10.81 | 28.20 | 35.14 |
| 50 | 3.35 | 68.92 | 3693.04 | 264.8569 | 10.36 | 28.12 | 36.12 |
| 60 | 3.35 | 70.88 | 3640.52 | 266.1079 | 10.37 | 28.23 | 35.19 |
| Qtr. Load | | | | | | | |
| 20 | 3.36 | 64.29 | 2824.91 | 253.4269 | 3.88 | 13.74 | 18.73 |
| 30 | 3.37 | 55.74 | 2835.06 | 238.568 | 3.84 | 14.14 | 22.07 |
| 40 | 3.36 | 50.76 | 2831.75 | 236.5363 | 3.70 | 14.26 | 24.33 |
| 50 | 3.38 | 53.46 | 2837.16 | 244.5775 | 3.79 | 14.57 | 23.67 |
| 55 | 3.36 | 57.59 | 2836.96 | 250.7884 | 3.80 | 14.00 | 21.20 |

$$m'_{exh.half} = \begin{pmatrix} 0.061 \\ 0.061 \\ 0.061 \\ 0.062 \\ 0.061 \end{pmatrix} \frac{kg}{s} \qquad T_{exh.in.half} = \begin{pmatrix} 592.739 \\ 554.999 \\ 543.29 \\ 538.007 \\ 539.258 \end{pmatrix} K$$



www.manaraa.com

***Evaporator evaluation 2:*** $i := 1, 2 .. 5$

*It is stated that the maximum heat transfer between two fluid occurs when:*

$Q_{max} = C_{min} \cdot (T_{hot.in} - T_{cold.in})$ where $C_{min} = m' \cdot cp$ *the minimum heat capacity of the two fluids*

*For our case will we assume the exhaust gas (hot fluid) to be the fluid with the minimum heat capacity due to a forced phase change in the ORC.*

$$Q_{max} = m'_{exh} \cdot cp_{exh} \cdot (T_{exh.in} - T_2)$$

$$Q_{max.half_{i,j}} := m'_{exh.half_j} \cdot cp_{exh.half_j} \cdot (T_{exh.in.half_j} - T2_i)$$

| Injection timing | 20 | 30 | 40 | 50 | 60 | pressure |
|---|---|---|---|---|---|---|
| $Q_{max.half} =$ | 18.363 | 15.988 | 15.294 | 15.093 | 14.964 | 1 |
| | 18.336 | 15.96 | 15.267 | 15.065 | 14.937 | 1.5 |
| | 18.308 | 15.933 | 15.239 | 15.037 | 14.91 | 2 |
| | 18.281 | 15.905 | 15.212 | 15.01 | 14.882 | 2.5 |
| | 18.245 | 15.87 | 15.176 | 14.974 | 14.847 | 3.15 |

$\cdot kW$

*The above matrix varies with engine injection timing and pump pressures. From left to right the number vary with injection timing (20, 30 40, 50, 60 degrees BTDC). From top to bottom the numbers vary with pump pressure (1.0, 1.5, 2.0, 2.5, 3.15 MPa). The following matrices have similar setup.*

*Use a range of effectiveness to find the actual heat transfer in different conditions:*

*effectiveness* $\varepsilon = \frac{Q_{actual}}{Q_{max}}$ $\varepsilon := \begin{pmatrix} 0.80 \\ 0.75 \\ 0.70 \\ 0.65 \\ 0.60 \end{pmatrix}$ $Q_{actual.half_{i,j}} := \varepsilon_i \cdot Q_{max.half_{i,j}}$

$Q_{actual.half.1_{i,j}} := \varepsilon_1 \cdot Q_{max.half_{i,j}}$

$$Q_{actual.half.1} = \begin{pmatrix} 14.691 & 12.79 & 12.236 & 12.074 & 11.971 \\ 14.669 & 12.768 & 12.214 & 12.052 & 11.95 \\ 14.647 & 12.746 & 12.192 & 12.03 & 11.928 \\ 14.625 & 12.724 & 12.169 & 12.008 & 11.906 \\ 14.596 & 12.696 & 12.141 & 11.979 & 11.877 \end{pmatrix} \cdot kW$$



www.manaraa.com

$$Q_{actual.half.2} := \varepsilon_2 \cdot Q_{max.half} \qquad Q_{actual.half.2} = \begin{pmatrix} 13.773 & 11.991 & 11.471 & 11.32 & 11.223 \\ 13.752 & 11.97 & 11.45 & 11.299 & 11.203 \\ 13.731 & 11.949 & 11.43 & 11.278 & 11.182 \\ 13.711 & 11.929 & 11.409 & 11.257 & 11.162 \\ 13.684 & 11.902 & 11.382 & 11.23 & 11.135 \end{pmatrix} \cdot kW$$

$$Q_{actual.half.3} := \varepsilon_3 \cdot Q_{max.half} \qquad Q_{actual.half.3} = \begin{pmatrix} 12.854 & 11.191 & 10.706 & 10.565 & 10.475 \\ 12.835 & 11.172 & 10.687 & 10.546 & 10.456 \\ 12.816 & 11.153 & 10.668 & 10.526 & 10.437 \\ 12.797 & 11.134 & 10.648 & 10.507 & 10.417 \\ 12.772 & 11.109 & 10.623 & 10.482 & 10.393 \end{pmatrix} \cdot kW$$

$$Q_{actual.half.4} := \varepsilon_4 \cdot Q_{max.half} \qquad Q_{actual.half.4} = \begin{pmatrix} 11.936 & 10.392 & 9.941 & 9.81 & 9.727 \\ 11.918 & 10.374 & 9.924 & 9.792 & 9.709 \\ 11.9 & 10.356 & 9.906 & 9.774 & 9.691 \\ 11.883 & 10.338 & 9.888 & 9.756 & 9.673 \\ 11.859 & 10.315 & 9.865 & 9.733 & 9.65 \end{pmatrix} \cdot kW$$

$$Q_{actual.half.5} := \varepsilon_5 \cdot Q_{max.half} \qquad Q_{actual.half.5} = \begin{pmatrix} 11.018 & 9.593 & 9.177 & 9.056 & 8.979 \\ 11.002 & 9.576 & 9.16 & 9.039 & 8.962 \\ 10.985 & 9.56 & 9.144 & 9.022 & 8.946 \\ 10.969 & 9.543 & 9.127 & 9.006 & 8.929 \\ 10.947 & 9.522 & 9.106 & 8.984 & 8.908 \end{pmatrix} \cdot kW$$

*From the actual heat transfer the exit exhaust temperature can be found:*

$$T_{exh.out.half.1_{i,j}} := T_{exh.in.half_j} - \frac{Q_{actual.half.1_{i,j}}}{m'_{exh.half_j} \cdot cp_{exh.half_j}}$$

$$T_{exh.out.half.1} = \begin{pmatrix} 357.748 & 350.2 & 347.858 & 346.801 & 347.052 \\ 358.1 & 350.552 & 348.21 & 347.153 & 347.404 \\ 358.452 & 350.904 & 348.562 & 347.505 & 347.756 \\ 358.804 & 351.256 & 348.914 & 347.857 & 348.108 \\ 359.26 & 351.712 & 349.37 & 348.313 & 348.564 \end{pmatrix} K$$

$$T_{exh.out.half.2_{i,j}} := T_{exh.in.half_j} - \frac{Q_{actual.half.2_{i,j}}}{m'_{exh.half_j} \cdot cp_{exh.half_j}}$$



www.manaraa.com

$$T_{exh.out.half.2} = \begin{pmatrix} 372.435 & 363 & 360.073 & 358.752 & 359.064 \\ 372.765 & 363.33 & 360.403 & 359.082 & 359.394 \\ 373.095 & 363.66 & 360.733 & 359.412 & 359.724 \\ 373.425 & 363.99 & 361.063 & 359.742 & 360.054 \\ 373.852 & 364.417 & 361.49 & 360.169 & 360.482 \end{pmatrix} K$$

$$T_{exh.out.half.3_{i,j}} := T_{exh.in.half_j} - \frac{Q_{actual.half.3_{i,j}}}{m'_{exh.half_j} \cdot cp_{exh.half_j}}$$

$$T_{exh.out.half.3} = \begin{pmatrix} 387.122 & 375.8 & 372.287 & 370.702 & 371.077 \\ 387.43 & 376.108 & 372.595 & 371.01 & 371.385 \\ 387.738 & 376.416 & 372.903 & 371.318 & 371.693 \\ 388.046 & 376.724 & 373.211 & 371.626 & 372.001 \\ 388.445 & 377.123 & 373.61 & 372.025 & 372.4 \end{pmatrix} K$$

$$T_{exh.out.half.4_{i,j}} := T_{exh.in.half_j} - \frac{Q_{actual.half.4_{i,j}}}{m'_{exh.half_j} \cdot cp_{exh.half_j}}$$

$$T_{exh.out.half.4} = \begin{pmatrix} 401.809 & 388.6 & 384.502 & 382.652 & 383.09 \\ 402.095 & 388.886 & 384.788 & 382.938 & 383.376 \\ 402.381 & 389.172 & 385.074 & 383.224 & 383.662 \\ 402.667 & 389.458 & 385.36 & 383.51 & 383.948 \\ 403.037 & 389.828 & 385.73 & 383.881 & 384.319 \end{pmatrix} K$$

$$T_{exh.out.half.5_{i,j}} := T_{exh.in.half_j} - \frac{Q_{actual.half.5_{i,j}}}{m'_{exh.half_j} \cdot cp_{exh.half_j}}$$

$$T_{exh.out.half.5} = \begin{pmatrix} 416.496 & 401.4 & 396.716 & 394.603 & 395.103 \\ 416.76 & 401.664 & 396.98 & 394.867 & 395.367 \\ 417.024 & 401.928 & 397.244 & 395.131 & 395.631 \\ 417.288 & 402.192 & 397.508 & 395.395 & 395.895 \\ 417.63 & 402.534 & 397.85 & 395.737 & 396.237 \end{pmatrix} K$$



www.manaraa.com

*Find the orc mass flow rate from the actual heat transfer*

$$\dot{m}'_{orc.half.1_{i,j}} := \frac{Q_{actual.half.1_{i,j}}}{\left(h3_i - h2_i\right)}$$

$$\dot{m}'_{orc.half.1} = \begin{pmatrix} 0.067 & 0.058 & 0.055 & 0.055 & 0.054 \\ 0.063 & 0.055 & 0.053 & 0.052 & 0.052 \\ 0.061 & 0.053 & 0.051 & 0.05 & 0.05 \\ 0.06 & 0.052 & 0.05 & 0.049 & 0.049 \\ 0.059 & 0.051 & 0.049 & 0.049 & 0.048 \end{pmatrix} \frac{kg}{s}$$

$$\dot{m}'_{orc.half.2_{i,j}} := \frac{Q_{actual.half.2_{i,j}}}{\left(h3_i - h2_i\right)}$$

$$\dot{m}'_{orc.half.2} = \begin{pmatrix} 0.062 & 0.054 & 0.052 & 0.051 & 0.051 \\ 0.059 & 0.052 & 0.049 & 0.049 & 0.048 \\ 0.058 & 0.05 & 0.048 & 0.047 & 0.047 \\ 0.056 & 0.049 & 0.047 & 0.046 & 0.046 \\ 0.055 & 0.048 & 0.046 & 0.046 & 0.045 \end{pmatrix} \frac{kg}{s}$$

$$\dot{m}'_{orc.half.3_{i,j}} := \frac{Q_{actual.half.3_{i,j}}}{\left(h3_i - h2_i\right)}$$

$$\dot{m}'_{orc.half.3} = \begin{pmatrix} 0.058 & 0.051 & 0.049 & 0.048 & 0.047 \\ 0.055 & 0.048 & 0.046 & 0.046 & 0.045 \\ 0.054 & 0.047 & 0.045 & 0.044 & 0.044 \\ 0.053 & 0.046 & 0.044 & 0.043 & 0.043 \\ 0.052 & 0.045 & 0.043 & 0.043 & 0.042 \end{pmatrix} \frac{kg}{s}$$

$$\dot{m}'_{orc.half.4_{i,j}} := \frac{Q_{actual.half.4_{i,j}}}{\left(h3_i - h2_i\right)}$$

$$\dot{m}'_{orc.half.4} = \begin{pmatrix} 0.054 & 0.047 & 0.045 & 0.044 & 0.044 \\ 0.051 & 0.045 & 0.043 & 0.042 & 0.042 \\ 0.05 & 0.043 & 0.042 & 0.041 & 0.041 \\ 0.049 & 0.043 & 0.041 & 0.04 & 0.04 \\ 0.048 & 0.042 & 0.04 & 0.039 & 0.039 \end{pmatrix} \frac{kg}{s}$$

$$\dot{m}'_{orc.half.5_{i,j}} := \frac{Q_{actual.half.5_{i,j}}}{\left(h3_i - h2_i\right)}$$

$$\dot{m}'_{orc.half.5} = \begin{pmatrix} 0.05 & 0.043 & 0.042 & 0.041 & 0.041 \\ 0.048 & 0.041 & 0.04 & 0.039 & 0.039 \\ 0.046 & 0.04 & 0.038 & 0.038 & 0.038 \\ 0.045 & 0.039 & 0.038 & 0.037 & 0.037 \\ 0.044 & 0.039 & 0.037 & 0.036 & 0.036 \end{pmatrix} \frac{kg}{s}$$

*Now the power output of the ORC can be found:*

$$W_{orc.half.1_{i,j}} := \dot{m}'_{orc.half.1_{i,j}} \cdot \left[\left(h3_i - h4.a_i\right) - \left(h2_i - h1\right)\right]$$



www.manaraa.com

$$W_{orc.half.1} = \begin{pmatrix} 2.609 & 2.271 & 2.173 & 2.144 & 2.126 \\ 2.824 & 2.458 & 2.351 & 2.32 & 2.301 \\ 2.964 & 2.58 & 2.467 & 2.435 & 2.414 \\ 3.052 & 2.656 & 2.54 & 2.506 & 2.485 \\ 3.129 & 2.721 & 2.603 & 2.568 & 2.546 \end{pmatrix} \cdot kW$$

$$W_{orc.half.2_{i,j}} := m'_{orc.half.2_{i,j}} \cdot \left[ \left( h3_i - h_{4.a_i} \right) - \left( h2_i - h_1 \right) \right]$$

$$W_{orc.half.2} = \begin{pmatrix} 2.446 & 2.129 & 2.037 & 2.01 & 1.993 \\ 2.648 & 2.305 & 2.204 & 2.175 & 2.157 \\ 2.779 & 2.418 & 2.313 & 2.283 & 2.263 \\ 2.862 & 2.49 & 2.381 & 2.35 & 2.33 \\ 2.933 & 2.551 & 2.44 & 2.407 & 2.387 \end{pmatrix} \cdot kW$$

$$W_{orc.half.3_{i,j}} := m'_{orc.half.3_{i,j}} \cdot \left[ \left( h3_i - h_{4.a_i} \right) - \left( h2_i - h_1 \right) \right]$$

$$W_{orc.half.3} = \begin{pmatrix} 2.283 & 1.987 & 1.901 & 1.876 & 1.86 \\ 2.471 & 2.151 & 2.058 & 2.03 & 2.013 \\ 2.594 & 2.257 & 2.159 & 2.13 & 2.112 \\ 2.671 & 2.324 & 2.222 & 2.193 & 2.174 \\ 2.738 & 2.381 & 2.277 & 2.247 & 2.228 \end{pmatrix} \cdot kW$$

$$W_{orc.half.4_{i,j}} := m'_{orc.half.4_{i,j}} \cdot \left[ \left( h3_i - h_{4.a_i} \right) - \left( h2_i - h_1 \right) \right]$$

$$W_{orc.half.4} = \begin{pmatrix} 2.119 & 1.845 & 1.765 & 1.742 & 1.727 \\ 2.295 & 1.997 & 1.911 & 1.885 & 1.869 \\ 2.409 & 2.096 & 2.005 & 1.978 & 1.961 \\ 2.48 & 2.158 & 2.064 & 2.036 & 2.019 \\ 2.542 & 2.211 & 2.115 & 2.086 & 2.069 \end{pmatrix} \cdot kW$$

$$W_{orc.half.5_{i,j}} := m'_{orc.half.5_{i,j}} \cdot \left[ \left( h3_i - h_{4.a_i} \right) - \left( h2_i - h_1 \right) \right]$$



www.manaraa.com

$$W_{orc.half.5} = \begin{pmatrix} 1.956 & 1.703 & 1.629 & 1.608 & 1.594 \\ 2.118 & 1.844 & 1.764 & 1.74 & 1.725 \\ 2.223 & 1.935 & 1.851 & 1.826 & 1.811 \\ 2.289 & 1.992 & 1.905 & 1.88 & 1.864 \\ 2.347 & 2.041 & 1.952 & 1.926 & 1.91 \end{pmatrix} \cdot kW$$

*Total thermal efficiency of engine plus ORC:*

$$\eta_{th.total.half.1_{i,j}} := \frac{W_{half.engine_j} + W_{orc.half.1_{i,j}}}{\left(m'_{d.half_j} \cdot Q_{LHV.d}\right) + \left(m'_{ng.half_j} \cdot Q_{LHV.ng}\right)}$$

$$\eta_{th.total.half.1} = \begin{pmatrix} 34.01 & 37.795 & 41.649 & 42.721 & 41.706 \\ 34.32 & 38.099 & 41.97 & 43.047 & 42.021 \\ 34.522 & 38.296 & 42.178 & 43.259 & 42.225 \\ 34.648 & 38.42 & 42.309 & 43.391 & 42.352 \\ 34.758 & 38.527 & 42.421 & 43.505 & 42.462 \end{pmatrix} \cdot \%$$

$$\eta_{th.total.half.2_{i,j}} := \frac{W_{half.engine_j} + W_{orc.half.2_{i,j}}}{\left(m'_{d.half_j} \cdot Q_{LHV.d}\right) + \left(m'_{ng.half_j} \cdot Q_{LHV.ng}\right)}$$

$$\eta_{th.total.half.2} = \begin{pmatrix} 33.776 & 37.564 & 41.405 & 42.474 & 41.467 \\ 34.066 & 37.849 & 41.706 & 42.779 & 41.762 \\ 34.255 & 38.035 & 41.902 & 42.978 & 41.953 \\ 34.374 & 38.15 & 42.024 & 43.101 & 42.073 \\ 34.477 & 38.25 & 42.129 & 43.208 & 42.176 \end{pmatrix} \cdot \%$$

$$\eta_{th.total.half.3_{i,j}} := \frac{W_{half.engine_j} + W_{orc.half.3_{i,j}}}{\left(m'_{d.half_j} \cdot Q_{LHV.d}\right) + \left(m'_{ng.half_j} \cdot Q_{LHV.ng}\right)}$$

$$\eta_{th.total.half.3} = \begin{pmatrix} 33.542 & 37.334 & 41.162 & 42.226 & 41.228 \\ 33.813 & 37.6 & 41.442 & 42.511 & 41.503 \\ 33.989 & 37.773 & 41.625 & 42.696 & 41.682 \\ 34.1 & 37.881 & 41.739 & 42.812 & 41.793 \\ 34.196 & 37.974 & 41.837 & 42.911 & 41.89 \end{pmatrix} \cdot \%$$



www.manaraa.com

$$\eta_{th.total.half.4_{i,j}} := \frac{W_{half.engine_j} + W_{orc.half.4_{i,j}}}{\left(m'_{d.half_j} \cdot Q_{LHV.d}\right) + \left(m'_{ng.half_j} \cdot Q_{LHV.ng}\right)}$$

$$\eta_{th.total.half.4} = \begin{pmatrix} 33.307 & 37.103 & 40.918 & 41.978 & 40.989 \\ 33.559 & 37.35 & 41.179 & 42.243 & 41.244 \\ 33.723 & 37.511 & 41.348 & 42.415 & 41.41 \\ 33.826 & 37.611 & 41.454 & 42.522 & 41.514 \\ 33.915 & 37.698 & 41.545 & 42.615 & 41.603 \end{pmatrix} \cdot \%$$

$$\eta_{th.total.half.5_{i,j}} := \frac{W_{half.engine_j} + W_{orc.half.5_{i,j}}}{\left(m'_{d.half_j} \cdot Q_{LHV.d}\right) + \left(m'_{ng.half_j} \cdot Q_{LHV.ng}\right)}$$

$$\eta_{th.total.half.5} = \begin{pmatrix} 33.073 & 36.873 & 40.674 & 41.731 & 40.75 \\ 33.305 & 37.101 & 40.915 & 41.975 & 40.986 \\ 33.456 & 37.249 & 41.071 & 42.134 & 41.139 \\ 33.551 & 37.341 & 41.169 & 42.233 & 41.234 \\ 33.634 & 37.421 & 41.253 & 42.318 & 41.317 \end{pmatrix} \cdot \%$$

*Percentage increase in thermal efficiency:*

$$Pct_{inc.half.1_{i,j}} := 1 - \frac{\eta_{th.half.engine_j}}{\eta_{th.total.half.1_{i,j}}}$$

$$Pct_{inc.half.1} = \begin{pmatrix} 17.201 & 15.624 & 20.431 & 15.452 & 15.624 \\ 17.949 & 16.297 & 21.039 & 16.092 & 16.255 \\ 18.428 & 16.729 & 21.429 & 16.502 & 16.66 \\ 18.726 & 16.996 & 21.671 & 16.757 & 16.911 \\ 18.983 & 17.226 & 21.878 & 16.974 & 17.126 \end{pmatrix} \cdot \%$$

$$Pct_{inc.half.2_{i,j}} := 1 - \frac{\eta_{th.half.engine_j}}{\eta_{th.total.half.2_{i,j}}}$$



www.manaraa.com

$$Pct_{inc.half.2} = \begin{pmatrix} 16.627 & 15.106 & 19.962 & 14.959 & 15.137 \\ 17.338 & 15.745 & 20.54 & 15.567 & 15.737 \\ 17.794 & 16.155 & 20.91 & 15.956 & 16.121 \\ 18.078 & 16.41 & 21.14 & 16.197 & 16.359 \\ 18.322 & 16.628 & 21.337 & 16.404 & 16.564 \end{pmatrix} \cdot \%$$

$$Pct_{inc.half.3_{i,j}} := 1 - \frac{\eta_{th.half.engine_j}}{\eta_{th.total.half.3_{i,j}}}$$

$$Pct_{inc.half.3} = \begin{pmatrix} 16.044 & 14.581 & 19.488 & 14.46 & 14.645 \\ 16.717 & 15.186 & 20.034 & 15.034 & 15.211 \\ 17.15 & 15.574 & 20.384 & 15.402 & 15.575 \\ 17.419 & 15.815 & 20.601 & 15.631 & 15.8 \\ 17.651 & 16.022 & 20.788 & 15.826 & 15.993 \end{pmatrix} \cdot \%$$

$$Pct_{inc.half.4_{i,j}} := 1 - \frac{\eta_{th.half.engine_j}}{\eta_{th.total.half.4_{i,j}}}$$

$$Pct_{inc.half.4} = \begin{pmatrix} 15.454 & 14.051 & 19.009 & 13.956 & 14.147 \\ 16.088 & 14.619 & 19.521 & 14.495 & 14.679 \\ 16.495 & 14.984 & 19.851 & 14.841 & 15.021 \\ 16.749 & 15.211 & 20.055 & 15.056 & 15.233 \\ 16.968 & 15.406 & 20.231 & 15.241 & 15.415 \end{pmatrix} \cdot \%$$

$$Pct_{inc.half.5_{i,j}} := 1 - \frac{\eta_{th.half.engine_j}}{\eta_{th.total.half.5_{i,j}}}$$

$$Pct_{inc.half.5} = \begin{pmatrix} 14.855 & 13.513 & 18.523 & 13.445 & 13.644 \\ 15.449 & 14.044 & 19.003 & 13.949 & 14.141 \\ 15.831 & 14.386 & 19.311 & 14.273 & 14.46 \\ 16.069 & 14.599 & 19.502 & 14.474 & 14.659 \\ 16.274 & 14.781 & 19.666 & 14.646 & 14.829 \end{pmatrix} \cdot \%$$



www.manaraa.com

*Chemical exergy* $\Psi_d := 47.4 \cdot \frac{MJ}{kg}$ $\Psi_{ng} := 51.8 \cdot \frac{MJ}{kg}$

*Reference: Russell et al. (1993)*

*Second law thermal efficiency for the engine:*

$$\eta_{th.2nd.engine.half_j} := \frac{W_{half.engine_j}}{\left(m'_{d.half_j} \cdot \Psi_d\right) + \left(m'_{ng.half_j} \cdot \Psi_{ng}\right)}$$

$$\eta_{th.2nd.engine.half} = \begin{pmatrix} 26.331 \\ 29.683 \\ 32.86 \\ 33.741 \\ 32.975 \end{pmatrix} \cdot \%$$

*Second law thermal efficiency for the engine plus the ORC:*

$$\eta_{th.2nd.total.half.1_{i,j}} := \frac{W_{half.engine_j} + W_{orc.half.1_{i,j}}}{\left(m'_{d.half_j} \cdot \Psi_d\right) + \left(m'_{ng.half_j} \cdot \Psi_{ng}\right)}$$

$$\eta_{th.2nd.total.half.1} = \begin{pmatrix} 29.594 & 32.894 & 36.255 & 37.191 & 36.305 \\ 29.863 & 33.159 & 36.535 & 37.475 & 36.579 \\ 30.039 & 33.33 & 36.716 & 37.659 & 36.756 \\ 30.149 & 33.438 & 36.829 & 37.774 & 36.867 \\ 30.245 & 33.531 & 36.927 & 37.873 & 36.963 \end{pmatrix} \cdot \%$$

$$\eta_{th.2nd.total.half.2_{i,j}} := \frac{W_{half.engine_j} + W_{orc.half.2_{i,j}}}{\left(m'_{d.half_j} \cdot \Psi_d\right) + \left(m'_{ng.half_j} \cdot \Psi_{ng}\right)}$$

$$\eta_{th.2nd.total.half.2} = \begin{pmatrix} 29.39 & 32.693 & 36.043 & 36.975 & 36.097 \\ 29.643 & 32.941 & 36.305 & 37.241 & 36.354 \\ 29.807 & 33.102 & 36.475 & 37.414 & 36.52 \\ 29.91 & 33.203 & 36.581 & 37.522 & 36.624 \\ 30 & 33.29 & 36.673 & 37.614 & 36.714 \end{pmatrix} \cdot \%$$



www.manaraa.com

$$\eta_{th.2nd.total.half.3_{i,j}} := \frac{W_{half.engine_j} + W_{orc.half.3_{i,j}}}{\left(m'_{d.half_j} \cdot \Psi_d\right) + \left(m'_{ng.half_j} \cdot \Psi_{ng}\right)}$$

$$\eta_{th.2nd.total.half.3} = \begin{pmatrix} 29.186 & 32.493 & 35.831 & 36.76 & 35.889 \\ 29.422 & 32.724 & 36.075 & 37.008 & 36.128 \\ 29.575 & 32.874 & 36.234 & 37.169 & 36.284 \\ 29.672 & 32.969 & 36.333 & 37.27 & 36.381 \\ 29.755 & 33.05 & 36.419 & 37.356 & 36.465 \end{pmatrix} \cdot \%$$

$$\eta_{th.2nd.total.half.4_{i,j}} := \frac{W_{half.engine_j} + W_{orc.half.4_{i,j}}}{\left(m'_{d.half_j} \cdot \Psi_d\right) + \left(m'_{ng.half_j} \cdot \Psi_{ng}\right)}$$

$$\eta_{th.2nd.total.half.4} = \begin{pmatrix} 28.982 & 32.292 & 35.619 & 36.544 & 35.68 \\ 29.201 & 32.507 & 35.846 & 36.774 & 35.903 \\ 29.344 & 32.647 & 35.993 & 36.924 & 36.047 \\ 29.433 & 32.734 & 36.085 & 37.017 & 36.138 \\ 29.511 & 32.809 & 36.165 & 37.098 & 36.215 \end{pmatrix} \cdot \%$$

$$\eta_{th.2nd.total.half.5_{i,j}} := \frac{W_{half.engine_j} + W_{orc.half.5_{i,j}}}{\left(m'_{d.half_j} \cdot \Psi_d\right) + \left(m'_{ng.half_j} \cdot \Psi_{ng}\right)}$$

$$\eta_{th.2nd.total.half.5} = \begin{pmatrix} 28.778 & 32.091 & 35.407 & 36.328 & 35.472 \\ 28.98 & 32.29 & 35.616 & 36.541 & 35.678 \\ 29.112 & 32.419 & 35.752 & 36.679 & 35.811 \\ 29.195 & 32.499 & 35.837 & 36.765 & 35.894 \\ 29.266 & 32.569 & 35.91 & 36.84 & 35.966 \end{pmatrix} \cdot \%$$

*Percentage increase in 2nd law thermal efficiency:*

$$Pct_{inc.2nd.half.1_{i,j}} := 1 - \frac{\eta_{th.2nd.engine.half_j}}{\eta_{th.2nd.total.half.1_{i,j}}}$$



www.manaraa.com

$$Pct_{inc.2nd.half.1} = \begin{pmatrix} 11.026 & 9.763 & 9.364 & 9.276 & 9.172 \\ 11.829 & 10.483 & 10.057 & 9.963 & 9.852 \\ 12.344 & 10.944 & 10.502 & 10.403 & 10.288 \\ 12.664 & 11.231 & 10.777 & 10.676 & 10.558 \\ 12.94 & 11.477 & 11.013 & 10.91 & 10.79 \end{pmatrix} \cdot \%$$

$$Pct_{inc.2nd.half.2_{i,j}} := 1 - \frac{\eta_{th.2nd.engine.half_j}}{\eta_{th.2nd.total.half.2_{i,j}}}$$

$$Pct_{inc.2nd.half.2} = \begin{pmatrix} 10.408 & 9.209 & 8.831 & 8.747 & 8.648 \\ 11.172 & 9.893 & 9.488 & 9.399 & 9.293 \\ 11.662 & 10.331 & 9.91 & 9.817 & 9.707 \\ 11.967 & 10.603 & 10.172 & 10.076 & 9.964 \\ 12.23 & 10.837 & 10.396 & 10.298 & 10.184 \end{pmatrix} \cdot \%$$

$$Pct_{inc.2nd.half.3_{i,j}} := 1 - \frac{\eta_{th.2nd.engine.half_j}}{\eta_{th.2nd.total.half.3_{i,j}}}$$

$$Pct_{inc.2nd.half.3} = \begin{pmatrix} 9.782 & 8.648 & 8.291 & 8.212 & 8.118 \\ 10.505 & 9.294 & 8.912 & 8.828 & 8.728 \\ 10.97 & 9.709 & 9.311 & 9.223 & 9.119 \\ 11.259 & 9.967 & 9.559 & 9.468 & 9.362 \\ 11.508 & 10.188 & 9.771 & 9.678 & 9.57 \end{pmatrix} \cdot \%$$

$$Pct_{inc.2nd.half.4_{i,j}} := 1 - \frac{\eta_{th.2nd.engine.half_j}}{\eta_{th.2nd.total.half.4_{i,j}}}$$

$$Pct_{inc.2nd.half.4} = \begin{pmatrix} 9.147 & 8.08 & 7.744 & 7.67 & 7.583 \\ 9.829 & 8.688 & 8.329 & 8.249 & 8.155 \\ 10.267 & 9.079 & 8.704 & 8.621 & 8.523 \\ 10.54 & 9.321 & 8.937 & 8.851 & 8.752 \\ 10.775 & 9.53 & 9.137 & 9.049 & 8.947 \end{pmatrix} \cdot \%$$



www.manaraa.com

$$Pct_{inc.2nd.half.5_{i,j}} := 1 - \frac{\eta_{th.2nd.engine.half_j}}{\eta_{th.2nd.total.half.5_{i,j}}}$$

$$Pct_{inc.2nd.half.5} = \begin{pmatrix} 8.504 & 7.505 & 7.192 & 7.122 & 7.04 \\ 9.142 & 8.074 & 7.738 & 7.663 & 7.576 \\ 9.553 & 8.439 & 8.089 & 8.011 & 7.92 \\ 9.808 & 8.666 & 8.307 & 8.227 & 8.133 \\ 10.029 & 8.862 & 8.494 & 8.412 & 8.316 \end{pmatrix} \cdot \%$$

*Pinch point analysis: Assuming that the exhaust temperature has a linear temperature profile as it moves through the evaporator, we can determine the slope.*

*H.2 will be the same for all five cases.*

$$H2_{i,j} := m'_{orc.half.1_{i,j}} \cdot \left(h2_i - h2_i\right) \qquad H_2 = \begin{pmatrix} 0 & 0 & 0 & 0 & 0 \\ 0 & 0 & 0 & 0 & 0 \\ 0 & 0 & 0 & 0 & 0 \\ 0 & 0 & 0 & 0 & 0 \\ 0 & 0 & 0 & 0 & 0 \end{pmatrix} W$$

*The slope of the exhaust gas is:*

$$m_{slope.half.1_{i,j}} := \frac{T_{exh.in.half_j} - T_{exh.out.half.1_{i,j}}}{Q_{actual.half.1_{i,j}} - H2_{i,j}}$$

$$m_{slope.half.1} = \begin{pmatrix} 15.996 & 16.012 & 15.972 & 15.836 & 16.055 \\ 15.996 & 16.012 & 15.972 & 15.836 & 16.055 \\ 15.996 & 16.012 & 15.972 & 15.836 & 16.055 \\ 15.996 & 16.012 & 15.972 & 15.836 & 16.055 \\ 15.996 & 16.012 & 15.972 & 15.836 & 16.055 \end{pmatrix} \cdot \frac{K}{kW}$$

$$m_{slope.half.2_{i,j}} := \frac{T_{exh.in.half_j} - T_{exh.out.half.2_{i,j}}}{Q_{actual.half.2_{i,j}} - H2_{i,j}}$$



www.manaraa.com

$$m_{slope.half.2} = \begin{pmatrix} 15.996 & 16.012 & 15.972 & 15.836 & 16.055 \\ 15.996 & 16.012 & 15.972 & 15.836 & 16.055 \\ 15.996 & 16.012 & 15.972 & 15.836 & 16.055 \\ 15.996 & 16.012 & 15.972 & 15.836 & 16.055 \\ 15.996 & 16.012 & 15.972 & 15.836 & 16.055 \end{pmatrix} \cdot \frac{K}{kW}$$

$$m_{slope.half.3_{i,j}} := \frac{T_{exh.in.half_j} - T_{exh.out.half.3_{i,j}}}{Q_{actual.half.3_{i,j}} - H_{2_{i,j}}}$$

$$m_{slope.half.3} = \begin{pmatrix} 15.996 & 16.012 & 15.972 & 15.836 & 16.055 \\ 15.996 & 16.012 & 15.972 & 15.836 & 16.055 \\ 15.996 & 16.012 & 15.972 & 15.836 & 16.055 \\ 15.996 & 16.012 & 15.972 & 15.836 & 16.055 \\ 15.996 & 16.012 & 15.972 & 15.836 & 16.055 \end{pmatrix} \cdot \frac{K}{kW}$$

$$m_{slope.half.4_{i,j}} := \frac{T_{exh.in.half_j} - T_{exh.out.half.4_{i,j}}}{Q_{actual.half.4_{i,j}} - H_{2_{i,j}}}$$

$$m_{slope.half.4} = \begin{pmatrix} 15.996 & 16.012 & 15.972 & 15.836 & 16.055 \\ 15.996 & 16.012 & 15.972 & 15.836 & 16.055 \\ 15.996 & 16.012 & 15.972 & 15.836 & 16.055 \\ 15.996 & 16.012 & 15.972 & 15.836 & 16.055 \\ 15.996 & 16.012 & 15.972 & 15.836 & 16.055 \end{pmatrix} \cdot \frac{K}{kW}$$

$$m_{slope.half.5_{i,j}} := \frac{T_{exh.in.half_j} - T_{exh.out.half.5_{i,j}}}{Q_{actual.half.5_{i,j}} - H_{2_{i,j}}}$$

$$m_{slope.half.5} = \begin{pmatrix} 15.996 & 16.012 & 15.972 & 15.836 & 16.055 \\ 15.996 & 16.012 & 15.972 & 15.836 & 16.055 \\ 15.996 & 16.012 & 15.972 & 15.836 & 16.055 \\ 15.996 & 16.012 & 15.972 & 15.836 & 16.055 \\ 15.996 & 16.012 & 15.972 & 15.836 & 16.055 \end{pmatrix} \cdot \frac{K}{kW}$$

*Slope - intercept:* $T = m_{slope} \cdot H + b_{int}$



www.manaraa.com

$$b_{int.half.1_{i,j}} := T_{exh.in.half_j} - m_{slope.half.1_{i,j}} \cdot Q_{actual.half.1_{i,j}}$$

$$b_{int.half.1} = \begin{pmatrix} 357.748 & 350.2 & 347.858 & 346.801 & 347.052 \\ 358.1 & 350.552 & 348.21 & 347.153 & 347.404 \\ 358.452 & 350.904 & 348.562 & 347.505 & 347.756 \\ 358.804 & 351.256 & 348.914 & 347.857 & 348.108 \\ 359.26 & 351.712 & 349.37 & 348.313 & 348.564 \end{pmatrix} K$$

$$b_{int.half.2_{i,j}} := T_{exh.in.half_j} - m_{slope.half.2_{i,j}} \cdot Q_{actual.half.2_{i,j}}$$

$$b_{int.half.2} = \begin{pmatrix} 372.435 & 363 & 360.073 & 358.752 & 359.064 \\ 372.765 & 363.33 & 360.403 & 359.082 & 359.394 \\ 373.095 & 363.66 & 360.733 & 359.412 & 359.724 \\ 373.425 & 363.99 & 361.063 & 359.742 & 360.054 \\ 373.852 & 364.417 & 361.49 & 360.169 & 360.482 \end{pmatrix} K$$

$$b_{int.half.3_{i,j}} := T_{exh.in.half_j} - m_{slope.half.3_{i,j}} \cdot Q_{actual.half.3_{i,j}}$$

$$b_{int.half.3} = \begin{pmatrix} 387.122 & 375.8 & 372.287 & 370.702 & 371.077 \\ 387.43 & 376.108 & 372.595 & 371.01 & 371.385 \\ 387.738 & 376.416 & 372.903 & 371.318 & 371.693 \\ 388.046 & 376.724 & 373.211 & 371.626 & 372.001 \\ 388.445 & 377.123 & 373.61 & 372.025 & 372.4 \end{pmatrix} K$$

$$b_{int.half.4_{i,j}} := T_{exh.in.half_j} - m_{slope.half.4_{i,j}} \cdot Q_{actual.half.4_{i,j}}$$

$$b_{int.half.4} = \begin{pmatrix} 401.809 & 388.6 & 384.502 & 382.652 & 383.09 \\ 402.095 & 388.886 & 384.788 & 382.938 & 383.376 \\ 402.381 & 389.172 & 385.074 & 383.224 & 383.662 \\ 402.667 & 389.458 & 385.36 & 383.51 & 383.948 \\ 403.037 & 389.828 & 385.73 & 383.881 & 384.319 \end{pmatrix} K$$

$$b_{int.half.5_{i,j}} := T_{exh.in.half_j} - m_{slope.half.5_{i,j}} \cdot Q_{actual.half.5_{i,j}}$$



www.manaraa.com

$$b_{int.half.5} = \begin{pmatrix} 416.496 & 401.4 & 396.716 & 394.603 & 395.103 \\ 416.76 & 401.664 & 396.98 & 394.867 & 395.367 \\ 417.024 & 401.928 & 397.244 & 395.131 & 395.631 \\ 417.288 & 402.192 & 397.508 & 395.395 & 395.895 \\ 417.63 & 402.534 & 397.85 & 395.737 & 396.237 \end{pmatrix} K$$

*With pressure and quality the enthalpy can be found when R113 is a saturated liquid:*

$$P_2 = \begin{pmatrix} 1 \\ 1.5 \\ 2 \\ 2.5 \\ 3.15 \end{pmatrix} \cdot MPa \qquad x := 0 \qquad find \qquad h_f := \begin{pmatrix} 171.4 \\ 197.8 \\ 218.6 \\ 235.5 \\ 251.5 \end{pmatrix} \cdot \frac{kJ}{kg}$$

$$H_{f.half.1_{i,j}} := m'_{orc.half.1_{i,j}} \cdot \left(h_{f_i} - h_{2_i}\right) \qquad H_{f.half.1} = \begin{pmatrix} 7.648 & 6.658 & 6.37 & 6.286 & 6.232 \\ 8.928 & 7.771 & 7.433 & 7.335 & 7.273 \\ 9.91 & 8.624 & 8.249 & 8.139 & 8.07 \\ 10.714 & 9.321 & 8.915 & 8.797 & 8.722 \\ 11.441 & 9.951 & 9.516 & 9.389 & 9.31 \end{pmatrix} \cdot kW$$

$$H_{f.half.2_{i,j}} := m'_{orc.half.2_{i,j}} \cdot \left(h_{f_i} - h_{2_i}\right) \qquad H_{f.half.2} = \begin{pmatrix} 7.17 & 6.242 & 5.972 & 5.893 & 5.843 \\ 8.37 & 7.285 & 6.969 & 6.877 & 6.818 \\ 9.29 & 8.085 & 7.733 & 7.631 & 7.566 \\ 10.044 & 8.739 & 8.358 & 8.247 & 8.177 \\ 10.726 & 9.329 & 8.922 & 8.803 & 8.728 \end{pmatrix} \cdot kW$$

$$H_{f.half.3_{i,j}} := m'_{orc.half.3_{i,j}} \cdot \left(h_{f_i} - h_{2_i}\right) \qquad H_{f.half.3} = \begin{pmatrix} 6.692 & 5.826 & 5.573 & 5.5 & 5.453 \\ 7.812 & 6.8 & 6.504 & 6.418 & 6.364 \\ 8.671 & 7.546 & 7.217 & 7.122 & 7.061 \\ 9.375 & 8.156 & 7.801 & 7.697 & 7.632 \\ 10.011 & 8.707 & 8.327 & 8.216 & 8.146 \end{pmatrix} \cdot kW$$

$$H_{f.half.4_{i,j}} := m'_{orc.half.4_{i,j}} \cdot \left(h_{f_i} - h_{2_i}\right) \qquad H_{f.half.4} = \begin{pmatrix} 6.214 & 5.41 & 5.175 & 5.107 & 5.064 \\ 7.254 & 6.314 & 6.04 & 5.96 & 5.909 \\ 8.052 & 7.007 & 6.702 & 6.613 & 6.557 \\ 8.705 & 7.574 & 7.244 & 7.147 & 7.087 \\ 9.296 & 8.085 & 7.732 & 7.629 & 7.564 \end{pmatrix} \cdot kW$$



www.manaraa.com

$$H_{f.half.5_{i,j}} := m'_{orc.half.5_{i,j}} \cdot \left(h_{f_i} - h_{2_i}\right) \qquad H_{f.half.5} = \begin{pmatrix} 5.736 & 4.994 & 4.777 & 4.714 & 4.674 \\ 6.696 & 5.828 & 5.575 & 5.501 & 5.455 \\ 7.432 & 6.468 & 6.186 & 6.104 & 6.052 \\ 8.035 & 6.991 & 6.686 & 6.597 & 6.541 \\ 8.581 & 7.463 & 7.137 & 7.042 & 6.982 \end{pmatrix} \cdot kW$$

*Temperature at pinch point:*

$$T_{pinch.half.1_{i,j}} := m_{slope.half.1_{i,j}} \cdot H_{f.half.1_{i,j}} + b_{int.half.1_{i,j}}$$

$$T_{pinch.half.1} = \begin{pmatrix} 480.081 & 456.816 & 449.598 & 446.341 & 447.112 \\ 500.905 & 474.982 & 466.939 & 463.31 & 464.17 \\ 516.965 & 488.99 & 480.311 & 476.394 & 477.322 \\ 530.18 & 500.514 & 491.31 & 487.157 & 488.14 \\ 542.269 & 511.055 & 501.371 & 497.002 & 498.036 \end{pmatrix} K$$

$$T_{pinch.half.2_{i,j}} := m_{slope.half.2_{i,j}} \cdot H_{f.half.2_{i,j}} + b_{int.half.2_{i,j}}$$

$$T_{pinch.half.2} = \begin{pmatrix} 487.122 & 462.952 & 455.453 & 452.07 & 452.871 \\ 506.645 & 479.983 & 471.711 & 467.979 & 468.863 \\ 521.701 & 493.115 & 484.247 & 480.245 & 481.193 \\ 534.09 & 503.919 & 494.559 & 490.335 & 491.335 \\ 545.423 & 513.801 & 503.991 & 499.564 & 500.613 \end{pmatrix} K$$

$$T_{pinch.half.3_{i,j}} := m_{slope.half.3_{i,j}} \cdot H_{f.half.3_{i,j}} + b_{int.half.3_{i,j}}$$

$$T_{pinch.half.3} = \begin{pmatrix} 494.164 & 469.089 & 461.309 & 457.799 & 458.63 \\ 512.385 & 484.984 & 476.483 & 472.647 & 473.556 \\ 526.437 & 497.241 & 488.183 & 484.096 & 485.064 \\ 538 & 507.324 & 497.807 & 493.513 & 494.53 \\ 548.577 & 516.548 & 506.611 & 502.127 & 503.189 \end{pmatrix} K$$

$$T_{pinch.half.4_{i,j}} := m_{slope.half.4_{i,j}} \cdot H_{f.half.4_{i,j}} + b_{int.half.4_{i,j}}$$

$$T_{pinch.half.4} = \begin{pmatrix} 501.205 & 475.225 & 467.165 & 463.528 & 464.389 \\ 518.124 & 489.985 & 481.255 & 477.316 & 478.249 \\ 531.173 & 501.367 & 492.119 & 487.947 & 488.935 \\ 541.91 & 510.73 & 501.056 & 496.691 & 497.725 \\ 551.732 & 519.294 & 509.231 & 504.69 & 505.765 \end{pmatrix} K$$



www.manaraa.com

$$T_{pinch.half.5_{i,j}} := m_{slope.half.5_{i,j}} \cdot H_{f.half.5_{i,j}} + b_{int.half.5_{i,j}}$$

$$T_{pinch.half.5} = \begin{pmatrix} 508.246 & 481.361 & 473.021 & 469.257 & 470.148 \\ 523.864 & 494.986 & 486.027 & 481.984 & 482.942 \\ 535.909 & 505.492 & 496.056 & 491.798 & 492.806 \\ 545.82 & 514.135 & 504.305 & 499.869 & 500.92 \\ 554.886 & 522.041 & 511.851 & 507.253 & 508.342 \end{pmatrix} K$$

*Pinch point temperature difference:*

$$\Delta T_{pinch.half.1_{i,j}} := T_{pinch.half.1_{i,j}} - T3_i$$

$$\Delta T_{pinch.half.1} = \begin{pmatrix} 67.931 & 44.666 & 37.448 & 34.191 & 34.962 \\ 65.655 & 39.732 & 31.689 & 28.06 & 28.92 \\ 63.415 & 35.44 & 26.761 & 22.844 & 23.772 \\ 61.23 & 31.564 & 22.36 & 18.207 & 19.19 \\ 56.119 & 24.905 & 15.221 & 10.852 & 11.886 \end{pmatrix} K$$

$$\Delta T_{pinch.half.2_{i,j}} := T_{pinch.half.2_{i,j}} - T3_i$$

$$\Delta T_{pinch.half.2} = \begin{pmatrix} 74.972 & 50.802 & 43.303 & 39.92 & 40.721 \\ 71.395 & 44.733 & 36.461 & 32.729 & 33.613 \\ 68.151 & 39.565 & 30.697 & 26.695 & 27.643 \\ 65.14 & 34.969 & 25.609 & 21.385 & 22.385 \\ 59.273 & 27.651 & 17.841 & 13.414 & 14.463 \end{pmatrix} K$$

$$\Delta T_{pinch.half.3_{i,j}} := T_{pinch.half.3_{i,j}} - T3_i$$

$$\Delta T_{pinch.half.3} = \begin{pmatrix} 82.014 & 56.939 & 49.159 & 45.649 & 46.48 \\ 77.135 & 49.734 & 41.233 & 37.397 & 38.306 \\ 72.887 & 43.691 & 34.633 & 30.546 & 31.514 \\ 69.05 & 38.374 & 28.857 & 24.563 & 25.58 \\ 62.427 & 30.398 & 20.461 & 15.977 & 17.039 \end{pmatrix} K$$

$$\Delta T_{pinch.half.4_{i,j}} := T_{pinch.half.4_{i,j}} - T3_i$$



www.manaraa.com

$$\Delta T_{pinch.half.4} = \begin{pmatrix} 89.055 & 63.075 & 55.015 & 51.378 & 52.239 \\ 82.874 & 54.735 & 46.005 & 42.066 & 42.999 \\ 77.623 & 47.817 & 38.569 & 34.397 & 35.385 \\ 72.96 & 41.78 & 32.106 & 27.741 & 28.775 \\ 65.582 & 33.144 & 23.081 & 18.54 & 19.615 \end{pmatrix} K$$

$$\Delta T_{pinch.half.5_{i,j}} := T_{pinch.half.5_{i,j}} - T3_i$$

$$\Delta T_{pinch.half.5} = \begin{pmatrix} 96.096 & 69.211 & 60.871 & 57.107 & 57.998 \\ 88.614 & 59.736 & 50.777 & 46.734 & 47.692 \\ 82.359 & 51.942 & 42.506 & 38.248 & 39.256 \\ 76.87 & 45.185 & 35.355 & 30.919 & 31.97 \\ 68.736 & 35.891 & 25.701 & 21.103 & 22.192 \end{pmatrix} K$$



www.manaraa.com

APPENDIX B

GRAPHS FOR R113 & PROPANE FROM EVALUTIONS 1 & 2 AT HALF LOAD



www.manaraa.com

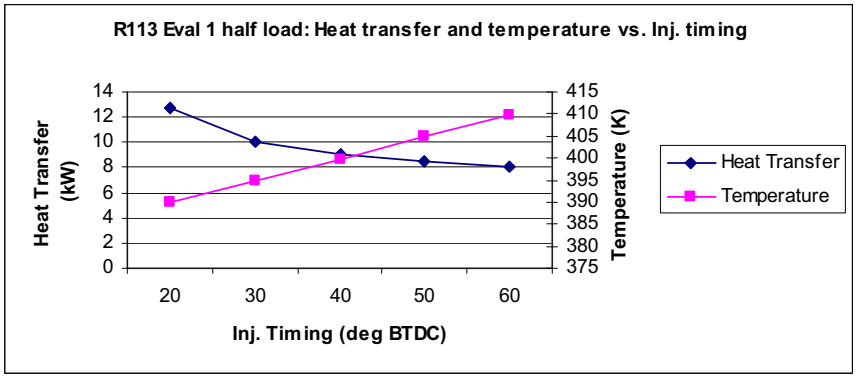


Figure 39 Evaluation 1 heat transfer and exhaust outlet temperature versus injection timing for R113 at half load

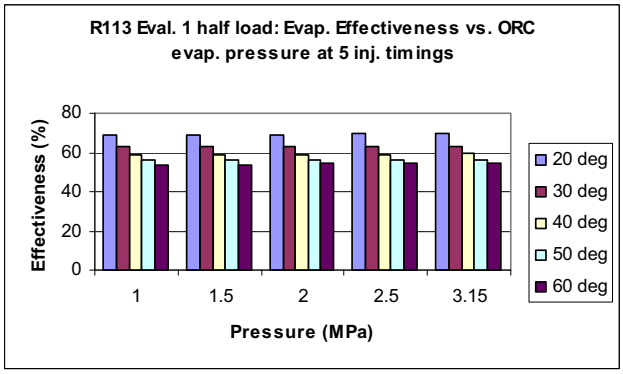


Figure 40 Evaluation 1 evaporator effectiveness versus pressure at 5 injection timings for R113 at half load

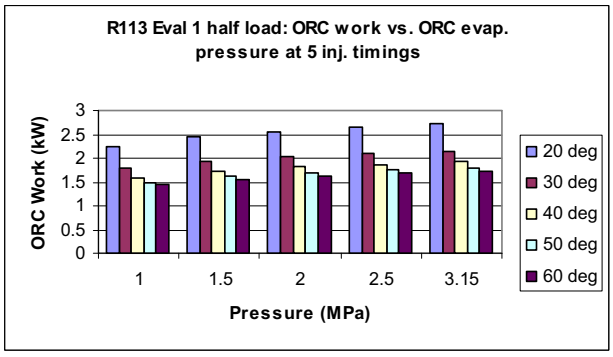


Figure 41 Evaluation 1work versus pressure at 5 injection timings for R113 at half load



www.manaraa.com

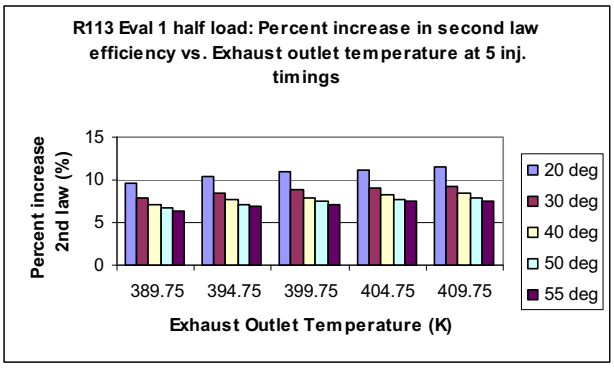


Figure 42 Evaluation 1 percent increase in second law efficiency versus exhaust outlet temperature at 5 injection timings for R113 at half load

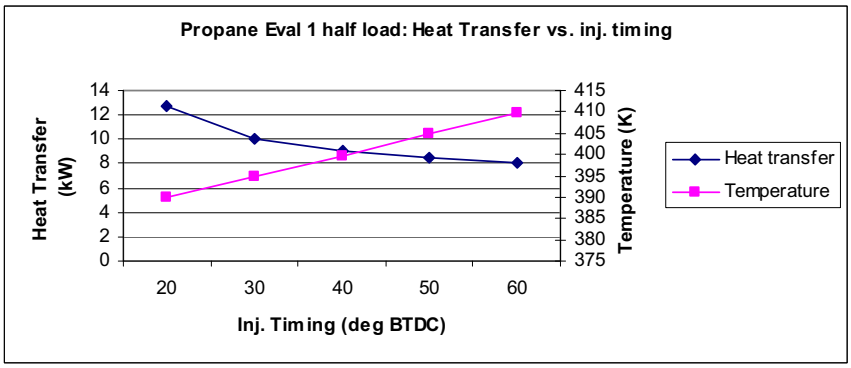


Figure 43 Evaluation 1 heat transfer and exhaust outlet temperature versus injection timing for propane at half load

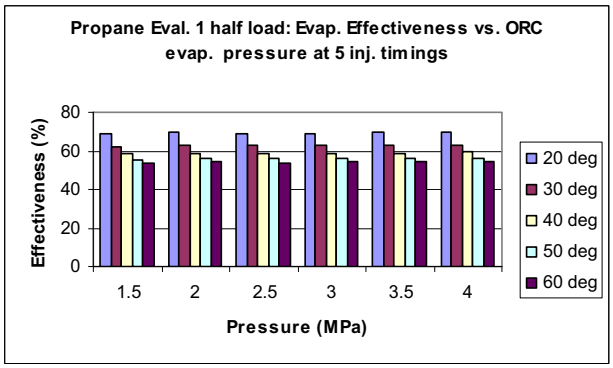


Figure 44 Evaluation 1 evaporator effectiveness versus pressure at 5 injection timings for propane at half load



www.manaraa.com

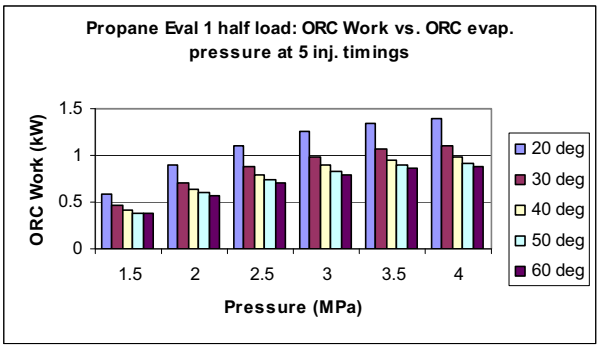


Figure 45 Evaluation 1 work versus pressure at 5 inj. timings for propane at half load

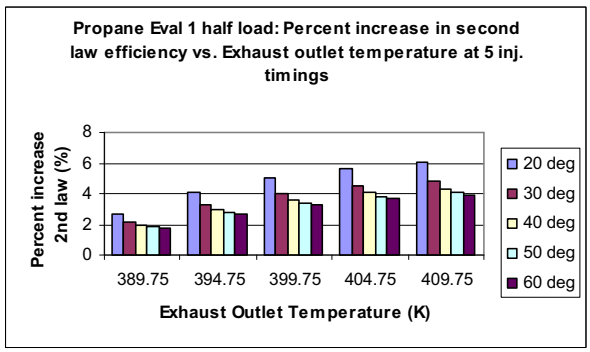


Figure 46 Evaluation 1 percent increase in second law efficiency versus exhaust outlet temperature at 5 injection timings for propane at half load

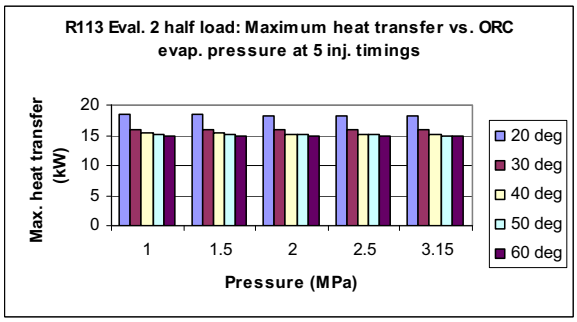


Figure 47 Evaluation 2 maximum heat transfer versus pressure at 5 injection timings for R113 at half load



www.manaraa.com

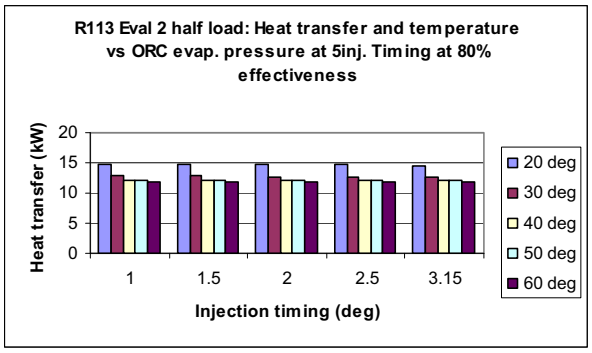


Figure 48 Evaluation 2 heat transfer at 80% effectiveness versus pressure at 5 injection timings for R113 at half load

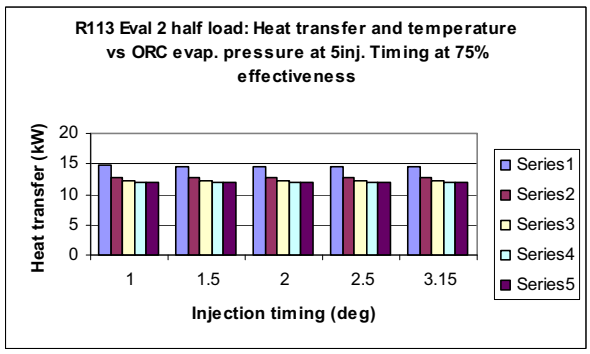


Figure 49 Evaluation 2 heat transfer at 75% effectiveness versus pressure at 5 injection timings for R113 at half load

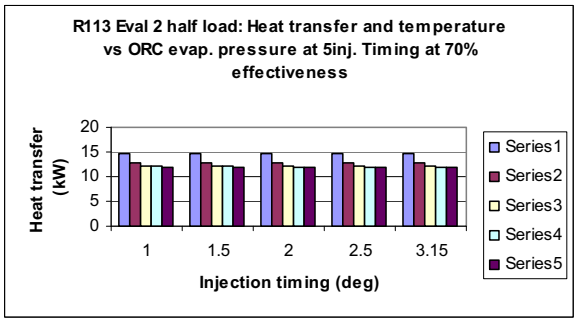


Figure 50 Evaluation 2 heat transfer at 70% effectiveness versus pressure at 5 injection timings for R113 at half load



www.manaraa.com

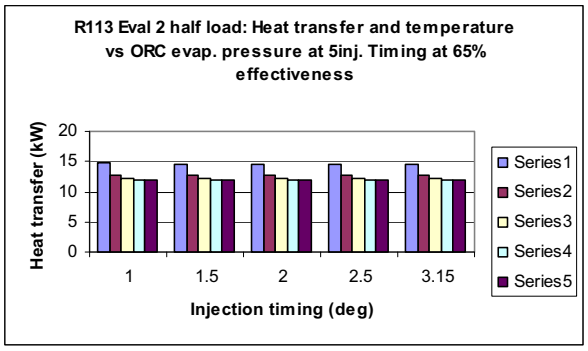


Figure 51 Evaluation 2 heat transfer at 65% effectiveness versus pressure at 5 injection timings for R113 at half load

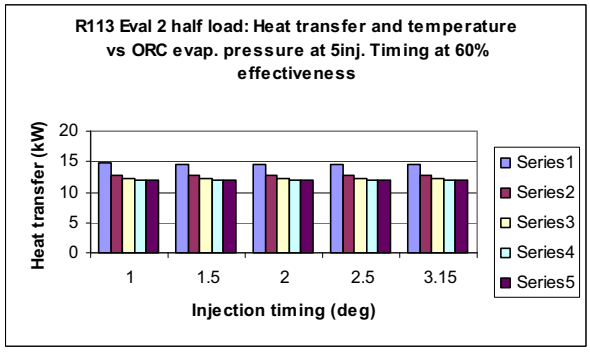


Figure 52 Evaluation 2 heat transfer at 60% effectiveness versus pressure at 5 injection timings for R113 at half load

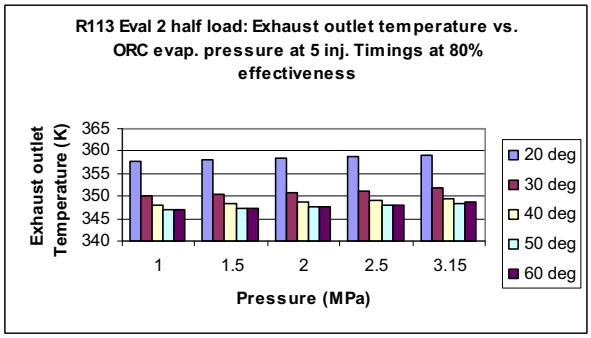


Figure 53 Evaluation 2 exhaust outlet temperature at 80% effectiveness versus pressure at 5 injection timings for R113 at half load



www.manaraa.com

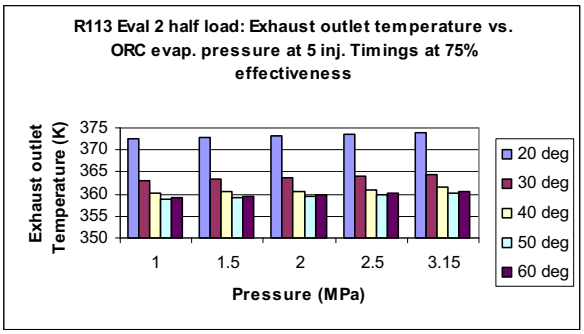


Figure 54 Evaluation 2 exhaust outlet temperature at 75% effectiveness versus pressure at 5 injection timings for R113 at half load

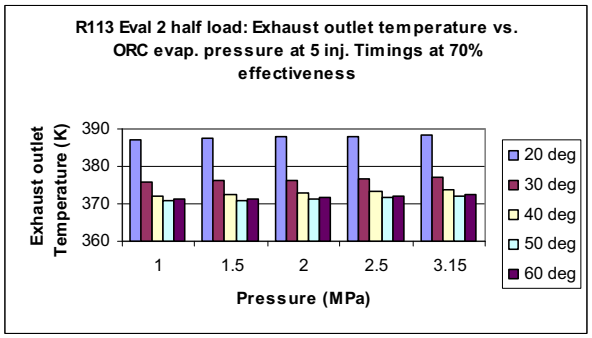


Figure 55 Evaluation 2 exhaust outlet temperature at 70% effectiveness versus pressure at 5 injection timings for R113 at half load

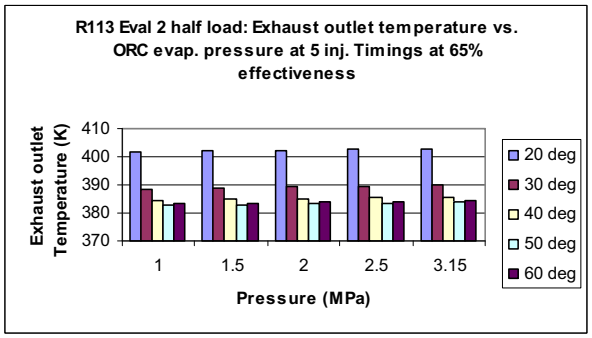


Figure 56 Evaluation 2 exhaust outlet temperature at 65% effectiveness versus pressure at 5 injection timings for R113 at half load



www.manaraa.com

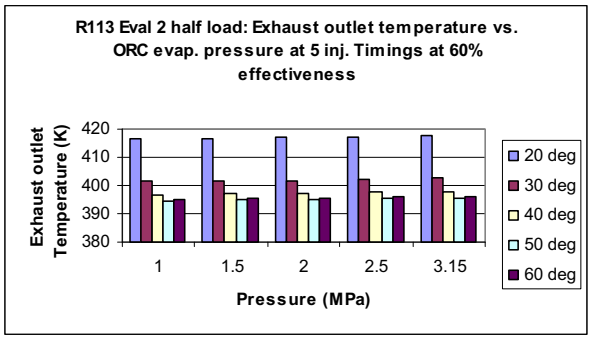


Figure 57 Evaluation 2 exhaust outlet temperature at 60% effectiveness versus pressure at 5 injection timings for R113 at half load

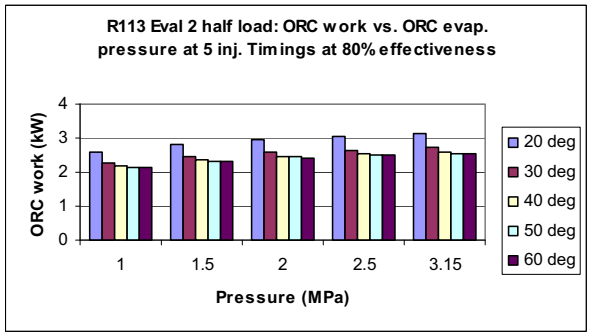


Figure 58 Evaluation 2 work at 80% effectiveness versus pressure at 5 injection timings for R113 at half load

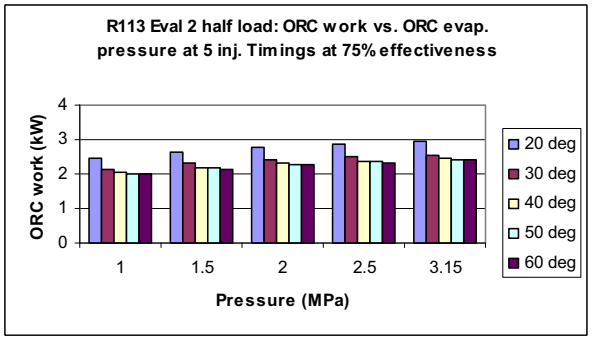


Figure 59 Evaluation 2 work at 75% effectiveness versus pressure at 5 injection timings for R113 at half load



www.manaraa.com

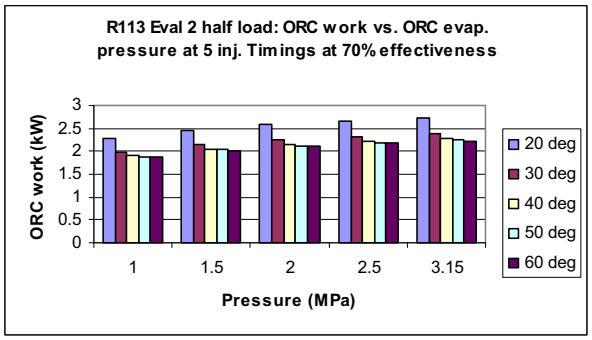


Figure 60 Evaluation 2 work at 70% effectiveness versus pressure at 5 injection timings for R113 at half load

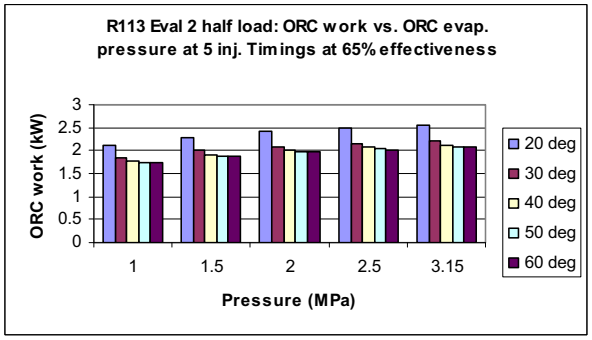


Figure 61 Evaluation 2 work at 65% effectiveness versus pressure at 5 injection timings for R113 at half load

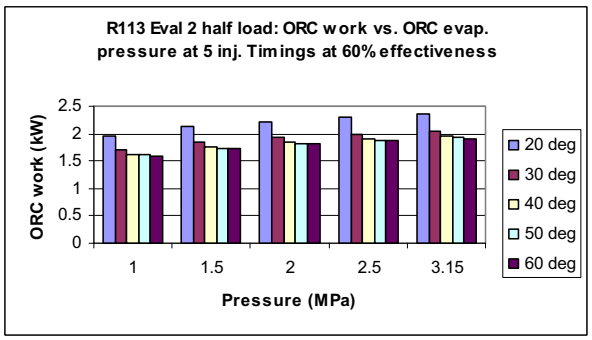


Figure 62 Evaluation 2 work at 60% effectiveness versus pressure at 5 injection timings for R113 at half load



www.manaraa.com

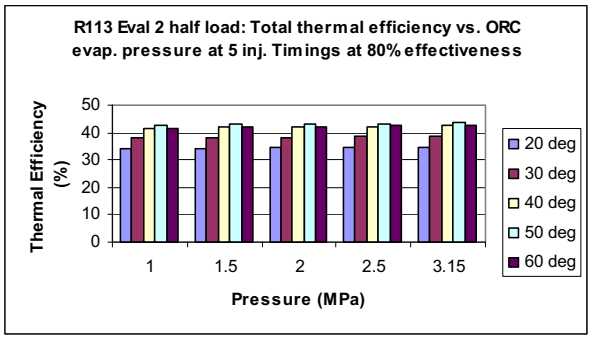


Figure 63 Evaluation 2 total thermal efficiency at 80% effectiveness versus pressure at 5 injection timings for R113 at half load

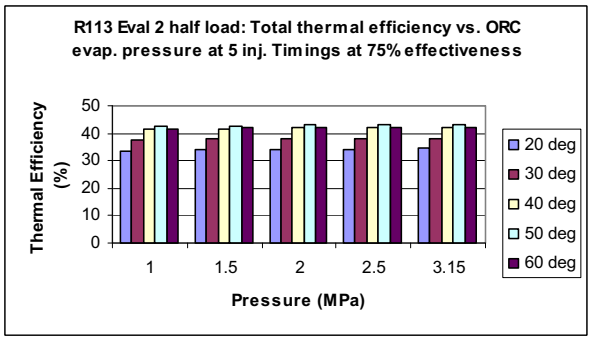


Figure 64 Evaluation 2 total thermal efficiency at 75% effectiveness versus pressure at 5 injection timings for R113 at half load

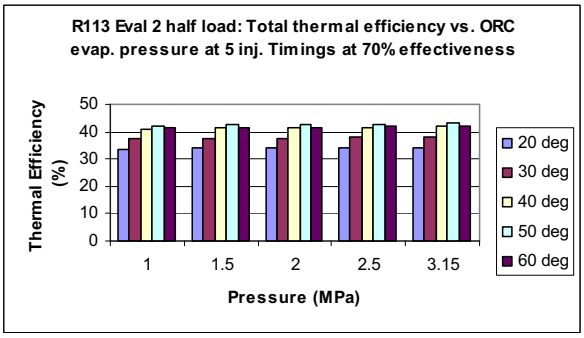


Figure 65 Evaluation 2 total thermal efficiency at 70% effectiveness versus pressure at 5 injection timings for R113 at half load



www.manaraa.com

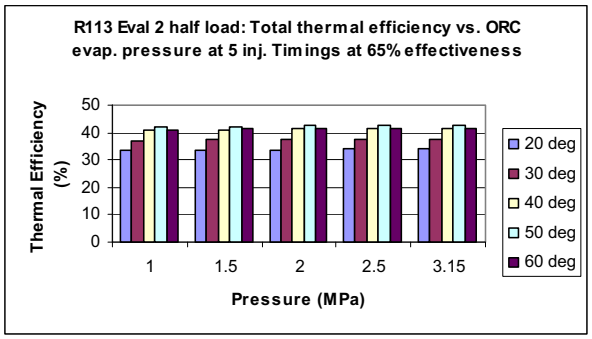


Figure 66 Evaluation 2 total thermal efficiency at 65% effectiveness versus pressure at 5 injection timings for R113 at half load

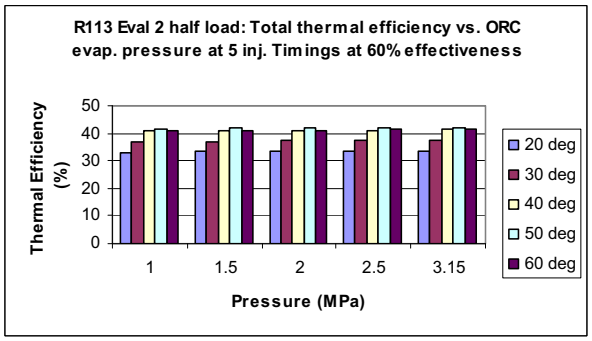


Figure 67 Evaluation 2 total thermal efficiency at 60% effectiveness versus pressure at 5 injection timings for R113 at half load

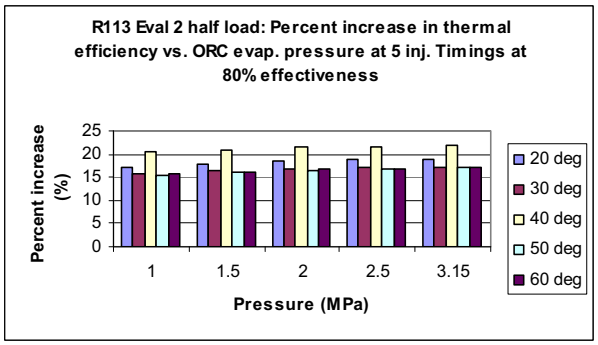


Figure 68 Evaluation 2 percent increase in thermal efficiency at 80% effectiveness versus pressure at 5 injection timings for R113 at half load



www.manaraa.com

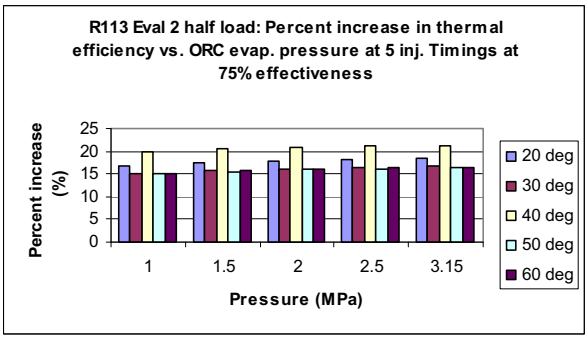


Figure 69 Evaluation 2 percent increase in thermal efficiency at 75% effectiveness versus pressure at 5 injection timings for R113 at half load

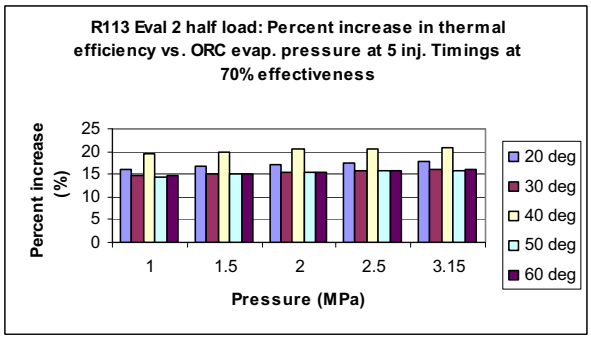


Figure 70 Evaluation 2 percent increase in thermal efficiency at 70% effectiveness versus pressure at 5 injection timings for R113 at half load

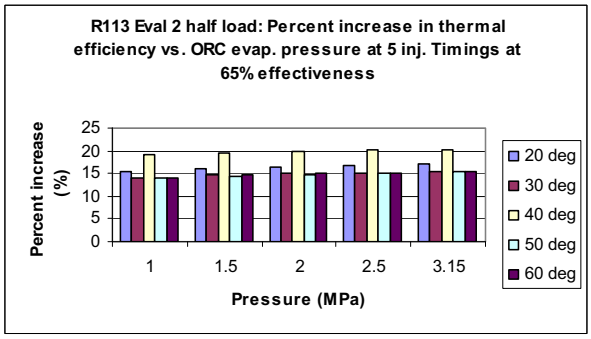


Figure 71 Evaluation 2 percent increase in thermal efficiency at 65% effectiveness versus pressure at 5 injection timings for R113 at half load



www.manaraa.com

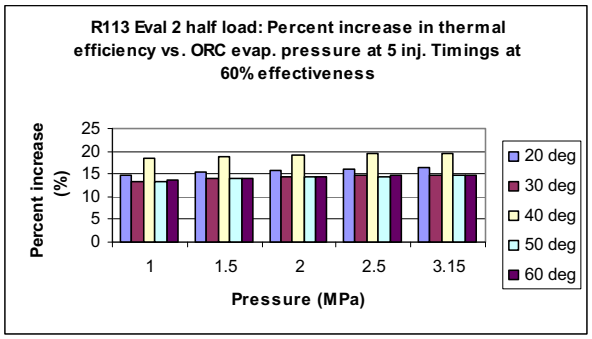


Figure 72 Evaluation 2 percent increase in thermal efficiency at 60% effectiveness versus pressure at 5 injection timings for R113 at half load

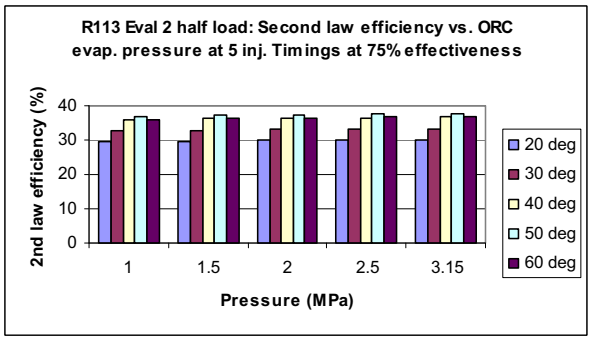


Figure 73 Evaluation 2 second law efficiency at 75% effectiveness versus pressure at 5 injection timings for R113 at half load

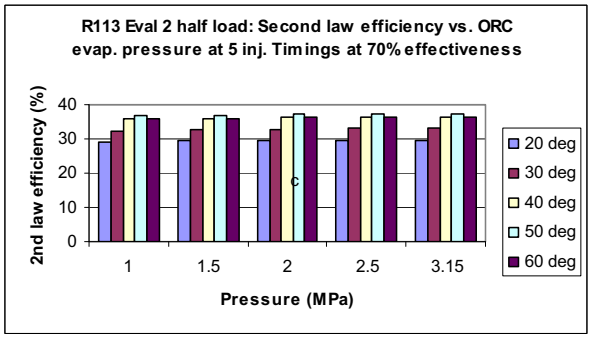


Figure 74 Evaluation 2 second law efficiency at 70% effectiveness versus pressure at 5 injection timings for R113 at half load



www.manaraa.com

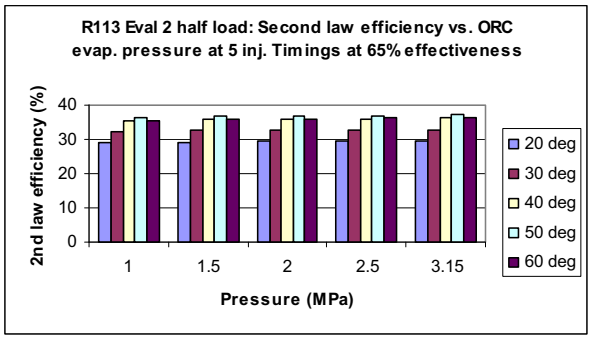


Figure 75 Evaluation 2 second law efficiency at 65% effectiveness versus pressure at 5 injection timings for R113 at half load

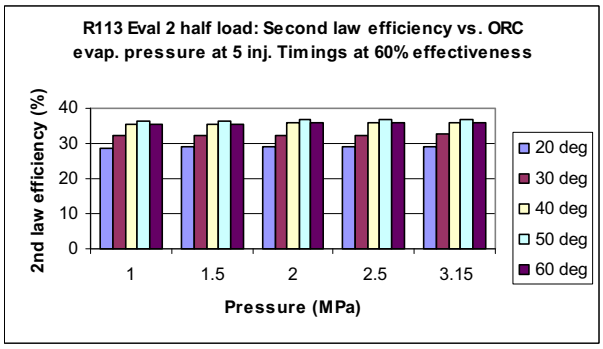


Figure 76 Evaluation 2 second law efficiency at 60% effectiveness versus pressure at 5 injection timings for R113 at half load

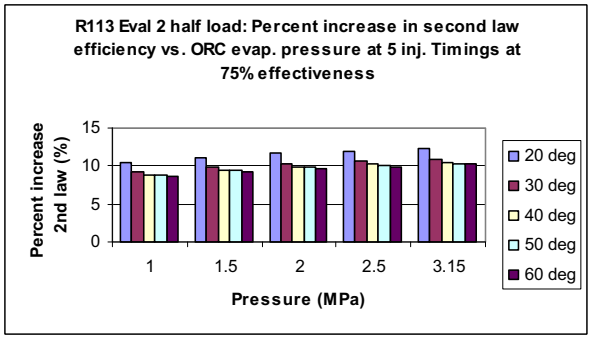


Figure 77 Evaluation 2 percent increase in second law efficiency at 75% effectiveness versus pressure at 5 injection timings for R113 at half load



www.manaraa.com

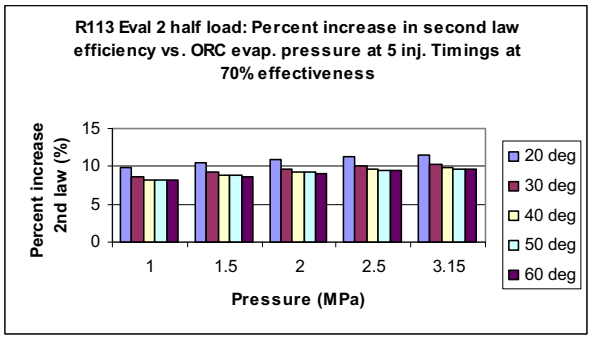


Figure 78 Evaluation 2 percent increase in second law efficiency at 70% effectiveness versus pressure at 5 injection timings for R113 at half load

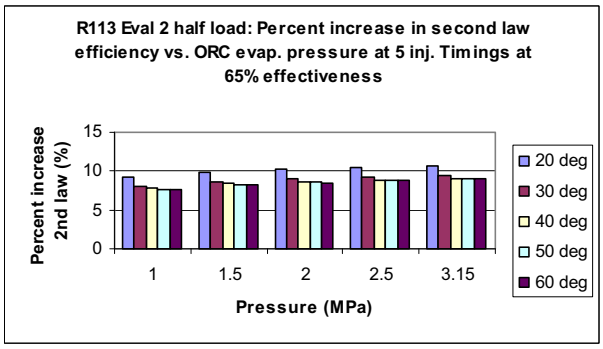


Figure 79 Evaluation 2 percent increase in second law efficiency at 65% effectiveness versus pressure at 5 injection timings for R113 at half load

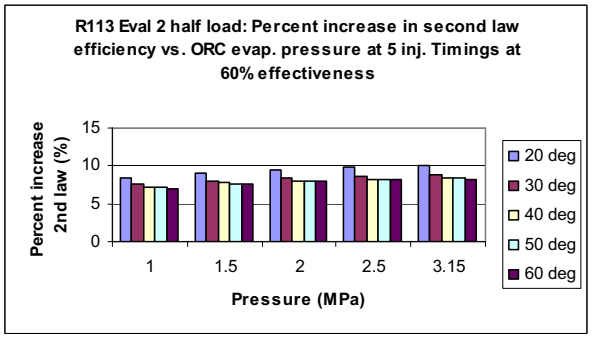


Figure 80 Evaluation 2 percent increase in second law efficiency at 60% effectiveness versus pressure at 5 injection timings for R113 at half load



www.manaraa.com

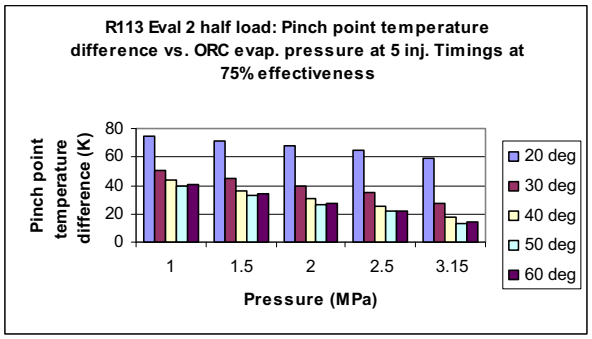


Figure 81 Evaluation 2 pinch point temperature difference at 75% effectiveness versus pressure at 5 injection timings for R113 at half load

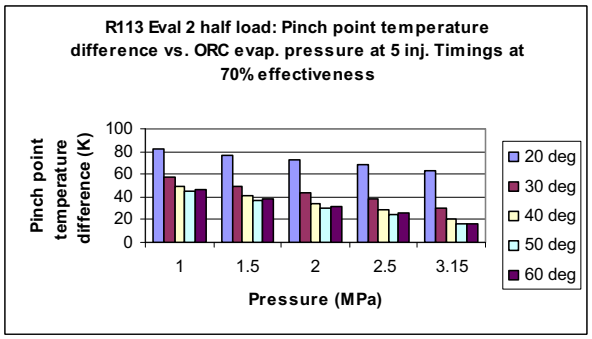


Figure 82 Evaluation 2 pinch point temperature difference at 70% effectiveness versus pressure at 5 injection timings for R113 at half load

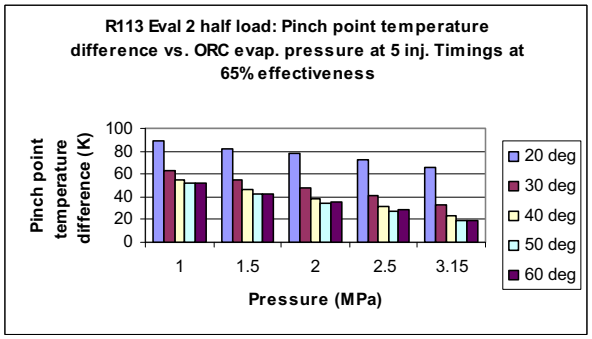


Figure 83 Evaluation 2 pinch point temperature difference at 65% effectiveness versus pressure at 5 injection timings for R113 at half load



www.manaraa.com

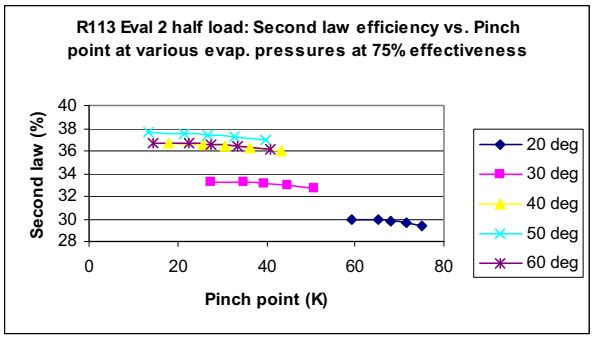


Figure 84 Evaluation 2 second law efficiency at 75% effectiveness versus pinch point at various pressures and 5 injection timings for R113 at half load

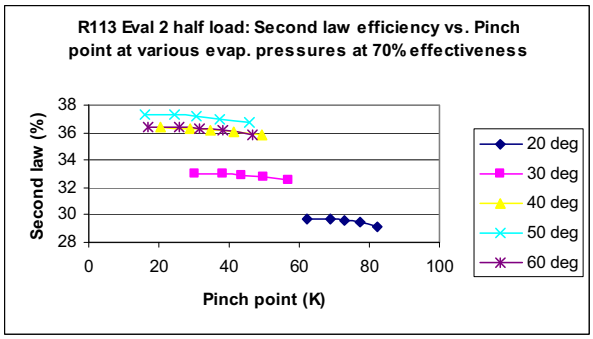


Figure 85 Evaluation 2 second law efficiency at 70% effectiveness versus pinch point at various pressures and 5 injection timings for R113 at half load

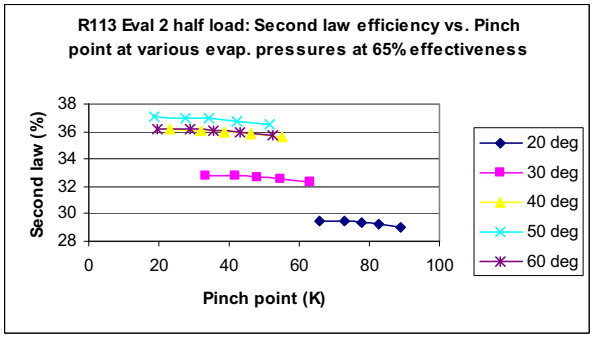


Figure 86 Evaluation 2 second law efficiency at 65% effectiveness versus pinch point at various pressures and 5 injection timings for R113 at half load



www.manaraa.com

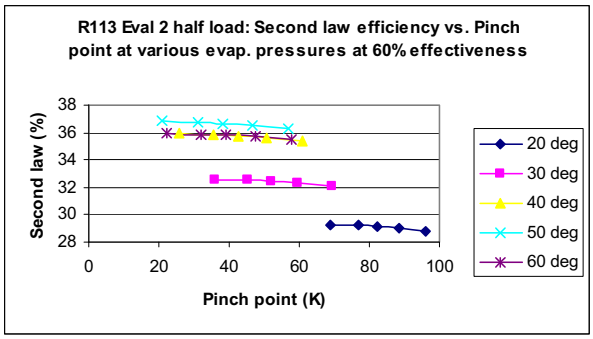


Figure 87 Evaluation 2 second law efficiency at 60% effectiveness versus pinch point at various pressures and 5 injection timings for R113 at half load

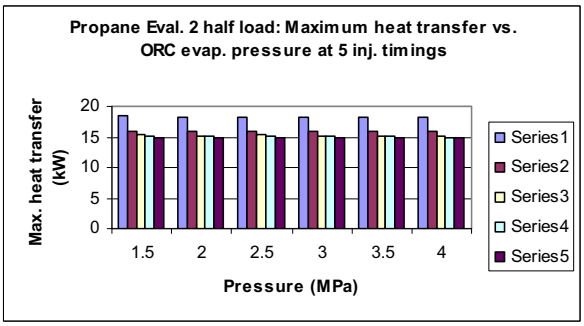


Figure 88 Evaluation 2 maximum heat transfer versus pressure at 5 injection timings for propane at half load

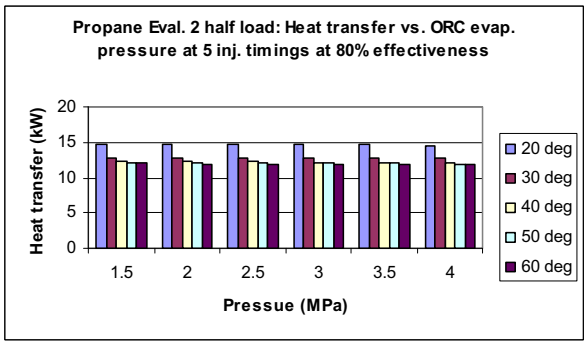


Figure 89 Evaluation 2 heat transfer at 80% effectiveness versus pressure at 5 injection timings for propane at half load



www.manaraa.com

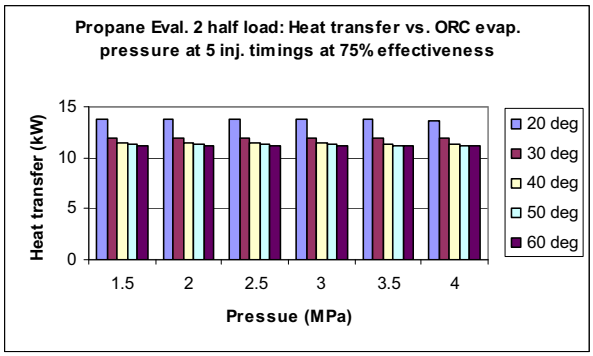


Figure 90 Evaluation 2 heat transfer at 75% effectiveness versus pressure at 5 injection timings for propane at half load

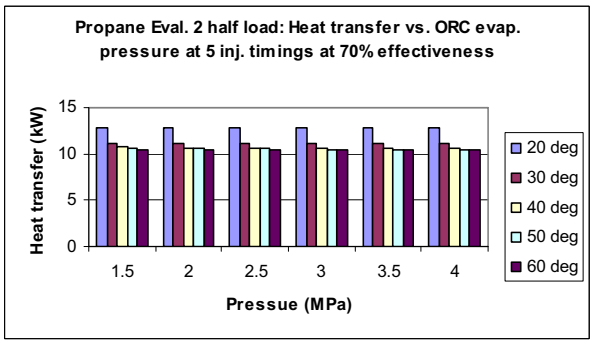


Figure 91 Evaluation 2 heat transfer at 70% effectiveness versus pressure at 5 injection timings for propane at half load

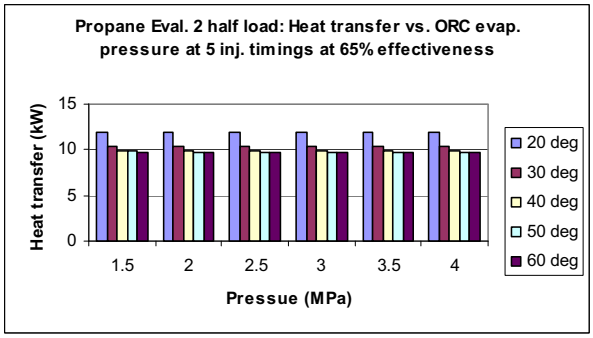


Figure 92 Evaluation 2 heat transfer at 65% effectiveness versus pressure at 5 injection timings for propane at half load



www.manaraa.com

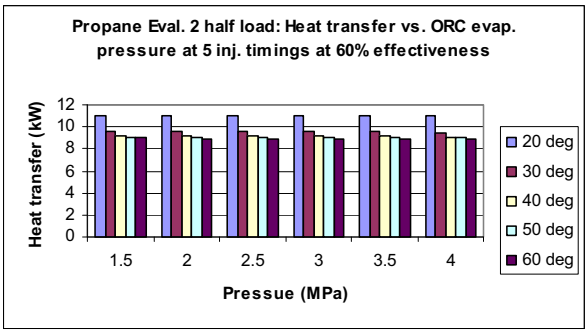


Figure 93 Evaluation 2 heat transfer at 60% effectiveness versus pressure at 5 injection timings for propane at half load

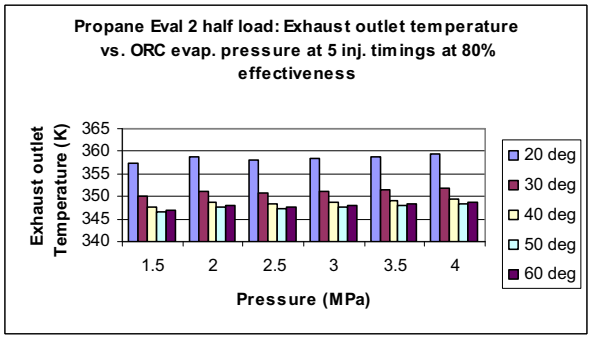


Figure 94 Evaluation 2 exhaust outlet temperature at 80% effectiveness versus pressure at 5 injection timings for propane at half load

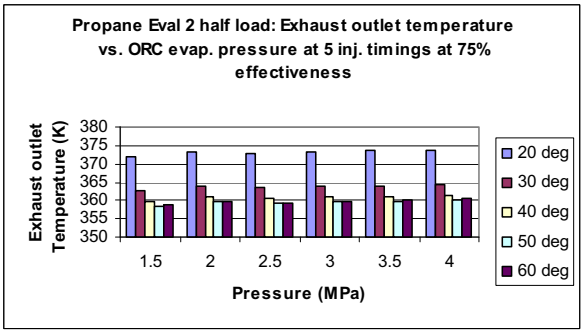


Figure 95 Evaluation 2 exhaust outlet temperature at 75% effectiveness versus pressure at 5 injection timings for propane at half load



www.manaraa.com

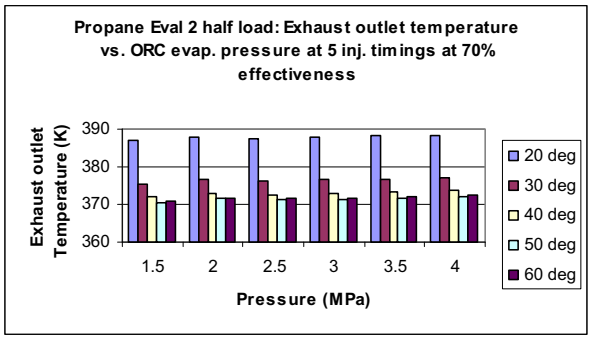


Figure 96 Evaluation 2 exhaust outlet temperature at 70% effectiveness versus pressure at 5 injection timings for propane at half load

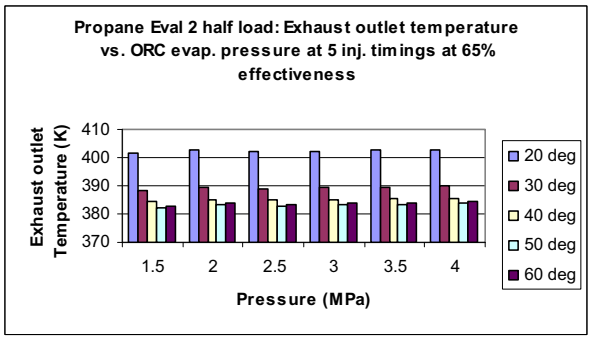


Figure 97 Evaluation 2 exhaust outlet temperature at 65% effectiveness versus pressure at 5 injection timings for propane at half load

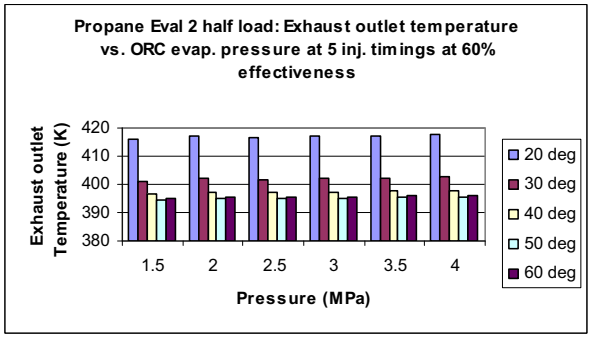


Figure 98 Evaluation 2 exhaust outlet temperature at 60% effectiveness versus pressure at 5 injection timings for propane at half load



www.manaraa.com

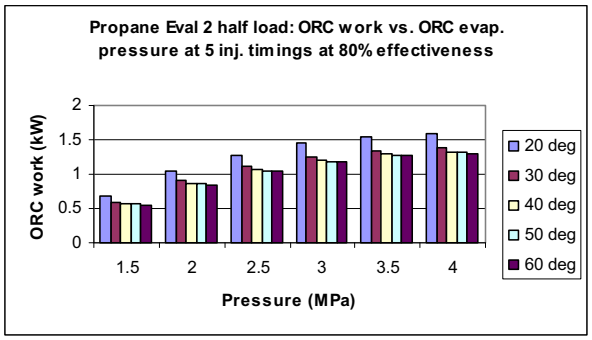


Figure 99 Evaluation 2 work at 80% effectiveness versus pressure at 5 injection timings for propane at half load

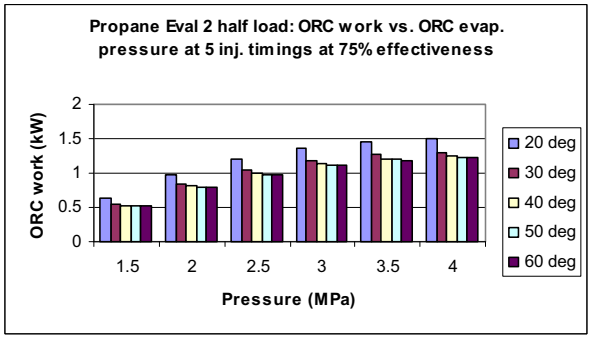


Figure 100 Evaluation 2 work at 75% effectiveness versus pressure at 5 injection timings for propane at half load

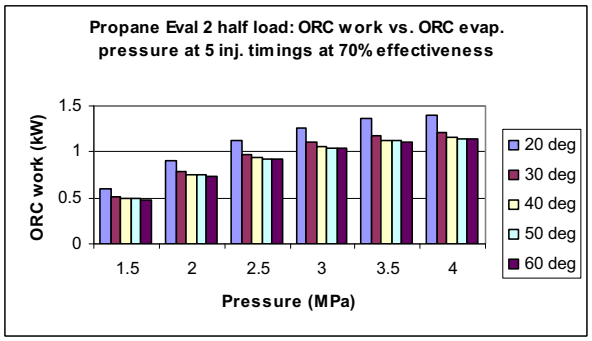


Figure 101 Evaluation 2 work at 70% effectiveness versus pressure at 5 injection timings for propane at half load



www.manaraa.com

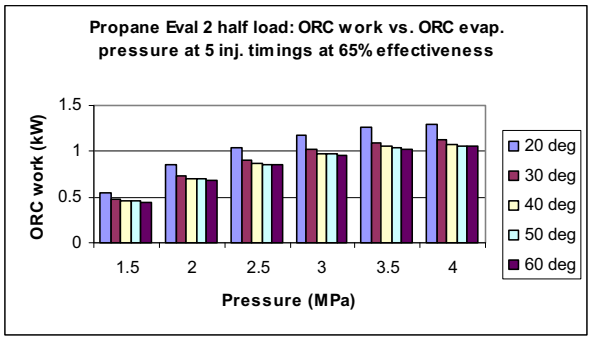


Figure 102 Evaluation 2 work at 65% effectiveness versus pressure at 5 injection timings for propane at half load

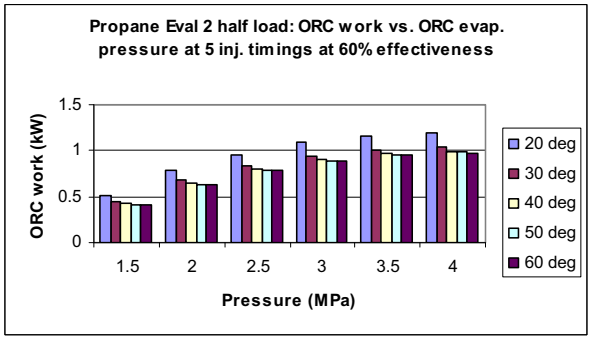


Figure 103 Evaluation 2 work at 60% effectiveness versus pressure at 5 injection timings for propane at half load

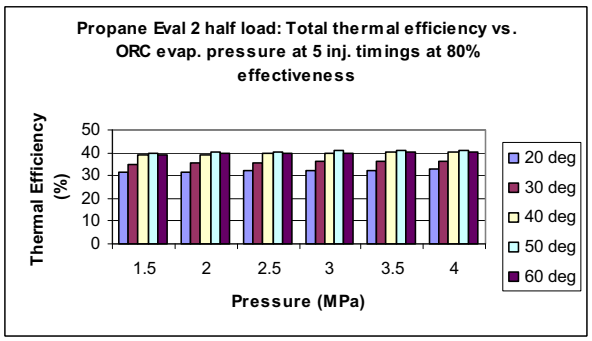


Figure 104 Evaluation 2 total thermal efficiency at 80% effectiveness versus pressure at 5 injection timings for propane at half load



www.manaraa.com

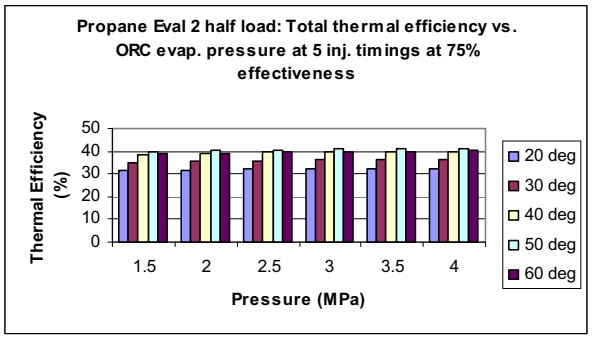


Figure 105 Evaluation 2 total thermal efficiency at 75% effectiveness versus pressure at 5 injection timings for propane at half load

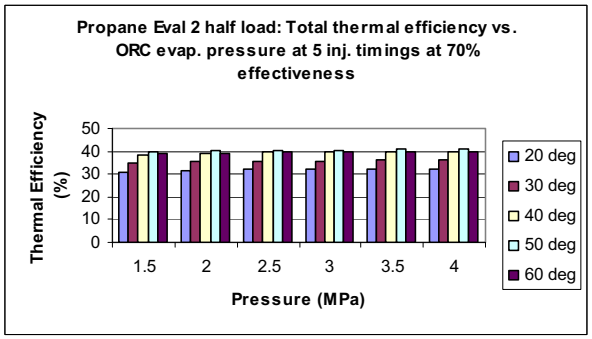


Figure 106 Evaluation 2 total thermal efficiency at 70% effectiveness versus pressure at 5 injection timings for propane at half load

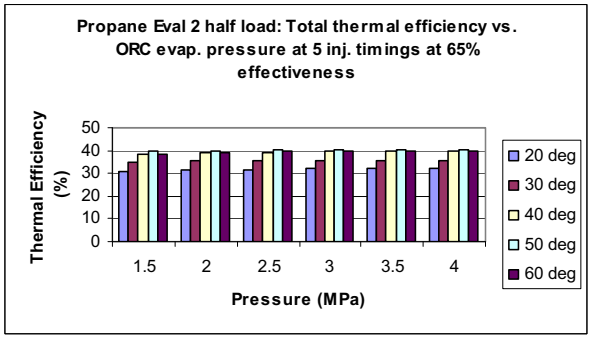


Figure 107 Evaluation 2 total thermal efficiency at 65% effectiveness versus pressure at 5 injection timings for propane at half load



www.manaraa.com

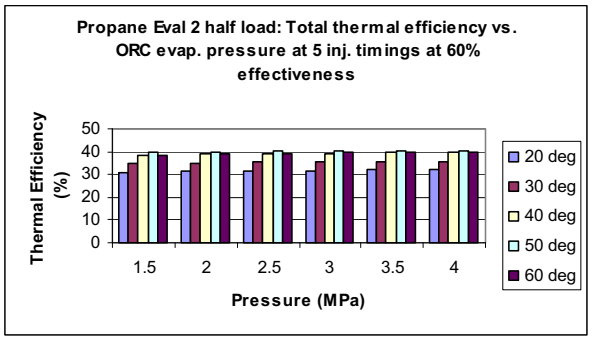


Figure 108 Evaluation 2 total thermal efficiency at 60% effectiveness versus pressure at 5 injection timings for propane at half load

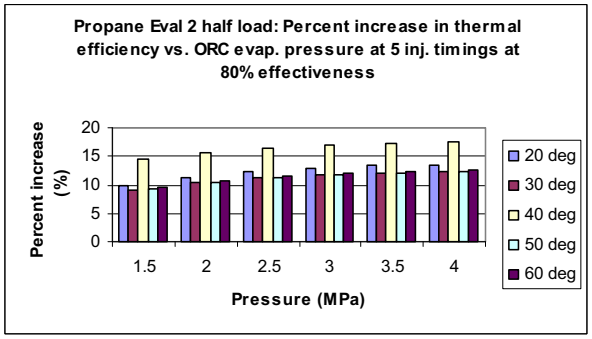


Figure 109 Evaluation 2 percent increase in thermal efficiency at 80% effectiveness versus pressure at 5 injection timings for propane at half load

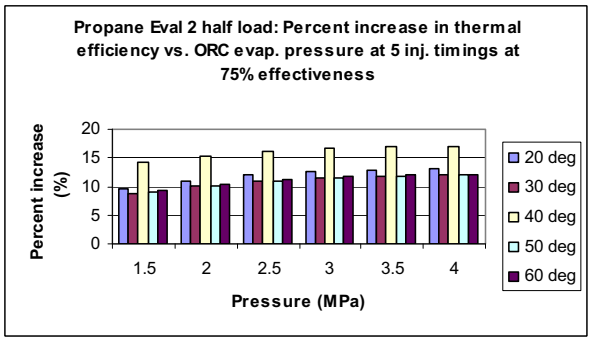


Figure 110 Evaluation 2 percent increase in thermal efficiency at 75% effectiveness versus pressure at 5 injection timings for propane at half load



www.manaraa.com

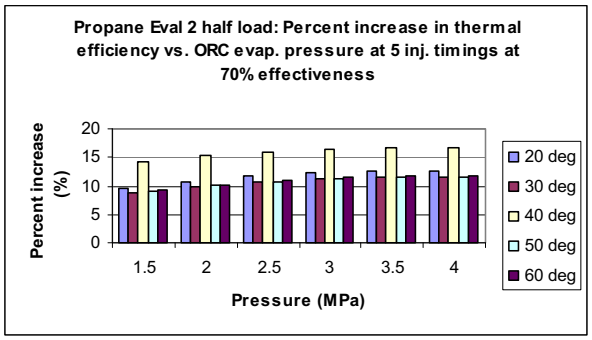


Figure 111 Evaluation 2 percent increase in thermal efficiency at 70% effectiveness versus pressure at 5 injection timings for propane at half load

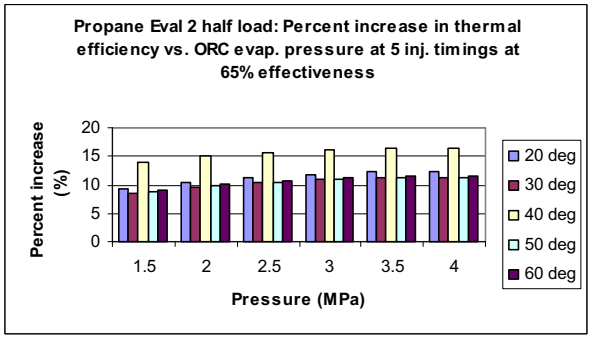


Figure 112 Evaluation 2 percent increase in thermal efficiency at 65% effectiveness versus pressure at 5 injection timings for propane at half load

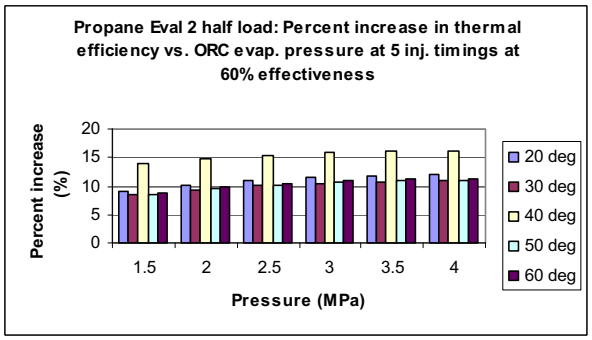


Figure 113 Evaluation 2 percent increase in thermal efficiency at 60% effectiveness versus pressure at 5 injection timings for propane at half load



www.manaraa.com

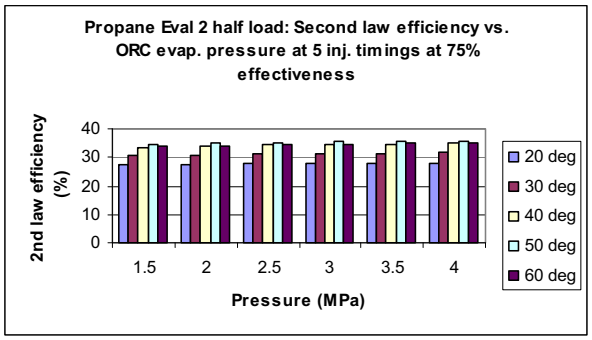


Figure 114 Evaluation 2 second law efficiency at 75% effectiveness versus pressure at 5 injection timings for propane at half load

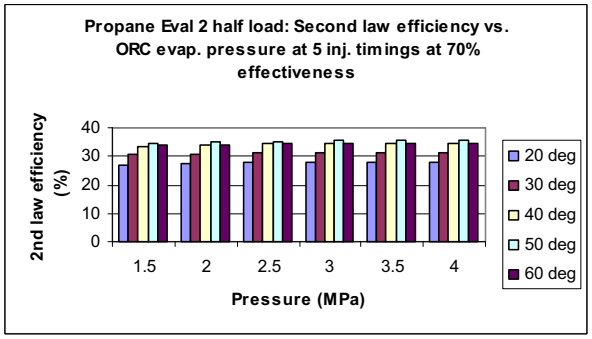


Figure 115 Evaluation 2 second law efficiency at 70% effectiveness versus pressure at 5 injection timings for propane at half load

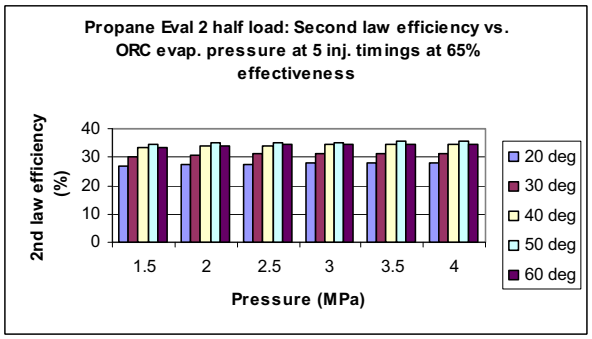


Figure 116 Evaluation 2 second law efficiency at 65% effectiveness versus pressure at 5 injection timings for propane at half load



www.manaraa.com

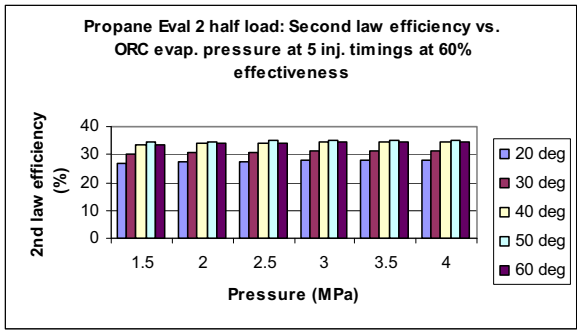


Figure 117 Evaluation 2 second law efficiency at 60% effectiveness versus pressure at 5 injection timings for propane at half load

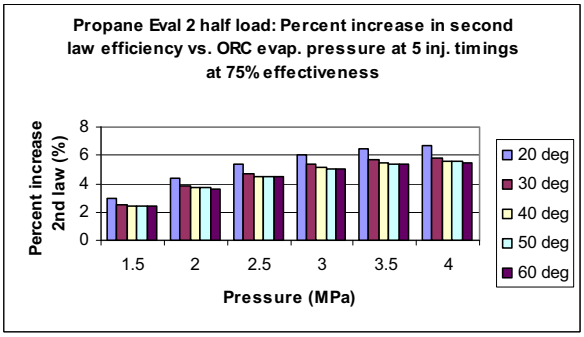


Figure 118 Evaluation 2 percent increase in second law efficiency at 75% effectiveness versus pressure at 5 injection timings for propane at half load

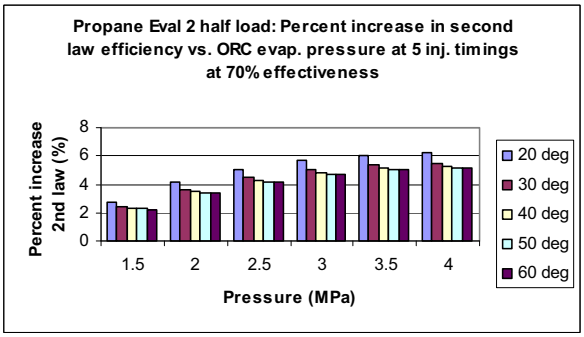


Figure 119 Evaluation 2 percent increase in second law efficiency at 70% effectiveness versus pressure at 5 injection timings for propane at half load



www.manaraa.com

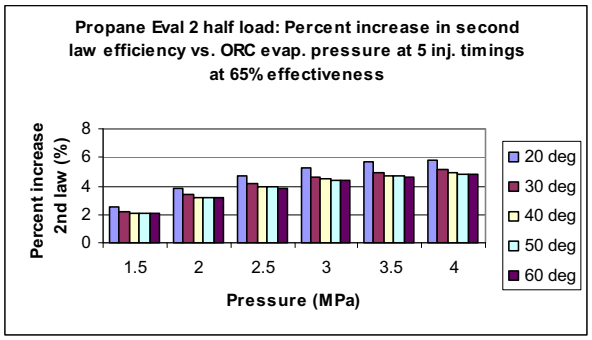


Figure 120 Evaluation 2 percent increase in second law efficiency at 65% effectiveness versus pressure at 5 injection timings for propane at half load

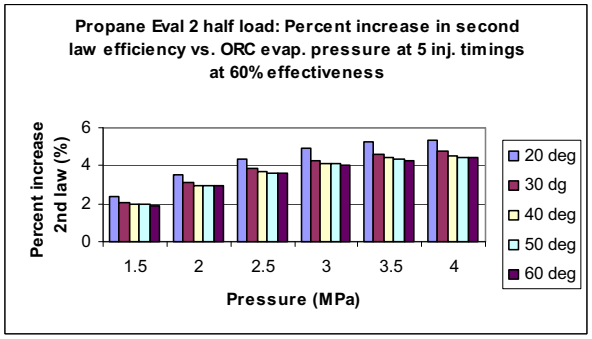


Figure 121 Evaluation 2 percent increase in second law efficiency at 60% effectiveness versus pressure at 5 injection timings for propane at half load



www.manaraa.com